CARACTÉRISATION DES PERTURBATIONS PARIÉTALES INDUITES PAR LA THAXTOMINE A CHEZ *ARABIDOPSIS THALIANA*

par

Fatima Awwad

Thèse présentée au département de Biologie en vue

de l'obtention du grade de docteur ès sciences (Ph.D.)

FACULTÉ DES SCIENCES

UNIVERSITÉ DE SHERBROOKE

Sherbrooke, Québec, Canada, octobre 2018

Le 25 octobre 2018

le jury a accepté la thèse de Madame Fatima Awwad
dans sa version finale.

Membres du jury

Professeure Nathalie Beaudoin

Directrice de recherche

Département de biologie

Professeur Daniel Kierzkowski

Évaluateur externe

Université de Montréal, Institut de recherche en biologie végétale

Professeure Carole Beaulieu

Évaluateur interne

Département de biologie

Professeur Peter Moffett

Président-rapporteur

Département de biologie

SOMMAIRE

Les cellules végétales, à la différence des cellules animales, sont munies d'une paroi cellulaire. Cette paroi confère à la cellule à la fois une rigidité lui permettant de confronter les stress environnants, et une flexibilité permettant l'élongation, la différenciation et la division. La présence de cette paroi protège la plante des agressions externes, comme par exemple l'infection par un agent phytopathogène ou une blessure. Une perturbation importante de la paroi, telle que causée par l'application d'un inhibiteur de synthèse de la cellulose, un composant majeur de la paroi, met également en place un programme de mort cellulaire programmée.

La thaxtomine A est un inhibiteur de synthèse de la cellulose qui induit ce type de programme de mort chez les cellules végétales sans activer les réponses typiques de la mort observée suite à une réponse hypersensible HR, comme la production d'espèces activées de l'oxygène ou la voie des protéines kinases activées par des mitogènes (MAPK). Cette toxine est secrétée par *Streptomyces scabies,* un agent responsable de la gale commune de la pomme de terre. La thaxtomine A est essentielle lors de l'infection des tubercules de pomme de terre pour la production des symptômes typiques de la maladie. La mort cellulaire induite par la thaxtomine A a été caractérisée dans le passé par notre laboratoire.

L'objectif de ma thèse est de décortiquer davantage les éléments impliqués dans la mort induite par la thaxtomine A. Pour ceci, plusieurs outils ont été déployés incluant l'utilisation d'inhibiteurs pharmacologiques et leurs effets sur la mort, l'analyse de la biomécanique de la surface cellulaire en mode de microscopie à force atomique, ainsi que l'imagerie en temps réel des composants du cytosquelette et des protéines de la membrane plasmique.

Dans ce travail, on montre qu'un traitement à la thaxtomine A de cellules d'*Arabidopsis* cultivées en suspension induit un efflux d'auxine, un signal calcique et une restriction de la taille cellulaire. On a aussi montré que la toxine cause une réorganisation rapide des microtubules et affecte la vitesse des protéines Cellulose Synthases. Également, on a démontré pour la première fois, que les microfibrilles de cellulose synthétisée en présence

de thaxtomine A sont plus courtes qu'en absence de traitement. Finalement, un lien a été établi entre l'absence de la flambée oxydative en présence de la thaxtomine A et son influence sur la rigidité de la paroi.

Mots clés : Thaxtomine A, paroi cellulaire, mort cellulaire programmée, auxine, cellulose, rigidité pariétale.

REMERCIEMENTS

Je tiens tout d'abord à remercier ma directrice de recherche, la Dre Nathalie Beaudoin pour m'avoir accueillie dans son laboratoire. Merci pour les encouragements dans les moments difficiles et aussi pendant la rédaction de cette thèse, pour tous les conseils et les corrections.

Je remercie également mes conseillers, la Dre Carole Beaulieu et le Dr Peter Moffett, qui ont participé activement à l'évaluation de cette thèse. Un grand merci pour les Drs Geoff Wasteneys (UBC) et Michel Grandbois (Fleurimont) pour m'avoir permis de faire des essais dans leurs laboratoires. J'aimerais remercier, de même, la Dre Miki Fujita de UBC pour son aide précieuse et son amitié.

J'aimerais dédier une partie importante de mes remerciements au Centre SÈVE, pour les bourses de stage et de participation à des congrès ainsi que pour toutes les formations enrichissantes. Je remercie particulièrement Chantal Binda, Anne-Marie Simao et Mina Zitouni, merci pour les discussions, les offres d'emploi, les encouragements. Sachez que votre implication dans mon cursus est gravée profondément.

Un grand merci à tous les collègues/amis(es) pour les pauses café et les encouragements et pour avoir supporté mes plaintes et mes angoisses : Mina, Jenia, Lauriane, Guillaume, Jessica, Camilia, Joël, Mohamad, Julien et Solange... Les amis qui me soutenaient depuis l'autre bout du monde : Hania, Maryam, Hicham, Farah, Jinane, Sarah et Rana... Un grand merci et beaucoup de gratitude pour Mylène Côté du programme de pharmacologie pour m'avoir confier les tâches d'auxiliaire d'enseignement mais aussi pour sa bonne humeur et ses anecdotes.

Enfin je tiens à remercier du fond du cœur ma famille qui m'a toujours soutenue et encouragée à supporter les distances nous séparant. Un merci spécial à mon conjoint, Mehdi, qui a pu supporter mon caractère durant la rédaction.

Finalement, pour celui qui m'a quitté physiquement depuis mes huit ans, mais qui m'a toujours accompagnée dans toutes mes décisions, à toi Papa, je dédie mon travail.

TABLES DES MATIÈRES

LISTE DES ABRÉVIATIONS

2,4-D	acide 2,4-dichlorophénoxyacétique
ADN	acide désoxyribonucléique
AFM	« Atomic Force Microscopy »
any1	*«anisotropy 1»*
CeSA	cellulose synthase
CoIP	co-immunoprécipitation
CSI	« Cellulose Synthase Interactive »
CSC	« Cellulose Synthase Complexe »
DCB	dichlobénile
GDP	guanosine di-phosphate
GTP	guanosine tri-phosphate
HG	homogalacturonanes
HR	réponse hypersensible
IAA	acide indole acétique
IXB	isoxabène
MAPK	protéine kinase active par des mitogènes
MCP	mort cellulaire programmée
NMR	résonnance magnétique nucléaire
PAL	phenylalanine ammonia-lyase

PDF	défensine végétale
PR1	«Pathogenesis related-1»
RG-I	rhamnogalacturonanes I
RG-II	rhamnogalacturonanes II
RH	réponse hypersensible
ROS	espèces réactives à l'oxygène
RSW	« Radial swelling»
TA	thaxtomine A
txr	*Thaxtomin-resistant*
MPa	mégapascal
µm	micromètre
µM	micromolaire
nM	nanomolaire

LISTE DES FIGURES

LISTE DES TABLEAUX

CHAPITRE 1

INTRODUCTION GÉNÉRALE

1.1 La paroi

Les cellules végétales présentent plusieurs spécificités, dont la paroi pectocellulosique, qui confère à la cellule sa forme et sa fonctionnalité tout en la protégeant des stress courants et permettant ainsi la survie des plantes face aux agents phytopathogènes et aux facteurs environnementaux. Presque toutes les cellules végétales ont une paroi primaire, quelques-unes possèdent une paroi secondaire qui ajoute de la rigidité à ces cellules. La paroi primaire est dotée d'une grande adaptabilité pour pouvoir répondre aux besoins de la cellule. C'est grâce aux composantes de la paroi qu'on est capable de produire du textile (ex : coton, lin), des biocarburants, de la papeterie et du bois. Il faut donc avouer que le progrès de la qualité de vie humaine est dû en partie à la paroi végétale dans toutes ses formes.

1.2 Les composants de la paroi

La paroi primaire est composée majoritairement de polysaccharides (cellulose, pectine et hémicellulose) ainsi qu'une faible portion de protéines. La paroi végétale se reconstitue dès la division des cellules. Lors de la division cellulaire, une plaque riche en pectine se forme entre les deux cellules-filles, qui deviendra la lamelle moyenne après la division. De même, une matrice extracellulaire composée de cellulose, d'hémicellulose et de pectine se forme à la frontière avec la membrane plasmique : c'est la paroi primaire. Dans certains types cellulaires comme les trachéides, une deuxième matrice se forme à l'intérieur de la paroi primaire qu'on appelle la paroi secondaire (Fig. 1.1).

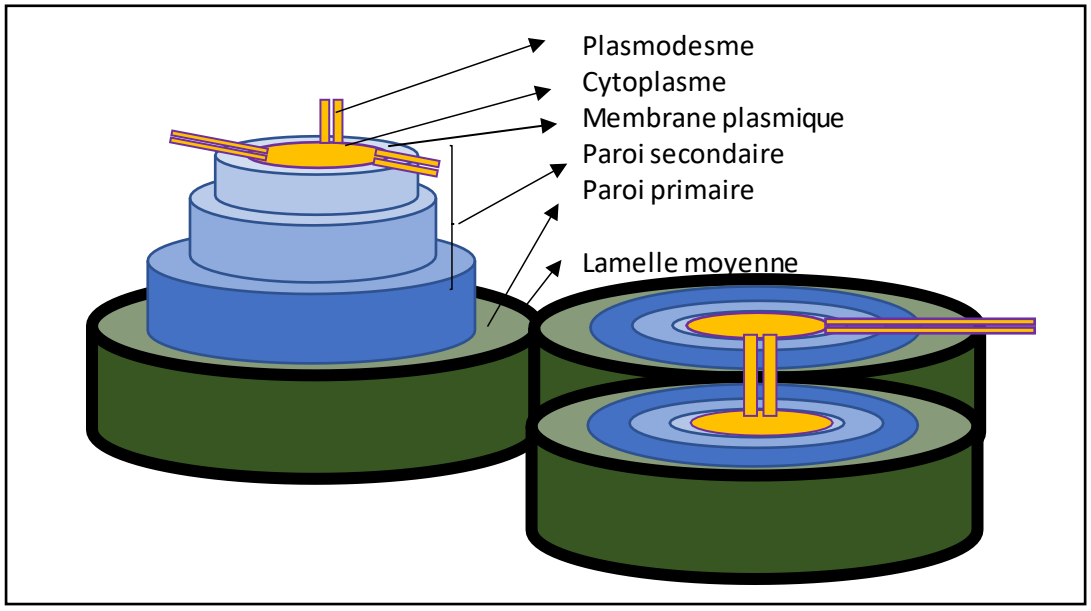

Figure 1.1 : Répartition des différentes couches de la matrice extracellulaire dans les cellules végétales. Le cytoplasme est délimité par une membrane plasmique (violet) caractérisée par la présence des plasmodesmes (communications intercellulaires), une ou plusieurs strates de la paroi secondaire (bleu), la paroi primaire (vert) et la lamelle moyenne (noir).

Il existe deux types de parois primaires : celle retrouvée chez les monocotylédones (type I) et celle chez les dicotylédones (type II). Elles diffèrent par la dominance de certains polysaccharides. La paroi primaire de type I est plus riche en pectine que celle de type II, qui elle est riche en phénylpropanoïdes et contient moins de xyloglucanes que de cellulose (Yokoyama and Nishitani, 2004). L'épaisseur de la paroi varie entre 0,1 µm et 10 µm (Fry, 2001). Cette variabilité dépend de l'espèce, du type cellulaire et des liaisons entre les différents constituants de la paroi (Fig. 1.2).

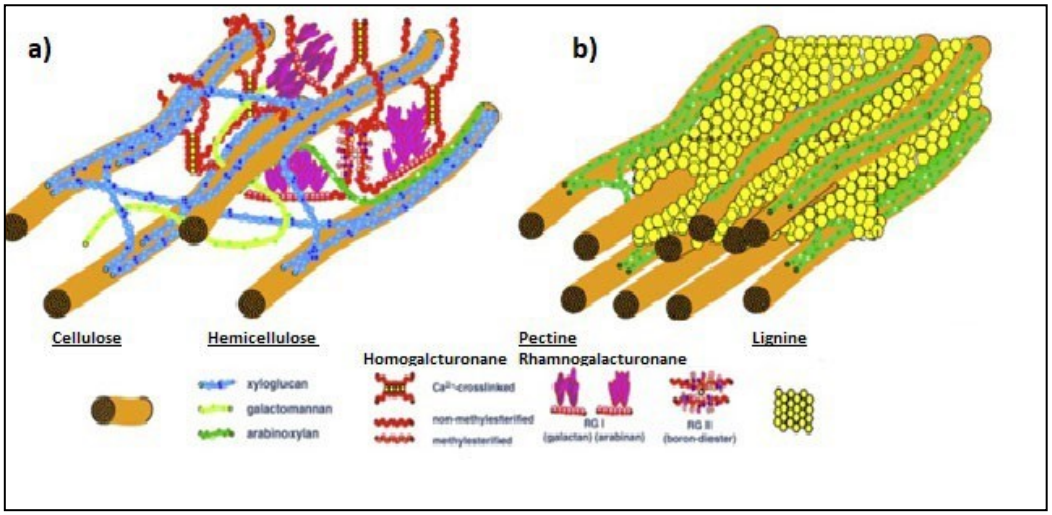

Figure 1.2 : Modèle schématique de la composition de la paroi primaire (a) et secondaire (b). Adaptée de Loqué, 2015.

1.2.1 Les protéines de la paroi

Les protéines de la paroi sont très diversifiées. Seulement chez la plante modèle *Arabidopsis thaliana*, on compte plus que 500 protéines dans la paroi qui sont exprimées avec des patrons tissu/cellule-spécifiques. Le quart de ces protéines sont des protéines qui agissent sur des polysaccharides, 15% sont des oxydoréductases, 12% des protéases, et le reste sont des protéines avec des domaines actifs, impliquées dans la signalisation ou à fonction inconnue pour la majorité (Francoz et al., 2015). Parmi ces protéines se trouve une grande famille de peroxydases de classe III (Fig. 1.3), qui peuvent agir directement sur la rigidité ou le ramollissement de la paroi primaire. Certaines enzymes de la membrane plasmique et de la paroi produisent dans l'apoplasme des espèces réactives de l'oxygène (ROS) tels que l'ion superoxyde ($O_2^{\cdot-}$), le peroxyde d'hydrogène (H_2O_2), l'oxygène singulet ($^1O_2$), et le radical hydroxyle ($^{\cdot}OH$). L'anion superoxyde $O_2^{\cdot-}$ est dismuté en H_2O_2 par la superoxyde dismutase, ou par l'acidité de la paroi. Les ROS jouent un rôle majeur dans le ramollissement de la paroi durant l'élongation cellulaire mais aussi durant l'inhibition de l'élongation. Parmi les enzymes de la paroi impliquées dans la formation de ROS, on retrouve les peroxydases de la classe III

qui sont capables de générer des ROS tels que ˙·OH et HOO· et de réguler le niveau de peroxyde d'hydrogène (H_2O_2). Ainsi, elles jouent un rôle central dans la croissance cellulaire en contrôlant l'équilibre entre le relâchement de la paroi cellulaire (via ·OH et HOO·) et la synthèse *de novo* de la paroi cellulaire ou son renforcement (via H_2O_2; Francoz et al., 2015, Kärkönen et Kuchitsu, 2015) .

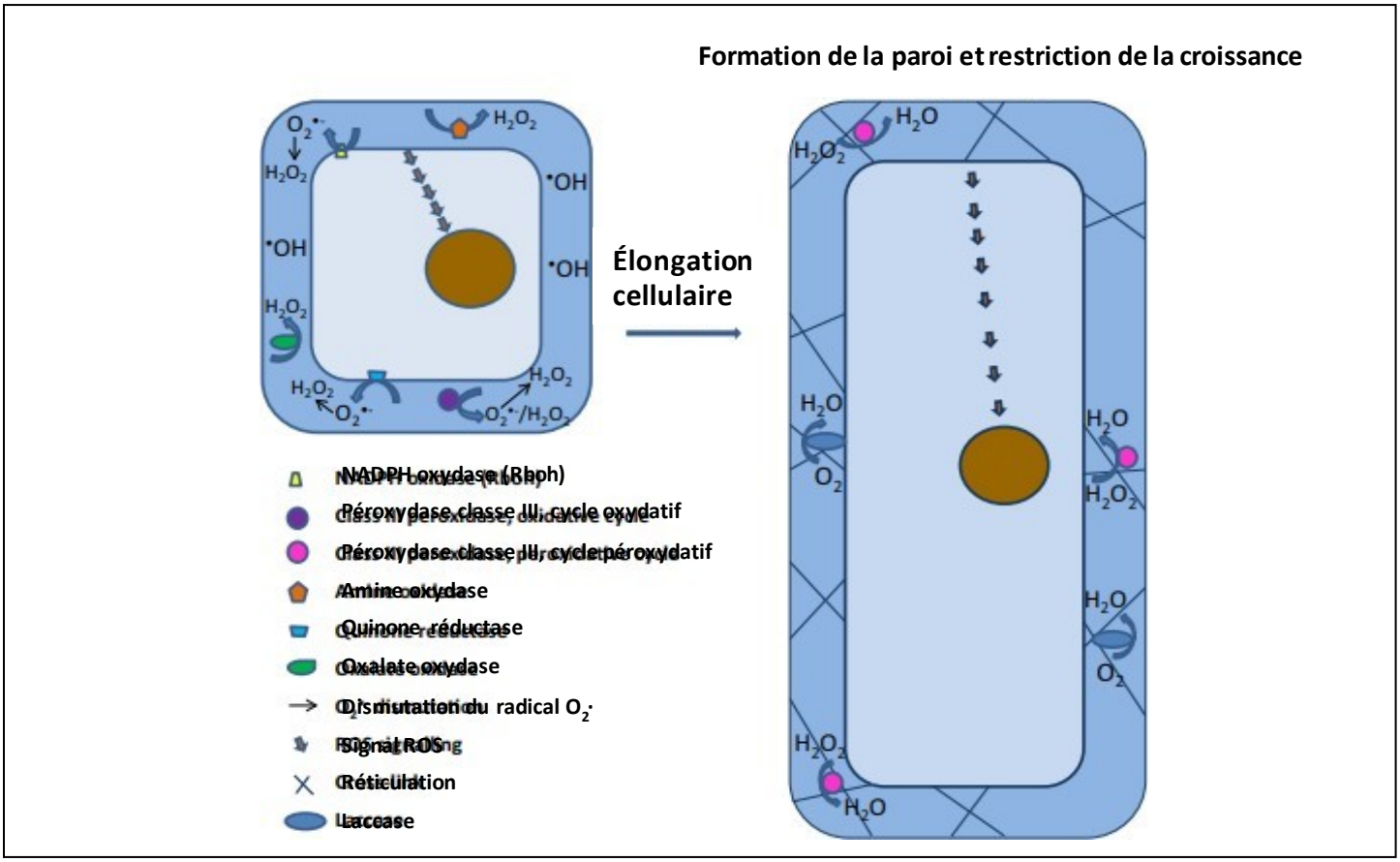

Figure 1.3 : Importance des péroxydases de classe III dans l'élongation cellulaire et la formation de la paroi. Les péroxydases de la paroi interviennent dans un cycle oxydatif ou péroxydatif agissant sur la concentration des espèces réactives à l'oxygène (ROS: l'anion superoxyde (O_2·-), le peroxyde d'hydrogène (H_2O_2), et le radical hydroxyle (**.**OH)), régulant ainsi le relâchement ou le durcissement de la paroi. (Adaptée de Kärkönen and Kuchitsu, 2015).

1.2.2 Les sucres de la paroi

La paroi primaire est dite pectocellulosique et contient majoritairement trois types de polymères de sucres : la cellulose, un homopolymère de glucose lié en β-(1→-4); l'hémicellulose, un hétéropolymère formé de plusieurs sucres comme les glucomannanes, les xylanes et les arabinogalactanes; et la pectine dont la chaîne prinicipale est composée des homogalacturonanes et qui joue un rôle important dans la viscoélasticité de la paroi (Chebli et Geitmann, 2017). La cellulose confèreà la paroi une rigidité avec ses microfibrilles plus ou moins cristallines. La fonction, synthèse et importance de la cellulose et des pectines seront discutées plus loin.

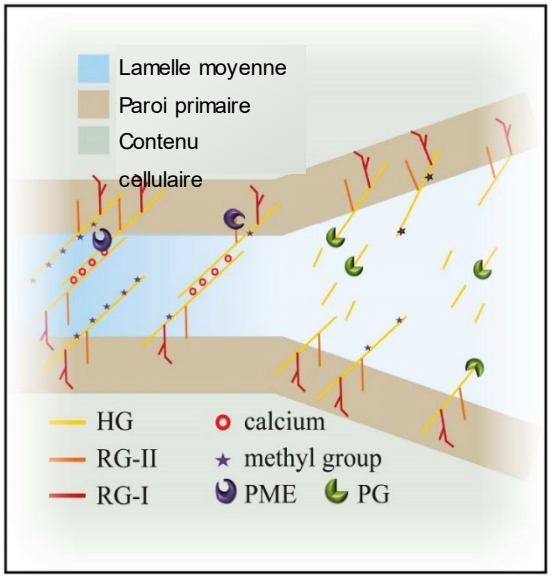

Figure 1.4 : Modèle de l'adhésion et de la séparation cellulaire. La liaison entre les polymères de pectines dé-estérifiées maintient l'adhésion cellulaire au niveau de la lamelle moyenne. Les polygalacturonases sont des enzymes qui ciblent les pectines dé-estérifiées et dégradent ainsi les liens en menant à la séparation des cellules. HG: homogalacturonane; RG: rhamanogalacturonane; PME: pectine méthyl-estérase; PG: polygalacturonase. (Adaptée de Daher et Braybrook, 2015).

1.2.2.1 La cellulose

La cellulose est le biopolymère le plus abondant sur terre. Sa production annuelle est de 10^{10}-10^{11} tonnes (Hon, 1994). La cellulose constitue environ 30% de la paroi primaire et 60% de la paroi secondaire chez les plantes, où sa structure est nettement plus cristalline (Meents et al., 2018). Les chaines de glucanes formant la cellulose sont reliées entre elles par des liaisons Van der Waals, ainsi que des liens hydrogènes inter- et intramoléculaires (Kim et al., 2013). Malgré son importance dans les fonctions des parois primaire et secondaire, la compréhension de l'assemblage et du degré de cristallinité de la cellulose reste faible. L'étude de la synthèse de la cellulose a évolué depuis 1972 grâce aux avancées génomiques et en microscopie qui ont permis d'identifier et de caractériser les protéines responsables de cette synthèse : les cellulose synthases.

1.2.2.2 Les complexes de cellulose synthase

La cellulose est synthétisée au niveau de la membrane plasmique par des celluloses synthases (CeSA ; McFarlane et al., 2014). La première CeSA a été découverte chez le coton (Pear et al., 1996). Les complexes de CeSA (CSC) sont assemblés en rosette, tel qu'observé pour la première fois en 1980 via la microscopie électronique par cryofracture des portions de la membrane plasmique (Mueller et Brown, 1980). De même que les avancées de la microscopie, l'analyse des mutants d'*Arabidopsis* a permis de comprendre plusieurs éléments impliqués dans la synthèse de la cellulose. Le mutant *radial swelling 1* ou *rsw1,* par exemple, est un mutant de *CeSA1* dont le contenu de cellulose dans la racine est compromis à température restrictive (31°C). La caractérisation de ce mutant a montré que la conformation en rosettes joue un rôle important dans l'assemblage de la cellulose (Williamson et al., 2001).

Chaque CSC contient trois isoformes de CeSA. Des expériences de co-immunoprécipitation (CoIP) ont démontré que lorsque l'expression de l'un des trois *CeSA* est réprimée et que la production d'une des protéines isoformes CeSA est abolie, le complexe CSC n'est plus détecté, les deux autres protéines CeSA n'interagissent plus et s'accumulent à des niveaux inférieurs à ceux trouvés dans la plante de type sauvage. Ceci a été observé autant pour les CeSA des parois primaires (Desprez et al., 2007) que celles des parois secondaires (Taylor et al., 2003). Les expériences de Western Blot et de CoIP suivies d'une analyse en spectrométrie de masse suggèrent que les trois classes de CeSA dans un complexe ont un rapport stœchiométrique de 1: 1: 1 (Hill et al., 2014). Les chercheurs ont proposé plusieurs modèles de CSC, la majorité proposant qu'il y aurait 36 CeSA par complexe CSC (Cosgrove, 2005). Par contre, on sait aujourd'hui que les complexes sont regroupés en rosette contenant 18 ou 24 CeSA de trois isoformes différents (Nixon et al., 2016; Oehme et al., 2015).

Tel que mentionné plus haut, le mutant *rsw1* poussé en condition de température restrictive montre une baisse de production de cellulose corrélant avec la perte de la conformation des rosettes de CSC dans la membrane plasmique (Arioli et al., 1998). Bien que cette conformation ait montré son importance dans différentes plantes, il est important de signaler qu'elle n'a pas été observée dans certaines espèces comme le coton (Kumar et Turner, 2015).

Dans les parois primaires, CeSA1 et CeSA3 forment les CSC de la paroi primaire chez *Arabidopsis thaliana*, en plus des CeSA2, 5, 6 ou 9 ; pour la paroi secondaire les CSC sont formés par CeSA4, 7 et 8 (Kaur et al., 2016). Chacun des isoformes des CSC est capable, d'un point de vue catalytique, de synthétiser seul la chaîne de glucose en β-(1→4) (Purushotham et al., 2016). La plupart des mutants de *CeSA* présentent du nanisme et un manque de structure, ce qui montre l'importance de la rigidité conférée par la cellulose dans l'établissement de la forme cellulaire. Dans les plantules d'*Arabidopsis thaliana*, la vélocité des CeSA est d'environ 300 nm min^{-1}, ce qui signifie que chaque chaine de glycanes est allongée de 10 nouvelles unités de glucose par seconde. L'imagerie des CeSA couplées à des protéines fluorescentes offre la possibilité de voir en détails le comportement des CeSA en différentes conditions (Kumar et Turner, 2015; McFarlane et al., 2014; Morgan et al., 2016)

La purification des cellulose synthases des plantes n'ayant pas été possible jusqu'à date, les chercheurs se servent donc des CeSA retrouvées chez certains genres bactériens (comme *Glucoacetobacter, Agrobacterium* et *Rhizobium*) pour comparer et élucider la structure et les domaines des CeSA végétales (Kumar et Turner, 2015). L'hélice multi-domaine des CeSA bactériennes joue un rôle essentiel dans la stabilisation des complexes chez les bactéries même si la synthèse de la cellulose en tant que tel n'a besoin que d'une faible portion protéique (Morgan et al., 2012). Ceci suggère la présence de partenaires protéiques ayant un rôle similaire chez les plantes. La source d'UDP-glucose dont les CeSA ont besoin pour la synthèse de la cellulose est assurée par l'association entre le partenaire protéique comme Sucrose Synthase SuSy et les CeSA dans le phloème et d'autre invertases dans les autres tissus (Almagro et al., 2012; Amor et al., 1995).

Le séquençage du génome d'*Arabidopsis* a permis l'identification de 10 gènes codant pour des isoformes CeSA1 à CeSA10 (Richmond et Somerville, 2000). La structure des CeSA (Fig.1. 5) chez les plantes compte un domaine cytoplasmique du côté N-terminal contenant une région riche en cystéine qui inclurait des motifs proposés pour l'interaction avec d'autres CeSA (Doblin et al., 2002). Ensuite, on trouve un noyau de deux domaines transmembranaires (TMD) mesurant 68 acides aminés, et un domaine centrale cytoplasmique ayant une activité β-glycosyltransférase et contenant des motifs D,D,D,QxxRW très conservés (Pear et al., 1996). Ce domaine central contient aussi d'autre régions assez conservées entre les différents isoformes de CeSA, qu'on appelle les régions classe-spécifique (« class-restricted » CR) représentées en vert dans la Fig. 1.5 (Vergara et Carpita, 2001). Il existe également un autre groupe de domaines transmembranaires (6 TMD prédits, 226 à 228 acides aminés, en noir dans la Fig. 1.5) et un petit domaine cytoplasmique du côté C-terminal (CT), qui s'est avéré important dans la production de cellulose pour CeSA3 (Wang et al., 2006).

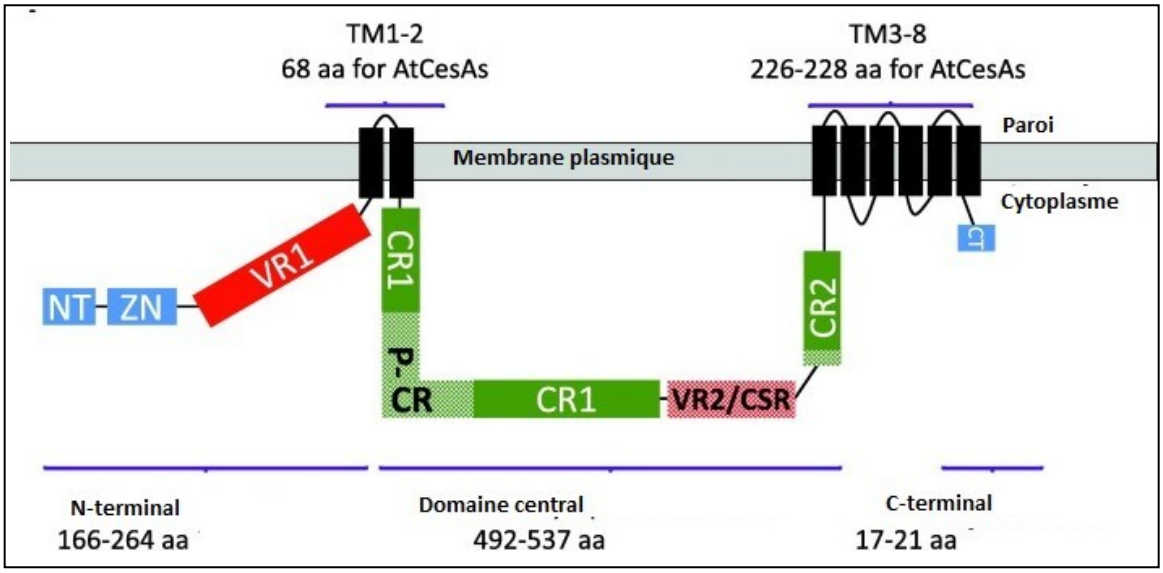

Figure 1.5 : Structure des cellulose synthase CeSA chez les plantes supérieures. (Adaptée de Kumar et Turner, 2015)

1.2.2.3 Le rôle des microtubules dans la synthèse de la cellulose

Le cytosquelette des cellules végétales est formé de filaments d'actine et des microtubules. Les deux sont formés par la polymérisation de leurs sous-unités et peuvent former plusieurs associations protéiques. Ce cytosquelette joue un rôle important dans l'acheminement des protéines et sucres requis pour la synthèse de la cellulose et des protéines associées.

Les microtubules, découverts en premier chez les plantes, sont des polymères dynamiques formés d'α et de β-tubulines arrangées dans 13 sous-unités. Ces microtubules et les protéines associées aux microtubules (MAP) jouent un rôle important à plusieurs niveaux, que ce soit durant la division cellulaire ou l'ouverture des stomates ou encore lors de la synthèse de la cellulose et de l'expansion cellulaire (Buschmann et Lloyd, 2008; Hashimoto, 2015). Les microtubules contrôlent ces aspects par leur capacité à ajouter un hétérodimère, donc à se polymériser ou à se dépolymériser. Le côté le plus dynamique en polymérisation et dépolymérisation des microtubules s'appellent le côté « + end ». En revanche, le côté « - end » subit moins les deux phénomènes (Ehrhardt et Shaw, 2006; Wasteneys et Ambrose, 2009). Le

côté '+ end' se termine par une β-tubuline qui va se lier à une α-tubuline du prochain dimère (Sedbrook et Kaloriti, 2008).Les α- et β-tubulines se lient à la guanosine triphosphate (GTP), mais cette liaison aboutit à un résultat différent dans chacune des sous-unités. La liaison entre le GTP et l'α-tubuline se situe à l'interface avec l'intradimère, ce qui augmenterait la stabilité du complexe (Menéndez et al., 1998). La liaison GTP - β-tubuline va mener à l'hydrolyse de la GTP en guanosine diphosphate (GDP) en déstabilisant les liens entre les tubulines, comme le montre la Fig.1.6. Les liens GTP- β tubulines stabilisent les protofilaments et permettent l'obtention d'une orientation précise droite (Alushin et al., 2014). Quand le lien du GTP avec la β-tubuline subit une hydrolyse après la polymérisation, le protofilament va se courber et changer de conformation ce qui augmente le désassemblage des microtubules (Drechsel et al., 1992). Les microtubules vont changer d'état selon les liens en passant par une croissance des microtubules, une pause de croissance ainsi qu'un rétrécissement, ces phases conférant aux microtubules leur importante instabilité dynamique, essentielle pour différentes fonctions biologique (Fig. 1.6; Dixit et Cyr, 2004).

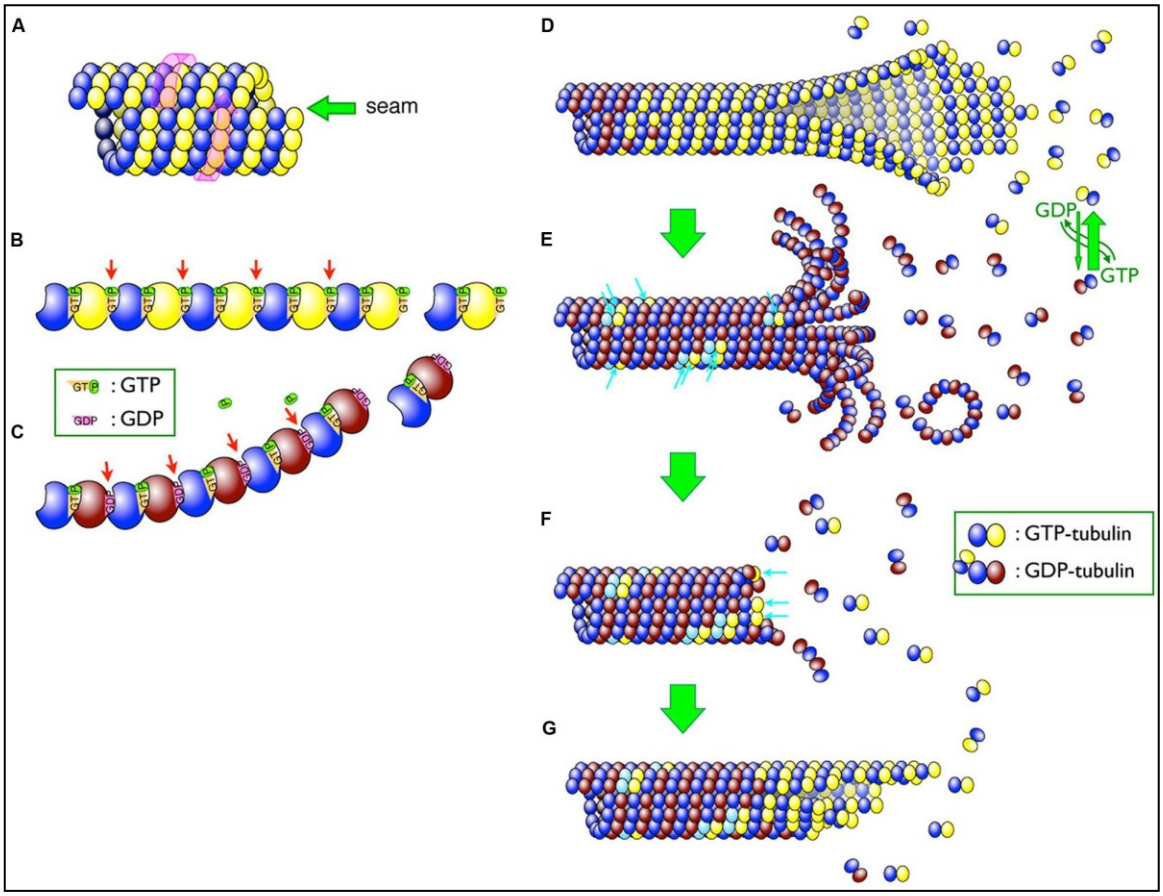

Figure 1.6 : L'instabilité dynamique des microtubules. (D'après Horio et Murata, 2014)

Les sous-unités d'un microtubule ont un sillon (*seam*, flèche verte) au niveau duquel la perturbation aura lieu (A). Les molécules de tubuline sont alignées latéralement le long de l'hélice à trois débuts avec rotation vers la gauche (flèche rose). (B, C) L'hydrolyse du GTP provoque un changement de conformation dans les protofilaments. La stabilité des GTP-tubulines (B) leur donne une direction fixe, alors que les GDP-tubulines (C) ont tendance à se courber vers l'extérieur, déstabilisant ainsi le microtubule. Les liaisons entre le GDP et β-tubuline sont en brun, celles avec la GTP sont en jaune. (D-G) Dépolymérisation et sauvetage des microtubules. La tubuline nouvellement ancrée est formée de GTP-tubuline (D), les molécules GTP-tubuline sont hydrolysées assez rapidement et la plupart des dimères du microtubule deviennent GDP-tubuline (ombrée en brun ; D) les GTP-tubulines restantes dans les microtubules sont indiquées par la flèche bleu (E). Les GTP-tubulines restantes peuvent faire le sauvetage et arrêter la dépolymérisation. (F). L'ajout de nouvelles molécules GTP-tubuline (flèches bleues dans F) mène à la reprise de la croissance, et à l'ajout des dimères de tubuline en continu (G).

Le rôle le plus important des microtubules, dans le cadre de cette étude, est sans doute le lien des microtubules avec les celluloses synthases. Les microtubules assurent le positionnement des CeSA dans la membrane plasmique et guident leurs mouvements, contrôlant ainsi l'expansion cellulaire (Gutierrez et al., 2009; Li et al., 2012). La perturbation des microtubules mène à des changements dans la vitesse du mouvement des CSC, et ainsi, affecte la cristallinité de la cellulose néo-produite (Fujita et al., 2011, 2013). Les celluloses synthases se lient aux microtubules grâce à des protéines comme la Cellulose Synthase Interactive 1 (CSI1, Fig. 1.7) et aux MAP (Endler et al., 2015; Lei et al., 2013; Li et al., 2012). Le lien exact et les étapes de guidage des CSC par les microtubules ne sont pas totalement élucidés.

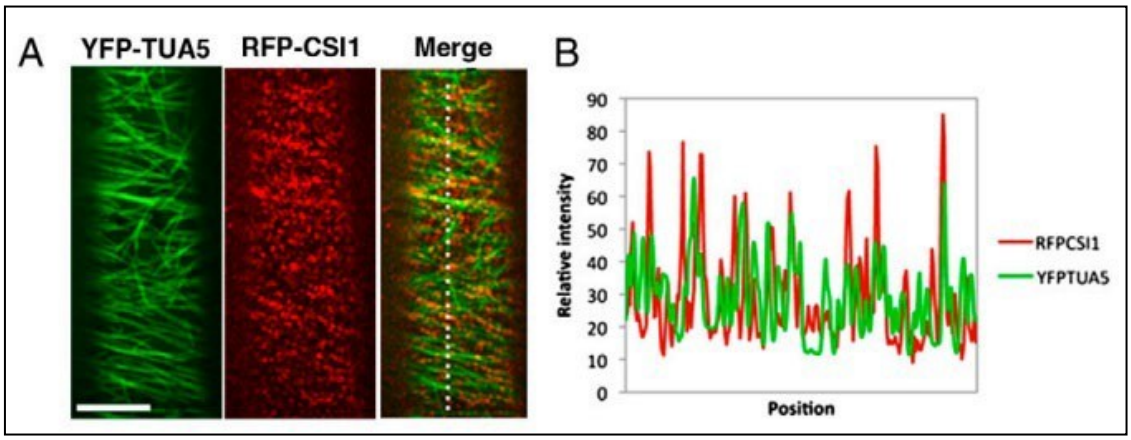

Figure 1.7 : Cellulose Synthase-Interactive 1 co-localise avec les microtubules corticaux.

(A) Image en microscopie confocale des cellules épidermiques de l'hypocotyle étiolé des plantules âgées de 3 jours et exprimant la tubuline avec la protéine jaune fluorescente (YFP-TUA5) et la protéine Cellulose Interactive 1 avec la protéine rouge fluorescente (RFP-CSI1). (Échelle = 5 µm.) (B) Corrélation entre la localisation de YFP-TUA5 et RFP-CSI1 (Li et al., 2012).

1.2.2.4 Les pectines

Les pectines forment un groupe de polysaccharides composé de résidus d'acides d-galacturoniques liés en α-1,4. Ces résidus peuvent être classés en homogalacturonanes (HG)

synthétisés au niveau du Golgi et en rhamnogalacturonanes (RG-I et RG-II) assemblés au niveau de la membrane plasmique (Atmodjo et al., 2013). Les pectines peuvent être méthylestérifiées au niveau des homogalacturonanes. D'ailleurs, le niveau de méthylestérification/acétylation dicte le niveau d'élasticité de la paroi (Levesque-Tremblay et al., 2015; Voiniciuc et al., 2018). Les différentes pectines interagissent entre elles par des liaisons covalentes et par le biais du calcium (Fig. 1.4), jouant ainsi un rôle important dans la distance entre les cellules adjacentes (Daher et Braybrook, 2015).

1.2.2.5 Liens entre les composants de la paroi

La matrice formée par les polysaccharides de la paroi et les protéines qui y sont associées est dynamique. Bien que les liens entre ces composants ne soient pas tout à fait élucidés, les études par résonnance nucléaire magnétique (NMR) et par microscopie électronique par balayage à émission de champ (FESEM), avec des combinaisons de traitements enzymatiques des débris de la paroi, ont permis d'étayer quelques hypothèses et d'en rejeter d'autres. On pensait que les hémicelluloses, plus particulièrement les xyloglucanes étaient essentiellement responsables des liens entre les microfibrille de cellulose d'une part et des pectines d'autre part. Mais récemment, cette théorie a été rejetée pour deux causes principales. Premièrement, l'analyse du double mutant d'*Arabidopsis* ne produisant aucune xyloglucane (*xxt1/xxt2*) a révélé que les liens entre les microfibrilles de cellulose se font même en absence de la majeure partie des hémicelluloses (Park et Cosgrove, 2012). Deuxièmement, les expériences effectuées en NMR montrent moins de liens cellulose-hémicellulose que prédit, mais une plus grande abondance de liaisons entre les pectines et les celluloses (Wang et al., 2015). On sait alors que les microfibrilles sont liées entre elles par des liaisons non-covalentes qui peuvent être détruites par des protéines de la paroi comme les expansines quand la cellule a besoin de croître (Wang et al., 2015).

1.3 L'importance de la paroi

Il existe 35 types différents de cellules végétales qui se caractérisent par des formes et fonctions variées. Cette diversité est due en grande partie aux différences retrouvées dans la composition de la paroi de ces types cellulaires (Cosgrove, 2005). Par exemple, la paroi pectocellulosique est fine et malléable dans les cellules en pleine croissance, permettant à ces cellules de remodeler leur forme et leur élongation, mais la paroi peut durcir et former une sorte de corset cellulaire rigide pendant la différenciation de certains types cellulaires (Cosgrove, 2016; Oda et al., 2005)

1.3.1 Le rôle de la paroi dans le développement

Le rôle de la paroi dans le développement peut se résumer en trois facteurs : la permission de l'élongation et de la division cellulaire, le rôle de la paroi dans la différenciation, et l'adaptabilité de la paroi dans les cellules avec un besoin continu de croissance.

En ce qui concerne l'élongation et la division cellulaire, la cellule végétale est encaissée dans sa paroi visco-élasto-plastique. Sans les modifications de cette dernière, aucune expansion ne peut avoir lieu (Chebli et Geitmann, 2017). Le matériel constituant la paroi peut s'étendre pour former une matrice plus lâche et permettre l'élongation, mais ceci n'est pas suffisant. La synthèse *de novo* des polymères de la paroi est donc nécessaire pour augmenter sa surface et ainsi permettre à la cellule de croître. Une preuve évidente de ce fait est l'activité continue des protéines cellulose synthase dans les cellules des hypocotyles étiolés (en croissance continue) par rapport aux cellules matures (Paredez et al., 2006).

Concernant la modification de la paroi pendant la différenciation des cellules, l'exemple le plus évident est observé chez les cellules vasculaires. Dans ces cellules, une déposition de la paroi secondaire est nécessaire pour activer une mort cellulaire programmée et mener à la différenciation et la fonctionnalité des cellules (Fukuda, 2004). La formation de la paroi

secondaire permet également chez certains types cellulaires (ex : fibres, sclérenchyme) la production d'autres polymères ayant une grande importance industrielle comme les fibres de coton et de lin (Kim et Triplett, 2001; Oda et al., 2005).

Finalement, l'adaptabilité de la paroi joue un rôle particulièrement important dans les cellules qui ont un besoin continuel d'élongation ou de réorientation, comme les poils absorbants, les trichomes et le grain de pollen. Ces types cellulaires nécessitent un remodelage continuel de la paroi cellulaire pour ajuster la forme et l'expansion des cellules. La paroi dans ces cellules est très dynamique et répond aux besoins de la cellule en se rigidifiant dans certaines fractions et se ramollissant dans d'autre (Fig. 1.8).

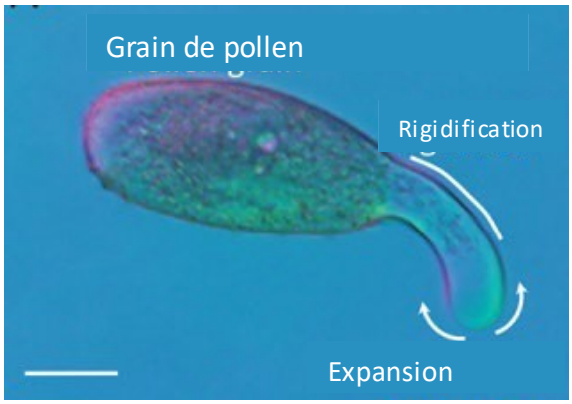

Figure 1.8 : Germination du grain de pollen. La ligne blanche indique les lieux de rigidification et les lignes avec des flêches indiquent d'expansion de la paroi au niveau du bout du tube de pollen en pleine formation (Adaptée de Gilroy, 2017).

Dans tous ces scénarios, l'adaptabilité de la paroi est due à un signal intracellulaire modifiant la vitesse de synthèse de cellulose ou l'état de méthyl estérification de ses pectines. Selon le concept de Ray, le ramollissement et l'extension de la paroi dépendent de deux constantes K1 et K2 (Fig. 1.9; Cosgrove, 2016). Le changement de la viscoélasticité est en lien avec l'absorption de l'eau, le changement de la taille de la vacuole d'un côté, ou la relaxation du stress et la rigidification d'autre côté (Cosgrove, 2005).

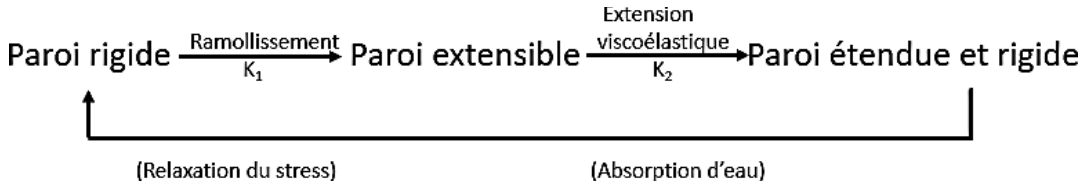

Figure 1.9: Concept de Ray de la réponse de la paroi au besoin de s'étendre. Le ramollissement et l'extension dépendent de deux constantes K1 et K2, qui diffèrent selon le type de la cellule et la composition de base de la paroi. (Adapté de Cosgrove, 2016).

1.3.2 Le rôle de la paroi dans la protection

Il est évident que la capacité de la paroi végétale à former une barrière physique et mécanique lui permet de jouer un rôle central dans la protection du cytosol contre les agressions externes. Mais le rôle de la paroi ne se résume pas à ceci, puisque les interactions entre la paroi et le milieu intracellulaire dépassent la définition de la paroi comme étant un exosquelette de la cellule. On peut classer les modes de protection en trois catégories : la biomécanique de la paroi et sa rigidité, les protéines de la paroi et leurs rôles signalétiques, et la dynamique de la paroi qui lui permet de s'adapter pour répondre aux agressions.

Par exemple, le traitement des plantes avec un éliciteur fongique peut induire une réponse de défense rapide qui est due en partie aux protéines riches en proline de la paroi. Les cellules végétales impliquées dans la réponse à l'éliciteur activeront une flambée oxydative au niveau du cytosol induisant un épaississement de la paroi. La mise en place d'un mécanisme similaire empêchera l'entrée de l'haustorium des agents phytopathogènes dans la cellule végétale (Bradley et al., 1992).

Les plantes possèdent différents mécanismes pour détecter l'invasion des agents pathogènes. Ces derniers secrètent des composés reconnus par les plantes grâce aux motifs moléculaires associés aux agents pathogènes (PAMP) qui peuvent être reconnus par des récepteurs membranaires, activant ainsi une cascade menant à la défense. Les plantes peuvent aussi détecter les changements dans l'intégrité de la paroi des cellules suite à sa dégradation par les enzymes des agents phytopathogènes (cellulase, xylanase, etc.). Cette reconnaissance active également la réponse immunitaire de la plante afin de survivre. Les réponses cellulaires aux PAMP tels que la flagelline 22 (flg22) ou la chitine sont très similaires aux réponses induites par la perturbation de la paroi cellulaire. Dans les deux cas, on observe la production des ROS, l'augmentation de la lignification ectopique ou de déposition de callose (Hématy et al., 2009).

Dans d'autres cas, la reconnaissance des molécules des agents pathogènes et des enzymes qui dégradent la paroi végétale ainsi que la pression mécanique appliquée par les champignons phytopathogènes au niveau de la paroi végétale activent la transduction d'un signal, la formation des microdomaines lipidiques et l'adhésion entre la paroi et la membrane plasmique (Fig.1. 10). Ainsi, la réorganisation du cytosquelette a lieu, accompagnée d'une production de métabolites secondaires et de peptides antifongiques, ce qui activera plusieurs mécanismes de défense chez la plante incluant la déposition de callose et l'inhibition des enzymes de dégradation de la paroi (Hématy et al., 2009; Hückelhoven, 2007).

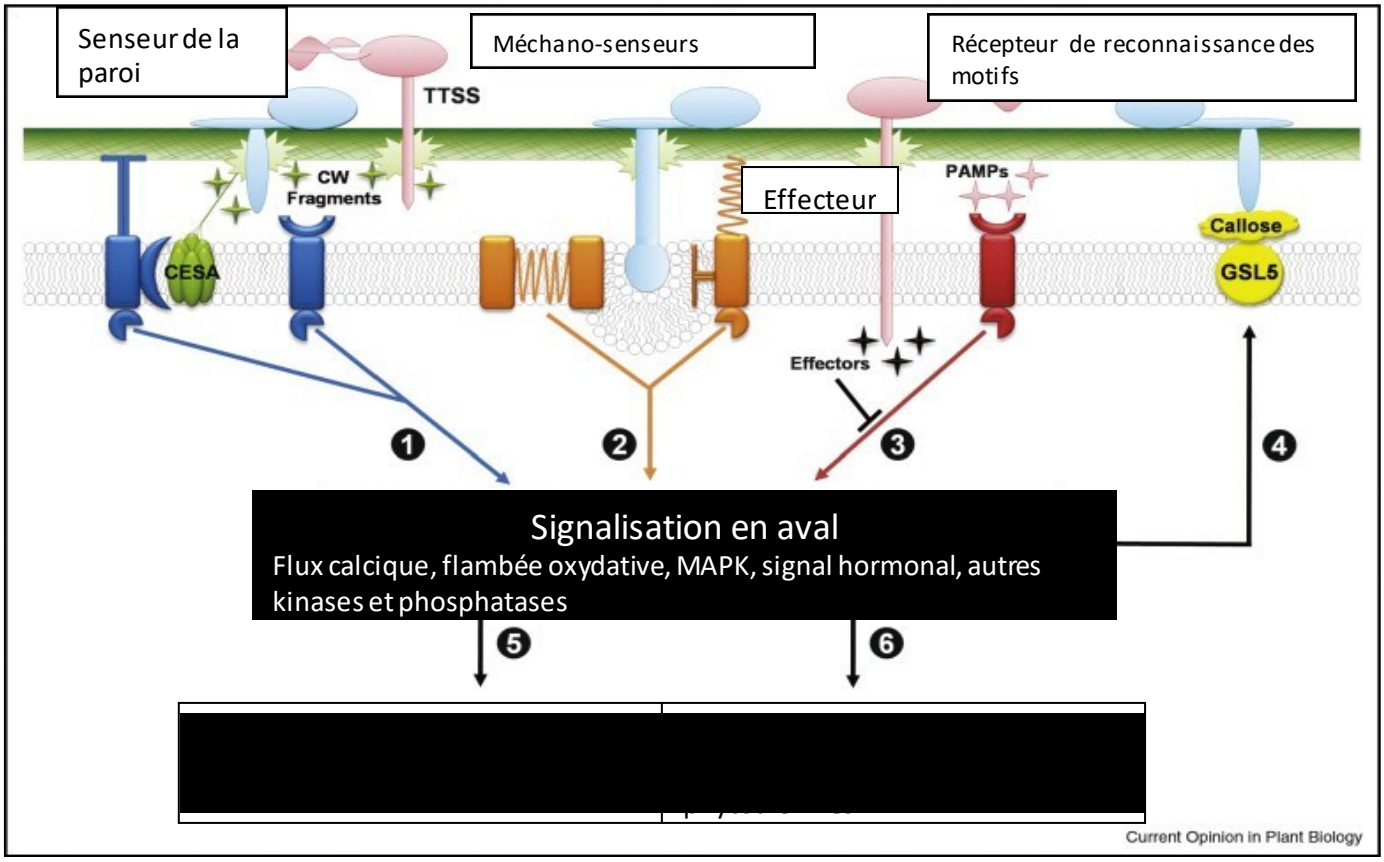

Figure 1.10 : Schématisation des composants de la signalisation cellulaire en réponse à une attaque pathogène. La cellule végétale perçoit les fragments de la paroi (CW fragment = étoile verte) ou les motifs moléculaires associés au pathogène (PAMP = étoiles roses). Chacun des ligands activent un récepteur spécifique qui, à son tour, active une cascade de signalisation en aval (Adaptée de Hématy et al., 2009).

De même, la paroi subit des changements en réponse aux changements environnementaux. Par exemple, durant un stress hydrique chez le blé, les pectines de la paroi subissent des modifications dans leur abondance et dans la longueur des chaines de rhamnogalacturonane I et II afin de limiter l'effet de la sécheresse (Leucci et al., 2008). D'un autre côté, la perception

du stress abiotique au niveau de la paroi implique différentes familles des 'receptor-like kinase' dont la plupart vont percevoir les changements extracellulaires au niveau de la paroi puis activer des messagers secondaires tel les espèces réactives à l'oxygènes (ROS) ou interagir avec d'autre molécules signal ou vont directement phosphoryler certains facteurs de transcription (Doblin et al., 2014; Tenhaken, 2015).

La paroi joue donc un rôle essentiel dans la perception des stresses biotiques et abiotiques permettant la défense, l'adaptation et la survie des cellules végétales.

1.4 Les perturbations de la paroi

La protection fournie pas la paroi peut être compromise suite à différentes perturbations. Celles-ci peuvent être causées par des stresses physiques, par exemple une blessure. Elles peuvent aussi être causées par les enzymes de dégradation de la paroi secrétées par les herbivores et les agents phytopathogènes. Les perturbations pariétales peuvent être étudiées grâce à l'ajout d'inhibiteurs de synthèse de cellulose (CBI) aux plantes. C'est ce type d'approche qui nous intéresse dans le cadre de cette étude.

Une vaste majorité des CBIs synthétiques entrent dans la composition d'herbicides commerciaux. Les CBIs sont classées en trois groupes (Tableau 1) selon leur effet sur la densité des CeSA dans la membrane plasmique, l'immobilisation des CeSA, ou le changement de la direction des particules (Tateno et al., 2016). Ces composés ont participé à l'élucidation du mode d'action des CeSA grâce à l'imagerie en temps réel des cellules vivantes. Parmi les CBIs les plus connus sont le dichlobénil (DCB) et l'isoxabène (IXB).

Table 1.1 : Classification des inhibiteurs de synthèse de cellulose (modifié de Tateno et al., 2016)

Groupe	Effet	CBI	Références
Groupe I	Diminution de la densité des CSC dans la membrane plasmique	Isoxabène	Gutierrez et al., 2009
		Quinoxyphène	Harris et al., 2012
		AE F150944	Gutierrez et al., 2009
		CGA 325'615	Crowell et al., 2009
		Thaxtomin A	Bischoff et al., 2010
		Flupoxam	Kudo et al., 1999
		Triazofénamide	Heim et al., 1998
		CESTRIN	Drakaki et al., 2011
		Acetobixan	Xia et al., 2014
Groupe II	Arrêt du mouvement des CeSA dans la membrane	Dichlobénil	Sabba et al., 1999
		Indaziflam	Brabham et al., 2014
Groupe III	Modification de la trajectoire des CeSA dans la membrane	Morlin	DeBolt et al., 2007
		Cobtorin	Yomeda et al., 2007

Le CBI d'intérêt dans cette étude est la thaxtomine A (TA), une toxine secrétée par *Streptomyces scabies*, l'agent causal de la gale commune chez la pomme de terre. La TA est la toxine principale secrétée par la bactérie pathogène filamenteuse *S. scabies*. Elle a été isolée pour la première fois, par le laboratoire de King en 1989, dans les lésions de gale commune sur les tubercules de pomme de terre (King et al., 1989). C'est une molécule de la famille des indoles (Fig. 1.11) ayant un cycle dioxopipérazine (Duval et al., 2005). Chez la bactérie, les deux gènes *txtA* et *txtB* sont impliqués dans la synthèse de la thaxtomine A (Kers et al., 2004). De même, il a été démontré que la virulence de *S. scabies* est dépendante de la présence de certains composants des cellules de la plante (principalement la subérine et la cellulose), et que selon le milieu, les bactéries pourront produire environ 14 différentes cellulases qui

dégraderont la cellulose végétale. Un lien existe entre la production de ces cellulases et l'expression des gènes de synthèse de TA, mais le mécanisme précis est encore nébuleux (Padilla-Reynaud et al., 2015).

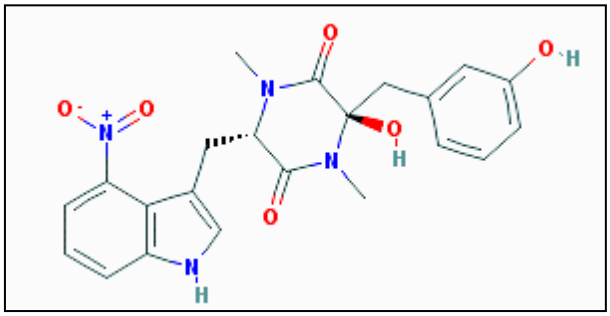

Figure 1.11 : Structure de la thaxtomine A. (Pubchem)

1.4.1 Les effets cellulaires et physiologiques de la thaxtomine A

La thaxtomine A est centrale dans la maladie de la gale commune. Ainsi, des *Streptomyces scabies* incapables de produire de la TA sont aussi incapables d'induire des lésions de gale à la surface des pommes de terre (Bignell et al., 2014). Cette toxine produit également différents effets chez d'autres tissus végétaux. Par exemple, un traitement des plantules d'oignon et de radis avec respectivement 50 et 500 nM de TA induit un retard de croissance ainsi qu'un gonflement des cellules (Fry et Loria, 2002).

De même, le traitement à la TA des cellules en suspension de tabac induit aussi le gonflement de ces cellules et la perte de la morphologie cellulaire. Ces aspects-là ont mené à croire que la cible de la TA est pariétale (Fry et Loria, 2002).

En 2003, l'équipe de Sommerville démontre que la TA inhibe l'incorporation de glucose marqué par l'isotope radioactif du carbone C^{14} dans la fraction cellulosique de la paroi. Pour expliquer cette inhibition de la synthèse de la cellulose, il a été proposé que les traitements à la TA inhiberaient la stabilité de CeSA3 au niveau de la membrane plasmique, ce qui diminuerait sa fonctionnalité et l'assimilation de carbone en cellulose (Bischoff et al., 2009).

Cette hypothèse a été appuyée par des résultats obtenus lors de la visualisation des effets de la TA sur les CSC au niveau de la membrane plasmique lors de la synthèse de la cellulose (Bischoff et al., 2003). Cette étude a montré que la TA perturbe la stabilité des CeSA3, tout en diminuant sa densité et sa présence dans la membrane plasmique (Bischoff et al., 2009). Cette équipe a aussi observé une baisse de l'expression des gènes qui codent pour les CeSA de la paroi primaire (Bischoff et al., 2009), démontrant que la TA ne perturbe pas uniquement les CeSA3.

Un mutant résistant à la thaxtomine A (*txr1*) a été identifié chez *Arabidopsis thaiana*. La mutation a été localisée sur le chromosome 3 (At3g58280) et la protéine codée par ce locus a été retrouvée dans le cytoplasme (Scheible et al., 2003). La fonction de cette protéine était inconnue, mais on a proposé qu'elle jouait le rôle d'un transporteur. Dernièrement, la protéine codée par *TXR1* a été à nouveau étudiée. Cette fois-ci, les chercheurs ont trouvé que le gène *TXR1* est allélique à *muse5*. Il s'agit d'un homologue de PAM16 de la levure *Saccharomyces cerevisiae* (PAM pour « pre-sequence translocase-associated protein import motor»). La protéine TXR1/MUSE5/PAM16 fonctionnerait comme régulateur négatif de l'immunité de la plante. Plus particulièrement, cette protéine serait responsable de la protection des cellules contre l'accumulation des ROS (Huang et al., 2013). La protéine TXR1/MUSE5/PAM16 a été localisée dans la membrane interne de la mitochondrie, contrairement aux énoncés précédents qui la localisait au niveau du cytoplasme (Huang et al., 2013; Bischoff et al., 2003)

Ces nouvelles informations ajoutent de la complexité au sujet et poussent à penser à des nouvelles pistes de protéines ciblées par les CBI tel que la TA.

1.4.2 La mort cellulaire programmée induite par la thaxtomine A

La mort cellulaire programmée (MCP) est un processus de grande importance chez les plantes pour sa nécessité dans le développement, la différenciation et la survie lors d'une défense (Fig.1.12). On distingue plusieurs types de MCP, mais généralement, les cascades signalétiques menant à la MCP impliquent un flux calcique, une fragmentation d'ADN, une

production de ROS et une activation des « Mitogen-Activated Protein Kinase» (MAPK; Van Hautegem et al., 2015).

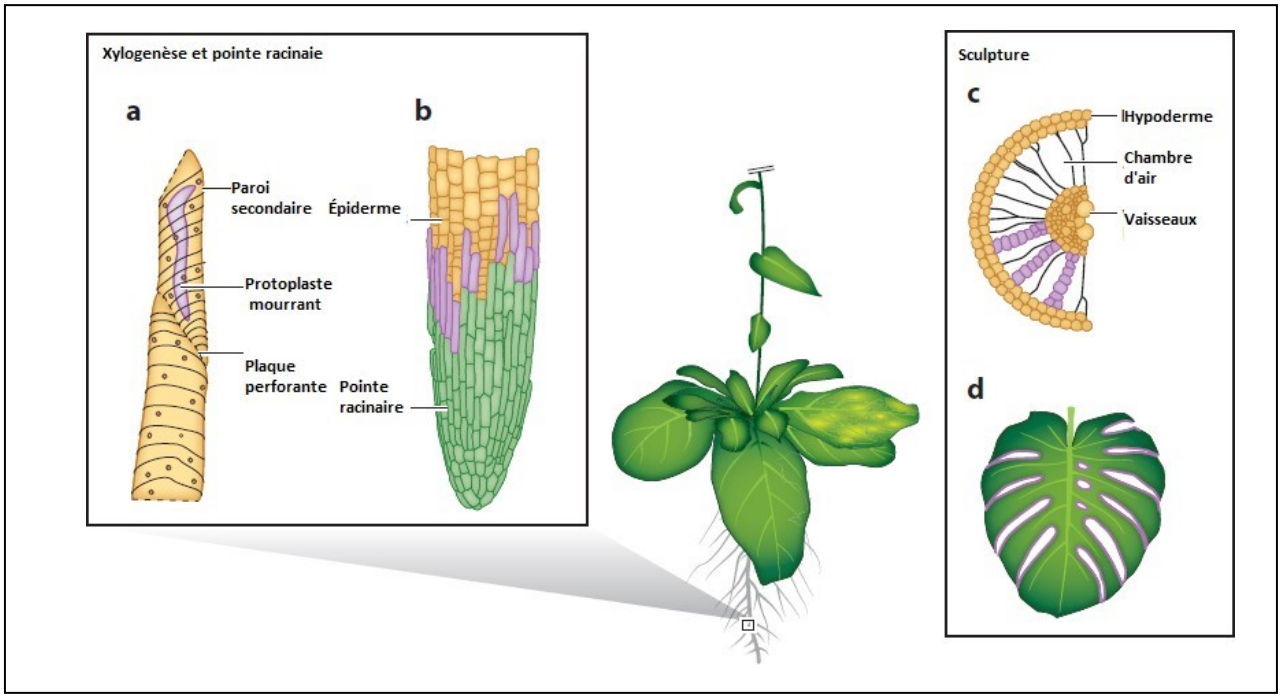

Figure 1.12 : Exemples de mort cellulaire programmée durant le développement. Mort cellulaire programmée durant la formation du xylème (a), la différenciation de la pointe racinaire (b), la formation de l'aérenchyme dans le riz (c) et dans la sculpture des feuilles de *Monstera deliciosa* (d). Les cellules en voie de mort sont indiquées en mauve. (Adaptée de Daneva et al., 2016).

Dans les cellules d'*Arabidopsis* en suspension, l'application de petites concentrations de TA (20-200 nM) suffit pour induire un programme de mort (Duval et al., 2005). La MCP induite par un traitement de TA est très similaire à celle induite par l'isoxabène. En plus des ressemblances morphologiques des cellules traitées, une forte corrélation existe entre les gènes induits dans les deux cas (Duval et Beaudoin, 2009). L'analyse transcriptomique dans les cellules en suspension d'*A. thaliana* réalisée dans notre laboratoire montre que 75% des gènes induits par la TA sont induits aussi par l'isoxabène et que la moitié de ces gènes-là sont communs aux voies de réponse aux défenses biotiques et abiotiques. Le gène codant pour la

phénylalanine ammonia-lyase (Pal) est parmi les gènes de défense activés par l'isoxabène et la TA. La Pal est une lyase liée à la défense et impliquée dans la première étape de la synthèse des phénylpropanoïdes chez les plantes (Lopez-Galvez, 1996). Cependant, d'autres gènes de défense dont l'expression est typiquement augmentée en réponse à l'acide salicylique, tel que *PR1*, ou en réponse à l'acide jasmonique et l'éthylène, tel que le gène codant pour la défensine 1.2 (*PDF1.2*) ne sont pas transcrits en réponse à la TA. De même, le traitement à la TA n'induit pas l'accumulation des ROS et n'active pas la voie des protéines kinases activées par les mitogènes (MAPK) comme dans la MCP de défense classique (Duval et Beaudoin, 2009).

Ces aspects combinés montrent que la TA induit un programme de mort atypique. L'action de cette molécule se traduit par un gonflement des cellules et une fragmentation de l'ADN. Ainsi, tout indique que la TA n'induit pas une réponse hypersensible (HR) dans les cellules puisque les gènes *PR1* et *PDF1.2* ne sont pas exprimés dans ces cellules, et que les niveaux de H_2O_2 n'y sont pas augmentés (Duval et al., 2005). Néanmoins, une activation de la transcription des gènes de novo se met en place, un flux de calcium vers le milieu intracellulaire a lieu ainsi qu'un efflux considérable des ions H^+ (Duval et Beaudoin, 2009; Errakhi et al., 2008; Tegg et al., 2005). Ces éléments regroupés permettent de conclure que la TA, comme l'isoxabène, induit une mort active ou bien un programme de mort atypique dans la cellule. C'est donc l'inhibition de la synthèse de la cellulose qui activerait ce programme de mort. Étant donné l'importance de la TA dans la maladie de la gale commune, il serait intéressant de mieux comprendre comment la TA agit sur les cellules végétales pour pouvoir mieux contrôler l'activation de cette MCP.

1.4.3 L'auxine et la thaxtomine A

L'auxine est l'hormone végétale la plus versatile. Le mot 'auxine' provient du grec, auxein, et signifie croître. Malgré la diversité des rôles joués par cette hormone, son implication dans l'élongation cellulaire reste l'aspect le plus étudié. Dans les cellules racinaires, par exemple,

c'est le ratio entre deux hormones, les cytokinines et l'auxine, qui régule l'activité des expansines, des pompes à protons et de certains facteurs de transcription pour contrôler l'élongation cellulaire (Pacifici et al., 2018). De même, la différenciation cellulaire et l'organogenèse suivent des patrons qui corrèlent avec le transport polaire de l'auxine via des transporteurs du genre PIN (Romero-Arias et al., 2017), ou la présence des protéines «Small Auxin Upregulated» (SAUR, Gallavotti, 2013). L'auxine a également été étudiée pour son rôle dans l'induction de la MCP durant l'organogenèse et la défense (Beckman, 2000; Xuan et al., 2016).

Au cours d'études s'intéressant aux mécanismes de résistance à la gale commune de la pomme de terre, il a été montré que l'ajout d'auxine ou des molécules "auxin-like", l'acide 2,4-dichlorophénoxyacétique (2,4-D), au niveau foliaire, peut réduire la sévérité de la gale commune sur les tubercules de pommes de terre (Tegg et al., 2008). De même, les travaux de recherche effectués dans notre laboratoire ont montré que l'ajout d'auxine exogène aux cellules en suspension de peuplier protège contre la mort induite par la TA et par un autre CBI le DCB (Brochu, 2005). D'autre travaux ont également montré qu'un pré-traitement à l'auxine réduit la MCP induite par la TA ou l'IXB dans les suspensions cellulaires d'*Arabidopsis thaliana* (Moneva, 2011). Il reste maintenant à comprendre comment l'auxine peut réduire les effets de la TA dans les cellules végétales.

1.5 Les objectifs du projet

Notre laboratoire s'intéresse à l'étude des facteurs modulant l'infection à la gale commune chez la pomme de terre et plus particulièrement à la thaxtomine A, étant donné qu'elle est essentielle pour que *Streptomyces scabies* puisse induire les symptômes de la maladie. Mon projet a été établi dans le but de mieux comprendre le mode d'action de la TA sur les cellules végétales et en particulier lors de l'activation de la MCP.

Mon premier objectif était de confirmer que l'auxine protège contre la MCP induite par la TA et d'étudier le mécanisme de protection. Plus particulièrement, j'ai investigué l'importance du transport de l'auxine dans l'induction de cette mort et j'ai caractérisé les effets de l'auxine et de la TA sur la rigidité de la paroi dans des cellules en suspensions d'*Arabidopsis thaliana*. Pour ce premier objectif, j'ai aussi réalisé ces mêmes expériences avec un autre inhibiteur de synthèse de la cellulose, soit l'isoxabène. Les résultats obtenus ont permis de déterminer si l'effet de la TA est spécifique à cette molécule ou associé au mode d'action plus générale des CBI de son groupe.

Deuxièmement, j'ai voulu étudier l'effet de la TA sur la structure de la cellulose, la dynamique du cytosquelette et l'activité des CeSA. Pour le faire, j'ai d'abord extrait de la cellulose à partir de cellules traitées à la TA. La qualité des microfibrilles a ensuite été évaluée par AFM. Pour analyser le cytosquelette et l'activité des CeSA en réponse à la TA, j'ai utilisé des lignées transgéniques exprimant la tubuline et la CeSA6 avec des protéines fluorescentes que j'ai analysées pour plusieurs critères, soient la vélocité des particules de CeSA6 dans la membrane la plasmique, la densité relative des CeSA6 et l'orientation des microtubules; et ce dans des plantules traitées au DMSO comme témoin ou à différentes concentrations et durée d'application de TA.

Finalement, mon troisième objectif était de valider et caractériser l'absence de la production des ROS après un traitement à la TA dans les cellules en suspensions. J'ai analysé l'activité de différentes enzymes impliquées dans la protection contre les ROS pour déterminer si elles sont impliquées dans la réduction des ROS. J'ai également observé qu'une augmentation exogène de peroxyde d'hydrogène pouvait réduire la mort induite par la TA, et que cet effet était associé à une augmentation de la rigidité pariétale.

L'ensemble de ces objectifs seront discutés dans les chapitres suivants pour arriver enfin à un modèle préliminaire de l'action de la TA sur les cellules végétales.

CHAPITRE 2

L'importance de l'auxine dans la mort cellulaire induite par la thaxtomine A et l'isoxabène dans les cellules en suspension d'*Arabidopsis thaliana*.

2.1 Introduction de l'article et contributions des auteurs

Les travaux de recherche effectués dans notre laboratoire ont montré un effet protecteur de l'auxine contre la mort induite par la TA dans les cellules d'*Arabidopsis* et du peuplier. Dans ce premier chapitre, j'ai étudié le mécanisme de protection conférée par l'auxine. Ici, je démontre que l'efflux de l'auxine est indispensable pour induire la MCP suite à l'ajout de la TA, et que l'auxine en tant que telle diminue la rigidité pariétale ce qui diminuerait le choc mécanique induit par la TA au niveau de la paroi.

Ma contribution à ce projet comprend l'exécution de la totalité des expériences présentées et la préparation du manuscrit pour la soumission. La partie concernant l'analyse des extraits de la paroi en microscopie à force atomique a été réalisé dans le laboratoire du Dr. Michel Grandbois à l'Institut de pharmacologie de l'université de Sherbrooke à Fleurimont. La totalité des travaux a été dirigé par Dre Nathalie Beaudoin.

Le manuscrit présenté ci-après a été préparé pour être soumis dans le journal BMC Plant Biology.

Auxin is involved in the cell life and death decisions in response to inhibition of cellulose synthesis in *Arabidopsis* cell cultures

Fatima Awwad, Guillaume Bertrand, Michel Grandbois and Nathalie Beaudoin*

***corresponding author**

2.2 Abstract

Cellulose microfibrils are the strongest components of the plant primary cell wall. Perturbation of cellulose synthesis by cellulose biosynthesis inhibitors (CBIs) compromises cell wall organization and induces an atypical program of cell death (PCD) in plant cells. However, little is known on the mechanisms that control PCD in response to cell wall perturbation. To address this question, we studied PCD in *Arabidopsis* cell cultures treated with two different CBIs, i.e., the herbicide isoxaben and the *Streptomyces scabies* phytotoxin thaxtomin A. The plant hormone auxin was proposed to play a role in controlling thaxtomin A toxicity. Accordingly, we found that exogenous addition of synthetic auxin 2,4-dichlorophenoxyacetic acid (2,4-D) and natural auxin IAA prior to CBI treatment inhibited cell death induced by thaxtomin A and isoxaben, two structurally different compounds. For both CBIs, induction of PCD was dependent on an early influx of calcium and was abrogated by auxin efflux inhibitors, suggesting that endogenous accumulation of auxin inhibits CBI-induced cell death. Since cell elongation was diminished in response to auxin, we speculated that auxin treatment should increase cell wall stiffness and compensate for reduced cellulose synthesis thus promoting cell survival. Atomic force microscopy (AFM) was used to measure cell wall stiffness in living cells treated with CBIs, auxin or a combination of both. However, both CBIs and auxin decreased cell wall stiffness, indicating that auxin does not prevent CBI-induced cell death by strengthening the cell wall. Unexpectedly, this also shows that decreased cell wall rigidity can be associated with reduced cell elongation.

Keywords: Programmed cell death, auxin, thaxtomin A, isoxaben, calcium, cell wall

2.3 Abbreviations

2,4-D 2,4-Dichlorophenoxyacetic acid

AFM Atomic Force Microscopy

CBI Cellulose Biosynthesis Inhibitor

CeSA Cellulose Synthase

CSC Cellulose Synthesis Complex

CTRL Control

IXB Isoxaben

PCD Programmed Cell Death

TA Thaxtomin A

2.4 INTRODUCTION

The plant cell wall plays essential roles in plant growth and development and determines cell form and size by regulating processes such as cell elongation, adhesion and water movement. As the cell wall surrounds the cell, it also participates in intercellular communication and offers cellular protection against biotic and abiotic aggression (Cosgrove 2005; Keegstra 2010). The primary cell wall is a strong but dynamic structure that can be modified by enzymatic and non-enzymatic proteins to modulate its elasticity and extensibility in response to growth signals or environmental changes (Cosgrove 2016; Cosgrove 2018).

Cellulose is the main structural constituent of the plant cell wall. This polysaccharide is made of chains of β-1-4 glucose subunits that are linked to each other by hydrogen bonds to form microfibrils which are embedded in a gel-like matrix made of pectins, hemicellulose and protein (Cosgrove 2016; McFarlane et al. 2014). Cellulose microfibrils are the strongest component of the cell wall (Tateno et al. 2016). One of the most recent conceptual model of the plant cell wall organization proposes that microfibrils form bundles by direct contacts between cellulose microfibrils and at load-bearing junctions where microfibrils intertwine with xyloglucan (Cosgrove 2018). These interactions would be necessary to increase cell wall mechanical resistance. Pectins, which bind the hydrophilic surface of cellulose, would fill the space between microfibrils (Cosgrove 2018). One important contribution of pectins is to regulate cell wall elasticity (Levesque-Tremblay et al. 2015), but they have also been implicated in maintaining and sensing cell wall integrity during salt stress (Feng et al. 2018) and pathogen interactions (Bethke et al. 2016; Lionetti et al. 2017).

Cellulose synthesis is mediated by different cellulose synthase (CeSA) proteins assembled in multiprotein complexes called cellulose synthesis complexes (CSCs) that can be seen as a rosette structure in the plasma membrane (Brabham and Debolt 2012; Keegstra 2010; McFarlane et al. 2014; Tateno et al. 2016). Pre-assembled CSCs are transported to the plasma membrane through the Golgi apparatus, the trans-Golgi network and ultimately in small compartments that associate with microtubules (McFarlane et al. 2014; Tateno et al. 2016). Any disruption in cellulose biosynthesis perturbs the function and organization of the cell wall, altering cell expansion and cell wall integrity. These effects can be studied using cellulose biosynthesis inhibitors (CBIs) (Tateno et al. 2016). The herbicide isoxaben (IXB) is a well-known CBI which was suggested to specifically target CeSA3 and CeSA6 (Desprez et al. 2002; Scheible et al. 2001). Inhibition of cellulose synthesis by IXB induces a wide range of responses in *Arabidopsis* seedlings, including inhibition of root elongation, root swelling, ectopic lignin deposition and expression of ethylene and jasmonate-mediated defense gene expression (Bischoff et al. 2009; Caño-Delgado et al. 2003; Ellis et al. 2002; Tsang et al. 2011).

The phytotoxin thaxtomin A (TA) is a natural CBI which is the main pathogenicity determinant of potato common scab-causing actinobacteria such as *Streptomyces scabies* (syn. *scabiei*) (Beaulieu et al. 2008; Braun et al. 2017; King et al. 1991; Loria et al. 2008; Scheible et al. 2003). Treatment of potato tubers with TA induces scab-like symptoms (King et al. 1992; Lawrence et al. 1990) and inhibition of TA synthesis in normally pathogenic strains abolishes the formation of scab-like symptoms on infected tubers (Goyer et al. 1998; Healy et al. 2000). Inhibition of cellulose synthesis by TA was proposed to facilitate bacterial penetration of plant cell walls (Loria et al. 2008). TA also induces various responses in different plant species and tissues (Beaulieu et al. 2008; Fry and Loria 2002; Loria et al. 2006). In *Arabidopsis*, the effects induced by TA in seedlings resemble those induced by IXB, including reduction of growth, induction of ectopic lignification and of defense-related gene expression (Bischoff et al. 2009; Scheible et al. 2003).

The responses to these inhibitors were studied at the cellular level in *Arabidopsis* cell suspensions. Both IXB and TA stimulate cellular hypertrophy and induce an atypical program of cell death (PCD) in *Arabidopsis* cell suspensions (Duval et al. 2005). This PCD is not associated with H_2O_2 production and would not involve defense-related mitogen-activated protein kinase (MAPK) signaling (Duval and Beaudoin 2009; Duval et al. 2005; Errakhi et al. 2008). Both CBIs also induce similar transcriptional changes that are comparable to wound-like and defense-related responses (Duval and Beaudoin 2009).

While the specific molecular target of TA has not yet been identified, it is most probably different from that of IXB, as mutant resistant to IXB are not resistant to TA (Tegg et al. 2013). Moreover, TA induces a different pattern of ectopic lignification than IXB and changes in gene expression induced by TA are not entirely mimicked by IXB treatment (Bischoff et al. 2009; Duval and Beaudoin 2009).

There is currently little information on the mechanisms of resistance to common scab (Braun et al. 2017). Since TA has a central role in the development of common scab symptoms in

potato tubers infected by pathogenic *Streptomyces* species, counteracting the effects of TA comes out as a promising strategy to reduce disease symptoms. It was shown that spraying potato plants with the synthetic auxin 2,4-dichlorophenoxyacetic acid (2,4-D) at the time of tuber induction increases resistance to common scab, an effect attributed to decreased TA toxicity (Tegg et al. 2008). However, it is not known how 2,4-D can increase tolerance to common scab or TA. 2,4-D could act at a systemic level, enhancing plant defense responses. Several studies have linked auxin to plant defense, but the role of auxin generally depends on plant pathogen type (Fu and Wang 2011; Kazan and Manners 2009). In most cases, auxin enhances plant disease susceptibility to biotrophic pathogens. In contrast, auxin signaling can be required to activate defense against necrotrophic pathogens. For example, it was shown that the natural auxin IAA has a protective effect against the fungus *Botrytis cineria* in harvested apple fruit (Yu et al. 2008) and against *Fusarium culmorum* in barley (Petti et al. 2012). It also induces in pear fruit wounds resistance against *Penicillium expansum* (Zhang et al. 2018) that was associated with increased expression of defense-related genes, suggesting that IAA would directly stimulate host-mediated resistance against pathogen. Yet, the reduction of TA toxicity in plant tissues by 2,4-D remains enigmatic.

This work addresses this question at the cellular level, using *Arabidopsis* cell cultures to study the impact of auxin on TA-treated cells. We found that auxin can protect cells from the TA-mediated induction of PCD (Duval et al. 2005). Moreover, we showed that auxin can also reduce IXB-induced PCD in cell cultures, indicating that the protective effect of auxin is not specific to the TA molecule but would somehow alter cellular responses activated by inhibition of cellulose synthesis. Induction of cell death by CBI was also decreased by inhibition of calcium influx and treatment with auxin transport (efflux) inhibitors, which were shown to increase intracellular auxin accumulation (Petrášek et al. 2003). To determine whether the protective effect of auxin may involve compensatory changes in cell wall rigidity, we used atomic force microscopy (AFM) to measure cell wall stiffness in cells treated with auxin, CBI or both. We discuss our results in the light of currently proposed mechanisms of action of auxin in relation to induction of cell death and the cell wall-cytoskeleton interactions.

2.5 MATERIALS AND METHODS

2.5.1 Plant material and treatments

Arabidopsis thaliana accession Landsberg *erecta* cell suspension cultures were graciously provided by Dr. Jean Rivoal (IRBV, Montréal, PQ, Canada). All chemicals were purchased from Sigma Aldrich unless otherwise indicated. Cell suspensions were grown in 45 mL Murashige and Skoog (MS) medium (pH 5.7) supplemented with B5 vitamins and 1 mg L^{-1} 2,4-dichlorophenoxyacetic acid (2,4-D) in 125 mL Erlenmeyer flasks kept on a rotary shaker (120 rpm) at 22°C in the dark. *Arabidopsis* cell cultures were subcultured every 7 d by diluting 15 mL cells into fresh medium. Treatments were performed using 10 mL log-phase cells 3 to 4 d after subculture. Thaxtomin A (TA) was prepared as described before (Duval et al. 2005). TA (stock of 1 mM) and isoxaben (IXB; stock of 10 mM) were prepared in methanol and added at a final concentration of 1 µM. The same volume of methanol (less than 0.1% of final volume) was added to control cells. 2,4-D and IAA were dissolved in ethanol and 1-naphtalenacetic acid (NAA) in water. These chemicals were added at the final concentration indicated in each experiment. Auxin transport inhibitors triiodobenzoic acid (TIBA), *N*-1-naphthylphthalamic acid (NPA), 2-naphthoxyacetic acid (2-NOA) and 3-chloro-4-hydroxyphenylacetic acid (CHPAA) were dissolved in ethanol and added to cell cultures at a final concentration of 10 µM. Calcium inhibitors ruthenium red (RR) and lanthanum chloride ($LaCl_3$) were diluted in water and filtered. Cells were treated with a final concentration of 50 nM of RR and 500 µM of $LaCl_3$.

2.5.2 Cell death assay

Cell death was assessed using trypan blue staining as described before (Duval et al. 2005). For microscopic evaluation, cells were incubated for 5 min in a fresh medium containing

fluorescein diacetate (FDA) at a final concentration of 50 µM and propidium iodide (PI) at a final concentration of 2.78 µM. Images were taken with a Zeiss Imager Z1 fluorescebce microscope (Carl Zeiss Canada Ltd, Ontario, Canada) equipped with a monochromatic camera using AxioVision 4.8.2 version. 40 µL of cell culture were examined using with excitation wavelength of 488 nm (FDA) and 535 nm (PI). FDA fluorescence was detected in living cells with a FITC filter (520 nm) and PI in dead cells with a rhodamine filter (617 nm). For each condition, at least 500 cells in groups of 100 were counted. Each experiment was repeated at least three times.

2.5.3 Measurement of cell dimensions

Cell dimensions were determined using Fiji software (Schindelin et al. 2012) by measuring the length of 300 cells per condition from three independent experiments.

2.5.4 Cell surface mechanics

The elastic modulus (Young's modulus) of individual cells was quantified from force/tip-sample separation curves recorded using atomic force microscopy (AFM). Cells were pretreated for 24 h with different combinations of methanol (control), TA, IXB, 2,4-D or IAA using the concentrations indicated in each experiment. A 40 µl-aliquot of each culture was laid on a poly-L-lysine (0.1 mg mL^{-1}) coated slide cover slip for 5 min to allow adhesion. The cover slip was washed three times with culture medium before fixing it with a minute drop of vacuum grease in a small petri dish that was filled with 2 mL of culture medium prior to analysis. AFM analysis was conducted in contact mode as described before (Radotić et al. 2012).

Briefly, AFM studies were performed with a JPK instrument NanoWizard® 4 V.6 (Berlin, Germany) mounted on top of an inverted Zeiss imager Z1 microscope (Carl Zeiss Canada Ltd, Ontario, Canada). MLCT cantilevers A with a nominal spring constant of 0.07 N/m were used (Bruker AFM probes, California, USA). For this cantilever we typically obtain a spring

constant ranging from 0.05 to 0.11 N/m, using the thermal noise technique (Hutter and Bechhoefer 1993). The Young's modulus was calculated using the Hertz model adapted for a four-sided pyramid indenter, built-in the JPK analysis software. The Young's modulus of the glass cover slip was considered infinitely rigid when compared to that of the measured cells. AFM trials were carried to precise adequate cell wall dept and cantilever tip distance to sample before usingthe same parameters for all further experiments. All studies were carried at room temperature. Force-curves were recorded at five different arbitrary locations in a 5 µm radius over the cell surface leading to five batches of 30 to 50 points per cell. We used 3 to 4 cells per experiment. Each experiment was repeated 3 times.

2.5.5 Statistics

Statistical analysis was performed with GraphPad Prism 7. For cell death assay and measurements, cells were counted in groups of 100 and the mean was calculated from 3 to 15 replicates. Each experiment was repeated at least three times. Data was analyzed using t-test followed by Holm-Šídák method with alpha = 0.05. Results were considered statistically different when p-value was < 0.05.

2.6 RESULTS AND DISCUSSION

2.6.1 Auxin protects *Arabidopsis* cells from CBI-induced cell death

Thaxtomin A (TA) inhibits root growth in *Arabidopsis*, tomato and potato plants (Tegg et al. 2005) and perturbs *Arabidopsis* seedling growth, an effect that can be reversed by the synthetic auxin 2,4-D or the natural auxin IAA (Tegg et al. 2008). Spray of 2,4-D on potato plants has also been shown to reduce common scab symptoms in potato tubers, and this outcome has been

attributed to the reduction of TA-induced necrosis in a tuber slice assay (Tegg et al. 2008). However, the mechanism of action of 2,4-D in the protection against TA has not yet been determined. We have chosen to study the effect of 2,4-D on the action of TA at the cellular level using *Arabidopsis* cell suspension cultures. In previous work, we showed that the CBIs TA and IXB induce PCD in *Arabidopsis* cell cultures (Duval et al. 2005). To evaluate whether 2,4-D could also prevent cell death induced by TA, *Arabidopsis* cell cultures were pretreated with 50 µM 2,4-D prior to TA treatment and dead cells were counted over 72 h. As shown in Fig. 2.1a, 2,4-D decreased the percentage of dead cells induced by TA 48 h after treatment from 79% to less than 18%, which was comparable to control levels. We also tested whether other auxins, such as IAA and NAA, could protect cells from TA-induced cell death (Suppl. Fig. S1). As observed with 2,4-D, pretreatment of cells with IAA significantly reduced the percentage of cell death in TA-treated cells for 48 h from 79% down to 49%, which was similar to IAA-treated samples. However, pretreatement of cells with 30 µM NAA increased cell death to a level similar to that induced by TA, making it impossible to determine whether it could effectively alter the response to TA. Lower concentrations of NAA did not protect cells from TA-induced cell death (data not shown). Nevertheless, these results demonstrate that both natural and synthetic auxins can significantly protect plant cells from the effects of TA. This also implicitly suggests that high levels of endogenous auxin may be able to protect plant cells from TA.

Auxins may exert their protective effect directly against the TA molecule itself (e.g., competition, interaction) or may protect cells from TA's ability to inhibit cellulose synthesis or its downstream consequences. To discriminate between these possibilities, we repeated the previous experiments using a structurally different inhibitor of cellulose biosynthesis, isoxaben (IXB), which can also induce a controlled cell death in *Arabidopsis* cell cultures (Duval et al. 2005). Cells were pretreated with various concentrations of 2,4-D and IAA followed by IXB treatment. Both 2,4-D and IAA used at a concentration of 50 µM and 1 µM respectively were able to reduce the level of cell death induced by IXB (Fig. 2.1b and data not shown), but the most efficient auxin was IAA, with a reduction of cell death from 84% down to 52%. We

concluded from these results that synthetic and natural auxins can protect cells from PCD induced by two structurally different inhibitors of cellulose synthesis, suggesting that auxinic compounds act against the action or downstream effects of CBIs and not through direct competition or interaction with TA or IXB.

2.6.2 Increase in cytosolic calcium is necessary for CBI-induced cell death

Calcium is an important second messenger implicated in a wide variety of cellular processes (Dodd et al. 2010). Rapid accumulation of cytosolic calcium can be detected in response to plant pathogens, specific elicitors and toxins but also in response to mechanical stimuli (Reddy 2001; White and Broadley 2003) (Kurusu et al. 2013). In general, alteration in calcium homeostasis precedes and is necessary for the induction of defense-related hypersensitive (HR) PCD induced in specific plant-pathogen interactions or in response to elicitors (Huysmans et al. 2017; Lecourieux et al. 2006). Likewise, a rapid and short calcium influx was detected in response to TA treatment (Errakhi et al. 2008; Tegg et al. 2005). This early increase in cytosolic calcium was required to activate the signaling cascade leading to the induction cell death by TA in *Arabidopsis* cells (Errakhi et al. 2008). In most cases, the calcium influx preceding defense-related PCD is associated with an oxidative burst characterized by the production of H_2O_2 (Hu et al. 2004) and the activation of a MAPK signaling pathway (Garcia-Brugger et al. 2006; Link et al. 2002). However, in the presence of TA, neither H_2O_2 production nor MAPK activation were detected (Duval et al. 2005; Errakhi et al. 2008), suggesting that the induced cell death pathway is different from classical defense-related PCD. Moreover, it was found that although TA also induces cell death in tobacco BY-2 cells, no calcium influx was required nor detected following TA treatment, suggesting the induction of different pathways leading to similar consequences in different species (Meimoun et al. 2009).

To determine whether the increase in cytosolic calcium required for the induction of cell death in *Arabidopsis* cells was a specific response to TA or a general reaction to inhibition of cellulose synthesis, we treated *Arabidopsis* cells with IXB combined with different calcium

transport inhibitors (Fig. 2.2), such as lanthanum chloride ($LaCl_3$), which inhibits extracellular calcium uptake, and ruthenium red (RR), which is thought to block calcium release from organelles (Choi et al. 2014). In TA-treated cells, $LaCl_3$ significantly reduced the level of cell death from 72% to 56% (Fig. 2.2a). The effect of $LaCl_3$ was even more important in IXB-treated cells, with a reduction of cell death from 84% down to 19%. This result confirms that the rapid increase in cytosolic calcium is a prerequisite for the induction of cell death by both TA and IXB. Treatment with RR also inhibited the induction of cell death mediated by both CBIs, decreasing cell death by 36% in TA-treated cells and by 54% for IXB treatment (Fig. 2.2). Therefore, the uptake of extracellular calcium as well as its release from intracellular stores both contribute to the increase in cytosolic calcium implicated in the activation of cell death in *Arabidopsis* cells. However, the downstream cascade activated by calcium leading to the induction of cell death remains unknown.

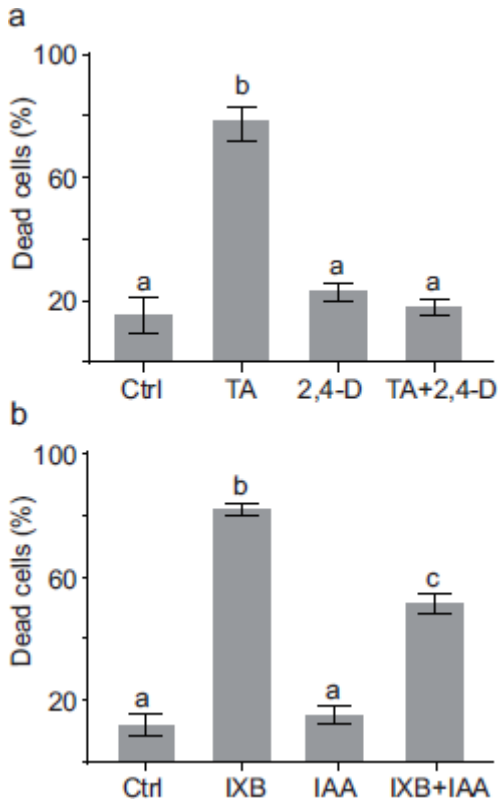

Figure. 2.1 Auxin protects *Arabidopsis* cells from CBI-induced cell death.
Percentage of dead cells in *Arabidopsis* suspension-cultured cells 48 h after addition of auxin and/or CBI. a) Cells were treated with thaxtomin A (TA; 1 µM), 2,4-dichlorophenoxyacetic acid (2,4-D; 50 µM), or 2,4-D 30 min before adding TA. b) Cells were treated with isoxaben

(IXB; 1 μM), IAA (1 μM), or IAA (1 μM) 30 min before adding IXB. Ctrl = control cells treated with equal volume of methanol as treated samples. Each value is the mean of n = 15 (100 cells each) ± SD. Statistically different values (t-test followed by Holm-Šídák method, $p < 0.05$) are indicated by different letters.

2.6.3 Inhibition of auxin efflux protects cells from IXB- and TA-induced cell death

As reported before, decreased cellulose synthesis by TA and IXB causes a radial expansion (hypertrophy and bulging) of cells at the end of cell files in suspension-cultured cells (Duval et al. 2005) (Suppl. Fig. S2). Interestingly, the hypertrophied cells remain alive longer than other cells in response to TA or IXB. These results suggest that cells with reduced elongation in response to CBI rapidly die while enlarged cells at the end of the cell files remain alive for a longer time. In tobacco BY-2 cell suspensions, cell axiality and cell file polarity are regulated by a unidirectional transport of auxin (Maisch and Nick 2007). In light of our results with auxins, we hypothesized that the survival of hypertrophied cells may be related to the polar transport and accumulation of auxin at the end of cell files. Accordingly, addition of exogenous auxin to cell cultures would increase the intracellular level of auxin and thus promote cell survival in most of the cells even after CBI-treatment.

It is possible to alter the endogenous levels of auxins using auxin efflux transport inhibitors such as *N*-1-naphthylphthalamic acid (NPA) and triiodobenzoic acid (TIBA) which were shown to increase accumulation of auxins within cells (Petrášek et al. 2003; Rubery and Sheldrake 1974). To test our hypothesis, we pretreated *Arabidopsis* cell suspensions with these inhibitors prior to CBI-treatment and counted dead cells. As shown in Fig. 2.3, TA-induced cell death was decreased from 87% to 65% and 40% when cells were pre-treated with the auxin efflux inhibitors NPA and TIBA respectively. In contrast, pretreatment with auxin influx inhibitors, such as 3-chloro-4-hydroxyphenylacetic acid (CHPAA) and 2-naphthoxyacetic acid (2-NOA), had no effect on TA-induced cell death. Again, this effect was not specific to the TA molecule itself but was also observed with IXB, with 25% to 28% less dead cells in NPA and TIBA pretreated cells (Fig.2. 2). This data suggests that perturbation of auxin efflux increases

the survival rate of CBI-treated cells, supporting our hypothesis that accumulation of endogenous auxins contributes to cell survival in response to TA and IXB.

This conclusion is also reinforced by other examples where auxin was shown to inhibit PCD occurring during plant development or in response to stress. For example, development of Norway spruce (*Picea abies*) somatic embryos involves the programmed elimination of suspensor and embryonal tube cells by PCD (Larsson et al. 2008). It was shown that inhibition of auxin transport using NPA inhibited PCD in suspensor and tube cells, suggesting that auxin accumulation in these cells perturbed PCD (Larsson et al. 2008). Auxin has also been involved in the protection of stem cell niche from chilling stress-induced PCD in root tissues (Hong et al. 2017). In this case, it was found that chilling stress, which perturbs root auxin levels and distribution, specifically induces PCD in columella stem cell daughters. As a result, auxin transport was disrupted, which re-established in the quiescent center cells an auxin maximum necessary to maintain stem cell niche integrity. This was shown to contribute to faster root growth recovery after chilling stress (Hong et al. 2017). Another example is the repression of cell death by auxin observed in harpin-treated tobacco (*Nicotiana tabacum*) leaves (Gopalan 2008) and grapevine (*Vitis rupestris)* cell cultures (Chang et al. 2015).

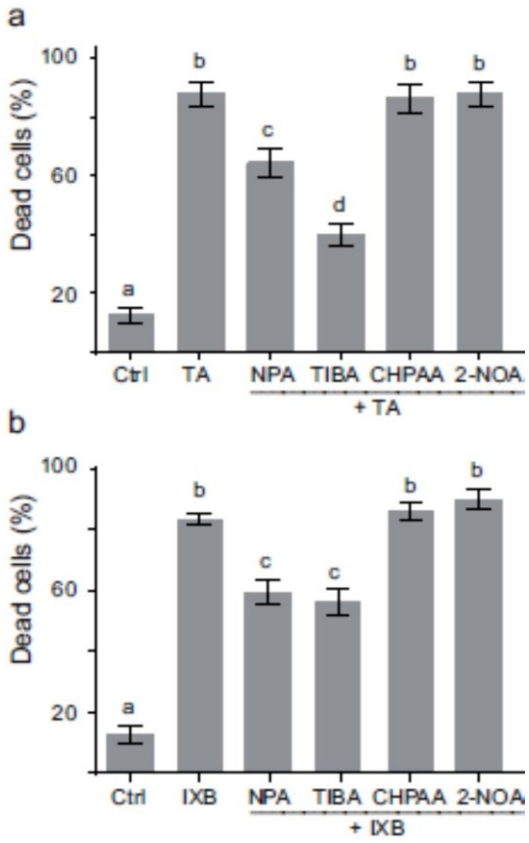

Figure 2.2 Inhibition of auxin transport (efflux) protects from CBI-induced cell death Percentage of dead cells in *Arabidopsis* cell cultures 72 h after addition of auxin transport inhibitor and/or CBI. a) Cell death was evaluated after treatment with thaxtomin A (TA; 1 µM) and in cells pretreated for 30 min with 10 µM of different auxin transport inhibitors: 2,3,5-triiodobenzoic acid (TIBA) and 1-N-naphthylphthalamic acid (NPA) as efflux inhibitors, 2-naphthoxyacetic acid (NOA) and 3-chloro-4-hydroxyphenylacetic acid (CHPAA) as influx inhibitors prior to TA treatment. b) Cell death was evaluated after treatment with isoxaben (IXB; 1 µM) and in cells pretreated for 30 min with the different auxin transport inhibitors prior to IXB addition. Ctrl = control cells treated with equal volume of methanol as treated samples. Each value is the mean of n = 15 (100 cells each) ± SD. Statistically different values (t-test followed by Holm-Šídák method, $p < 0.05$) are indicated by different letters.

The proteinaceous elicitor harpin from *Erwinia amylovora* activates a defense-related hypersensitive (HR) PCD in plant cells, a process accompanied by local and systemic resistance in plants. This PCD can be reversed by auxin (IAA and 2,4-D) without affecting the associated immune-related responses, suggesting that distinct auxin-dependent and

independent signaling pathways modulate the harpin induction of cell death and defense resistance separately (Chang et al. 2015; Gopalan 2008). The protective effect of auxin was proposed to depend on modifications of the level of actin organization and its interaction with the plasma membrane (Chang et al. 2015). Actin bundling is an early and essential event in PCD (Smertenko and Franklin-Tong 2011), but auxin treatment can restore a normal actin configuration (Chang et al. 2015; Nick 2010). Based on experimental results, Chang et al. (2015) suggested that harpin would perturb an auxin-dependent pathway involved in the remodeling of actin. Harpin treatment would lead to contraction of actin cables (actin bundling) and perturbation of membrane integrity that ultimately activates PCD. Accordingly, the life and death decision in response to harpin would depend on the dynamic subpopulation of membrane-associated actin (Chang et al. 2015). Hence, auxin treatment would stimulate cell survival by maintaining a dynamic actin configuration.

There is wide evidence that inhibition of cellulose synthesis can alter the organization of the plant cytoskeleton, with changes observed both at the level of the actin network and microtubules (Lehman et al. 2017). More specifically, it was shown that when cellulose synthesis is inhibited by IXB and TA for 2.5 h, most of CeSA3 proteins are moved from the plasma membrane to intracellular small microtubule associated compartments or MASCs (Bischoff et al. 2009; Paredez et al. 2006; Tateno et al. 2016). Disruption of the cell wall-plasma membrane interface by IXB also perturbs cortical microtubule alignment (Bischoff et al. 2009; Tolmie et al. 2017), reduces bulk remodeling of the actin cytoskeleton (Tolmie et al. 2017) and alters the localization of the polar auxin transporter PIN1 (Feraru et al. 2011; Lehman et al. 2017). However, there is little information on the effect of TA on the cytoskeleton. Most changes induced by IXB (root growth inhibition, changes in gene expression, CeSA relocalization to MASCs, etc.) are reproduced by TA treatments (Bischoff et al. 2009; Tegg et al. 2013). Nonetheless, it was reported that TA has no significant effect on the organization of microtubule array after a 2.5 h treatment (Bischoff et al. 2009). On the other hand, there is indirect evidence that TA treatment may alter auxin transport in *Arabidopsis* cell cultures and seedlings, a process that closely depends on the organization of the actin

cytoskeleton (Duval and Beaudoin 2009; Tegg et al. 2013). The auxin protection was also shown on that the application of TA on potato tuber cells induces disruption of the cell wall-plasma membrane interface (Goyer et al., 2000). Further studies will be required to determine the impact of TA on the plant cell cytoskeleton and to investigate whether the protective effect of auxin against CBI-induced cell death involves the cytoskeleton.

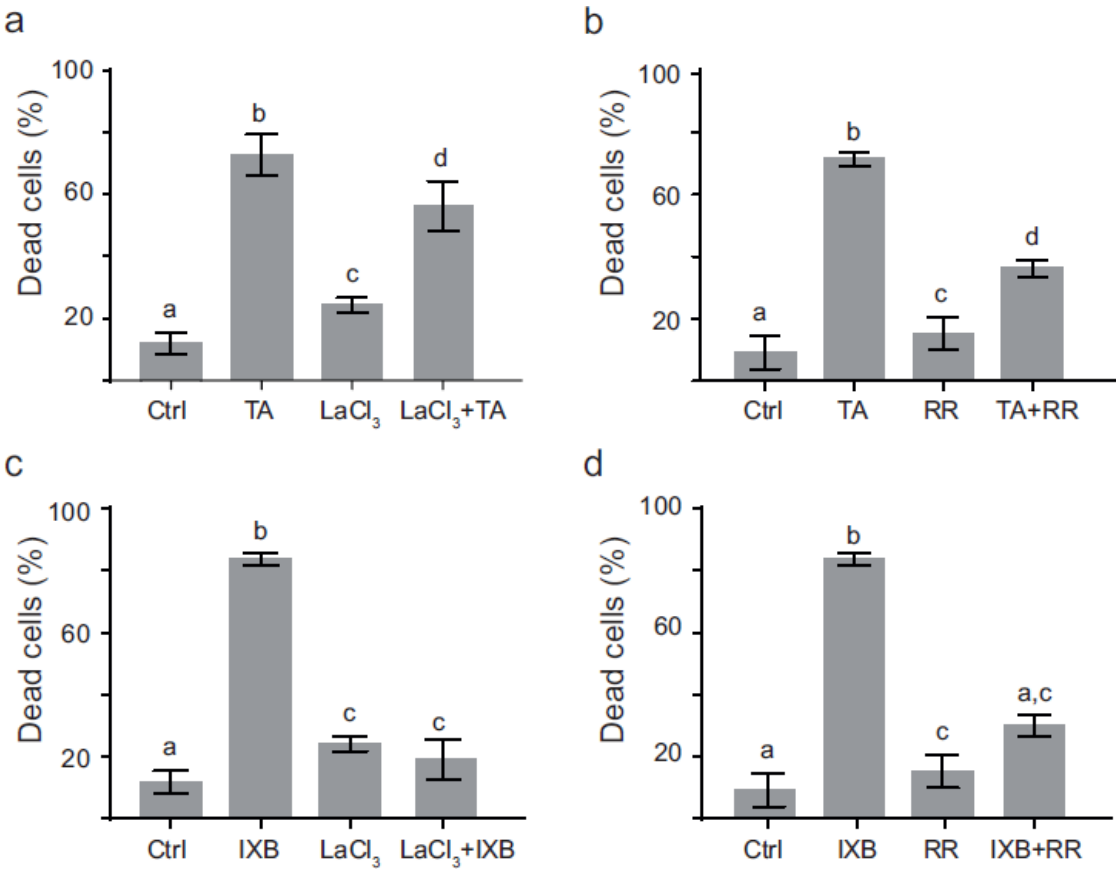

Figure 2. 3 Calcium influx is required for the CBI-induction of cell death.
Percentage of dead cells in *Arabidopsis* suspension cells 48 h after the addition of calcium transport inhibitors. a) and c) Cells were treated with thaxtomin A (TA; 1 µM), isoxaben (IXB; 1 µM) or lanthanum chloride ($LaCl_3$; 500 µM) alone, or pretreated with $LaCl_3$ (500 µM) 30 min before adding TA or IXB. b) and d) Cells were treated with TA (1 µM), IXB (1 µM) or ruthenium red (RR; 50 nM) alone, or pretreated with 50 nM of RR 30 min before adding TA or IXB. Ctrl = control cells treated with equal volume of methanol as treated samples. Each value is the mean of n = 15 (100 cells each) ± SD. Statistically different values (t-test followed by Holm-Šídák method, $p < 0.05$) are indicated by different letters.

Table 2.1 Distribution of cells according to cell length (µm) 24 h after treatment with cellulose biosynthesis inhibitors and auxins.

	Percentage of cells according to cell length[a]		
Treatment	**10-40 µm**	**40-60 µm**	**›60 µm**
Control (Methanol)	**44.0 ± 11.7**	**33.4 ± 2.4**	**26.6 ± 9.3**
Thaxtomin A	**75.5 ± 2.2***	**22.6 ± 0.2***	**4.1 ± 0.2***
Isoxaben	**67.9 ± 4.7***	**27.1 ± 1.5***	**10.9 ± 6.2**
2,4-D	**89.6 ± 6.3***	**7.2 ± 3.3***	**3.2 ± 2.8***
IAA	**72.1 ± 8.6***	**17.5 ± 5.7***	**10.4 ± 4.6***

[a]Cells stained with trypan blue were visualized by light microscopy and photographed. Cell dimensions were measured using Fiji software (Schindelin et al. 2012) for 300 cells per condition. Results show the mean percentage of cells in each category of length from 3 replicates ± SD. (*) indicates statistically significant difference with control in each category (t-test followed by Holm-Šídák method, $p < 0.05$)

2.6.4 TA and IXB as well as auxin decrease stiffness of the plant cell wall while restricting cell elongation

Inhibition of cellulose synthesis by TA and IXB in Arabidopsis cell cultures and seedlings induces the expression of genes involved in cell wall synthesis and ectopic accumulation of lignin (Bischoff et al. 2009; Duval and Beaudoin 2009). These responses may be activated to reinforce cell walls compromised by reduced cellulose synthesis in order to maintain cell wall mechanical properties and integrity required for cell elongation and growth (Bischoff et al. 2009). Moreover, resistance to CBI in plant cells habituated to TA or IXB has been associated with important changes in cell wall composition towards the production of pectins to compensate for loss of cellulose (Brochu et al. 2010; Manfield et al. 2004). Hence, modifications of the cell wall organization and composition may be a way to increase cell survival when cellulose content is reduced.

Auxin can also induce a variety of cell wall modifications. Auxin plays a central role in the control of cell elongation by stimulating cell wall loosening, in agreement with the acid growth hypothesis or by regulating cell wall modifying enzymes such as expansins and pectin methylesterase (Majda and Robert 2018; Nafisi et al. 2015). Increased cell wall extensibility

by auxin is required to stimulate rapid cell elongation. However, we observed that *Arabidopsis* cell cultures treated with auxin contained a high proportion of cells smaller than control cells (Table 1), indicating that cell elongation was reduced by auxin. Both CBIs and auxin halted cell elongation of *Arabidopsis* suspension-cultured cells. In response to a 24 h-treatment with IXB or TA, 67% to 75% of cells remained shorter than 40 μm, while only 44% of control cells were found in this category. Moreover, more than 26% of control cells were longer that 60 μm compared to only 4% to 10% for TA- or IXB-treated cells. A reduction in cell expansion was also observed in specific tissues of *Arabidopsis* seedlings treated with IXB or TA, where root hairs appear crowded in the differentiation zone due to shorter trichoblast cells (Tegg et al. 2005; Tsang et al. 2011). In our experimental conditions, 2,4-D also reduced cell elongation even more than CBI, with over 89% cells in the 10 to 40 μm category. On the other side, IAA inhibitory effect on cell elongation resembled that of CBIs (Table 1). While auxin can stimulate cell expansion following a concentration-dependent manner in light grown aerial tissues, high concentrations (above 10^{-8} M) are generally inhibitory in root tissues (Dünser and Kleine-Vehn 2015; Perrot-Rechenmann 2010). Enhanced cell elongation by auxin is explained by the "acid growth theory" which stipulates that extracellular acidification caused by auxin induces cell wall loosening, thus increasing cell wall extensibility and cell expansion (Majda and Robert 2018). However, the tissue-specific difference in auxin sensitivity of root tissues has not yet been elucidated (Dünser and Kleine-Vehn 2015). On the other hand, it was shown that root tip swelling induced by reduced cellulose synthesis, as observed in *fei1 fei2* mutants, can be inhibited by decreased auxin accumulation (Steinwand et al. 2014). It was speculated that reduced auxin might increase cell wall rigidity to constrict radial cell expansion caused by reduced cellulose synthesis in the *fei1 fei2* mutant (Steinwand et al. 2014). As noted earlier, *Arabidopsis* cell cultures with compromised cellulose synthesis after CBI treatment also show radial cell expansion at the end of cell files (Duval et al. 2005) (Suppl. Fig. S2). In contrast to results obtained in root tissues, addition of exogenous auxin to in Arabidopsis cell cultures inhibited cellular hypertrophy (Suppl. Fig. 2). It is possible that auxin induces modifications in the cell wall composition or organization. This would most likely affect the mechanical strength of the cell walls and prevent cell death induced by CBI. To explore this possibility,

we used Atomic Force Microscopy (AFM) to evaluate the elastic modulus of living cells treated or not with IXB, TA, auxin (IAA and 2,4-D) or a combination of auxin and CBI (Fig. 4). AFM can be used as a topographic imaging tool to visualize and characterize the cell wall and in particular, the cellulose microfibril network (Marga et al. 2005). Here, a modified AFM-based approach, called AFM stiffness tomography, was used to measure mechanical properties of the cell wall in living cells (Radotić et al. 2012).

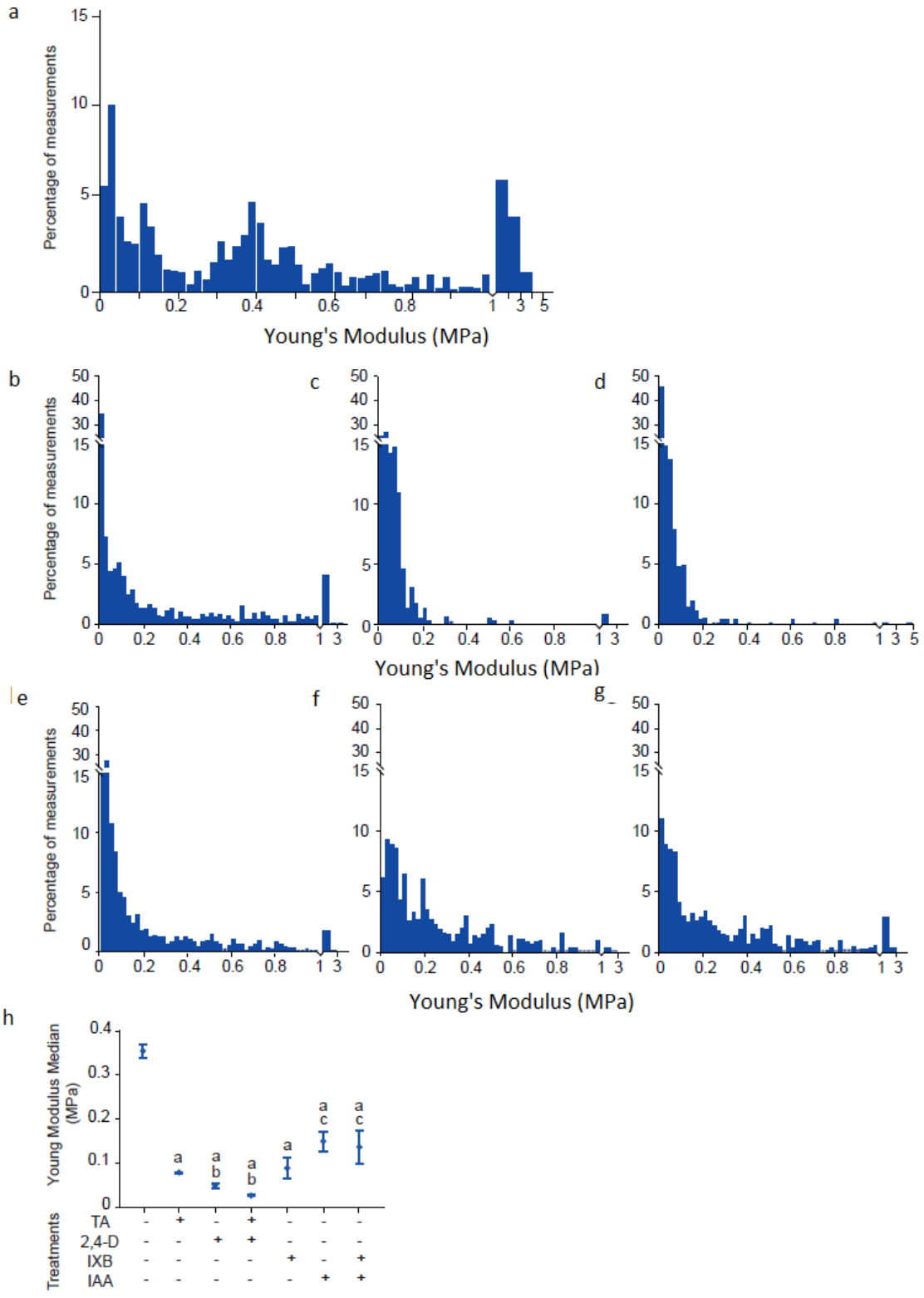
a
Percentage of measurements
Young's Modulus (MPa)
b
c
d
e
f
g
h
Young Modulus Median (MPa)
Treatments
TA
2,4-D
IXB
IAA

Figure 2.4 CBIs and auxin decrease cell wall stiffness

Atomic force microscopy (AFM) was used to measure cell wall stiffness profiles of *Arabidopsis* suspension-cultured cells treated with: a) methanol (control), b) thaxtomin A (TA; 1 µM), c) 2,4-dichlorophenoxyacetic acid (2,4-D; 50 µM), d) 2,4-D and TA, e) isoxaben (IXB; 1 µM), f), IAA (1 µM), g) IAA and IXB for 24 h. Force curves were recorded at the surface of 3 cells per condition in order to extract Young's modulus (MPa) values (see Material and Methods). Each histogram bar represents the relative proportion of Young's modulus values measured on the cell surface in each condition. Because of the low proportion of values measured above 1 MPa, a scale change was used after 1 MPa. h) Average median values of Young's modulus were calculated for each condition from 3 different experiments (3 to 4 cells per experiment). Error bars represent SD. Statistically different values (t-test followed by Holm-Šídák method, $p < 0.05$) are indicated by different letters.

Arabidopsis cells treated with the indicated concentrations of auxin and/or CBI were compared to untreated cells originating from the same culture. Hence, any differences in the elastic modulus (Young's modulus) measured on the cell surface could be attributed to changes induced by the different CBI and auxin treatments. Since cell wall elastic modulus can be altered by the presence of organelles below the measured points, we selected five regions on each cell and optical image to confirm the absence of organelles below each batch of measurements. The histograms in Fig. 2.4 show the distribution percentage of measured Young's modulus with values ranging from 0 to 5 MPa for each treatment. We also calculated the average median of Young's modulus values for each treatment as summarized in Fig.2. 4h.

In control cells (Fig. 2.4a), Young's modulus values were broadly distributed over the entire measuring range, with less than 39% of values found below 0.2 MPa, and about 30 % found between 0.2 and 1 MPa. In contrast, addition of TA or IXB to *Arabidopsis* cells lead to a decrease in Young's modulus values compared to the control (Fig. 2.4 b and e) with more than 60% of the measurements below 0.2 MPa. Accordingly, the Young's modulus average median values (Fig.2.4 h) calculated for TA- or IXB-treated cells (about 0.10 MPa) were significantly lower than the Young's modulus average median of control cells (0.35 MPa), demonstrating a significant drop in cell wall stiffness.

Auxin effect on cell wall rigidity was also evaluated. In 2,4-D-treated cells (Fig.2.4 c), more than 90% of Young's modulus values were found below 0.2 MPa, indicating a drastic reduction in cell wall stiffness. The combination of both 2,4-D and TA treatments decreased even further cell wall stiffness compared to individual treatments (Fig. 2.4 d). This effect was also reflected in calculated Young's modulus medians (Fig.2. 4 h). In comparison to control cells, cells treated with 2,4-D alone or in combination with TA showed significantly lower Young's modulus average median value of 0.05 and 0.03 MPa respectively, suggesting an additive effect of 2,4-D and TA on cell wall stiffness. Cells treated with the natural auxin IAA alone also showed a decreased cell wall rigidity, with 58% of Young's modulus values distributed below 0.2 MPa (Fig.2. 4g) and a Young's modulus average median of 0.15 MPa (Fig.2. 4h). However, this effect was not as dramatic as that of 2,4-D, which may be explained by the faster metabolic degradation of IAA compared to the metabolically stable 2,4-D (Seifertová et al. 2014). When IAA and IXB treatments were combined (Fig. 2.4g), we found a Young's modulus distribution of values comparable to that after IAA treatment, with 52% of Young's modulus values below 0.2 MPa, and a Young's modulus average median value of 0.14 MPa, indicating again a decrease in cell wall stiffness compared to control cells. However, in contrast to cells treated with both 2,4-D and TA, no cumulative effect was detected when IXB and IAA were added at the same time. Overall, these results indicated that CBI and auxin treatments all reduce cell wall stiffness.

Cellulose microfibrils are the main load-bearing components of the cell wall, it is not surprising that inhibition of cellulose synthesis by TA or IXB comprised the cell wall rigidity in *Arabidopsis* cell cultures. Reduced cell wall stiffness in response to auxin also corresponds to their widely recognized role in stimulating cell wall loosening that generally leads to turgor-driven cell expansion. However, our results indicate that the protective role of auxin against CBI-induced PCD does not rely on increasing cell wall stiffness to compensate for the mechanical perturbation induced by inhibition of cellulose synthesis. Still, our results do not exclude the possibility that other compensatory mechanisms in the composition and organization of the cell wall are induced by auxin, but these changes clearly do not increase

the cell wall stiffness. Interestingly, modulation of the cell wall composition has been reported in plant cells habituated to different CBIs, such as dichlobenil, isoxaben and thaxtomin A, suggesting that plant cells can survive to CBIs with a modified cell wall (Brochu et al. 2010; Encina et al. 2001; Manfield et al. 2004; Mélida et al. 2009). However, changes in the cell wall composition during cell habituation to CBI occur gradually over a long period of several weeks or even months. Whether auxin can rapidly stimulate similar changes in *Arabidopsis* cell cultures remains to be shown.

On the other hand, our results also show that auxin can repress cell elongation despite reducing cell wall stiffness, suggesting that reduced cell expansion is not, in this case at least, strictly associated with an increase in cell wall stiffness. Interestingly, work by Löfke et al., 2015, has shown that restriction of cell growth in root tissues by auxin may be based on an auxin-dependent signaling that controls the vacuolar morphology and occupancy of growing cells (Löfke et al. 2015). Accordingly, restriction of cellular vacuolarisation by auxin would limit cell growth. More recently, it was found that the auxin-regulated vacuolar occupancy is in fact controlled by an actin-dependent mechanism (Scheuring et al. 2016). It would be interesting to determine if changes in vascularization induced in root tissues by auxin are also associated with decreased cell wall stiffness. This indicates that decreased cell wall stiffness *in planta* does not necessarily correlate with cell elongation.

2.7 CONCLUSION

We have shown that exogenous addition of synthetic and natural auxins to *Arabidopsis* cell cultures can inhibit PCD induced by two structurally different CBIs, TA and IXB. For both CBIs, initiation of cell death depended on an increase in cytosolic calcium originating from external and internal sources, which suggests that calcium is an early step in the signaling cascade leading to CBI-induced PCD. Accumulation of endogenous auxin stimulated by auxin efflux inhibitors (NPA and TIBA) was also shown to protect cells from CBI-induced PCD. These findings corroborated work by others who showed that some development- or defense-

related PCDs can be inhibited by auxin. Auxin may also protect from CBI-induced cell death by inducing changes in the cell wall composition and organization to compensate for reduced cellulose synthesis. However, cell wall stiffness evaluated using AFM was reduced by auxin, showing that auxin-mediated protection against CBI-induced PCD does not depend on reinforcement of the cell wall.

These findings suggest that auxin plays an important role in the cell life and death decisions in response to cell wall perturbations. There are various possibilities that need to be investigated to explain the protective effect of auxin against CBI-induced PCD. One possibility is that auxin, which can restore a normal and dynamic actin configuration, would prevent cell death by inhibiting actin bundling that may occur in response to CBI and that normally precedes PCD. It is also possible that reduced cell wall stiffness induced by auxin is associated with cell wall modifications that alleviate changes induced by CBIs, as seen previously in CBI-habituated cells (Duval et al., 2005). Moreover, it was suggested that auxin or auxin signaling may interact with the signaling cascade induced by cell wall perturbation (Steinwand et al. 2014) that leads to PCD in *Arabidopsis* cell cultures. Finally, we cannot exclude the possibility that a combination of several events induced by auxin are involved in the inhibition of PCD. Further studies are currently in progress to evaluate these possibilities.

2.8 Conflict of interest

The authors declare that they have no conflict of interest.

2.9 REFERENCES

Beaulieu C, Goyer C, Beaudoin N (2008) Interaction between pathogenic streptomycetes and plants: The role of thaxtomins. In: Barka EA, Clément C (eds) Plant-Microbe Interactions. Research Signpost, pp 117-133

Bethke G et al. (2016) Pectin biosynthesis is critical for cell wall integrity and immunity in *Arabidopsis thaliana*. Plant Cell 28:537-556. doi:10.1105/tpc.15.00404

Bischoff V, Cookson SJ, Wu S, Scheible WR (2009) Thaxtomin A affects CeSA-complex density, expression of cell wall genes, cell wall composition, and causes ectopic lignification in *Arabidopsis thaliana* seedlings. J Exp Bot 60:955-965. doi:10.1093/jxb/ern344

Brabham C, Debolt S (2012) Chemical genetics to examine cellulose biosynthesis. Front Plant Sci 3:309. doi:10.3389/fpls.2012.00309

Braun S, Gevens A, Charkowski A, Allen C, Jansky S (2017) Potato common scab: A review of the causal pathogens, management practices, varietal resistance screening methods, and host resistance. Am J Potato Res 94:283-296. doi:10.1007/s12230-017-9575-3

Brochu V et al. (2010) Habituation to thaxtomin A in hybrid poplar cell suspensions provides enhanced and durable resistance to inhibitors of cellulose synthesis. BMC Plant Biol 10:272. doi:10.1186/1471-2229-10-272

Caño-Delgado A, Penfield S, Smith C, Catley M, Bevan M (2003) Reduced cellulose synthesis invokes lignification and defense responses in *Arabidopsis thaliana*. Plant J 34:351-362. doi:10.1046/j.1365-313X.2003.01729.x

Chang X, Riemann M, Liu Q, Nick P (2015) Actin as deathly switch? How auxin can suppress cell-death related defence. PLoS One 10:e0125498. doi:10.1371/journal.pone.0125498

Choi WG, Toyota M, Kim SH, Hilleary R, Gilroy S (2014) Salt stress-induced Ca^{2+} waves are associated with rapid, long-distance root-to-shoot signaling in plants. Proc Natl Acad Sci USA 111:6497-6502. doi:10.1073/pnas.1319955111

Cosgrove DJ (2005) Growth of the plant cell wall. Nat Rev Mol Cell Biol 6:850-861. doi:10.1038/nrm1746

Cosgrove DJ (2016) Plant cell wall extensibility: connecting plant cell growth with cell wall structure, mechanics, and the action of wall-modifying enzymes. J Exp Bot 67:463-476. doi:10.1093/jxb/erv511

Cosgrove DJ (2018) Diffuse growth of plant cell walls. Plant Physiol 176:16-27. doi:10.1104/pp.17.01541

Desprez T et al. (2002) Resistance against herbicide isoxaben and cellulose deficiency caused by distinct mutations in same cellulose synthase isoform CeSA6. Plant Physiol 128:482-490. doi:10.1104/pp.010822

Dodd AN, Kudla J, Sanders D (2010) The language of calcium signaling. Annu Rev Plant Biol 61:593-620. doi:10.1146/annurev-arplant-070109-104628

Dünser K, Kleine-Vehn J (2015) Differential growth regulation in plants - the acid growth balloon theory. Curr Opin Plant Biol 28:55-59. doi:10.1016/j.pbi.2015.08.009

Duval I, Beaudoin N (2009) Transcriptional profiling in response to inhibition of cellulose synthesis by thaxtomin A and isoxaben in *Arabidopsis thaliana* suspension cells. Plant Cell Rep 28:811-830. doi:10.1007/s00299-009-0670-x

Duval I, Brochu V, Simard M, Beaulieu C, Beaudoin N (2005) Thaxtomin A induces programmed cell death in *Arabidopsis thaliana* suspension-cultured cells. Planta 222:820-831. doi:10.1007/s00425-005-0016-z

Ellis C, Karafyllidis I, Wasternack C, Turner JG (2002) The *Arabidopsis* mutant *cev1* links cell wall signaling to jasmonate and ethylene responses. Plant Cell 14:1557-1566. doi:10.1105/tpc.002022

Encina AE, Moral RM, Acebes JL, Álvarez JM (2001) Characterization of cell walls in bean (*Phaseolus vulgaris* L.) callus cultures tolerant to dichlobenil. Plant Sci 160:331-339. doi:10.1016/S0168-9452(00)00397-6

Errakhi R et al. (2008) An early Ca^{2+} influx is a prerequisite to thaxtomin A-induced cell death in *Arabidopsis thaliana* cells. J Exp Bot 59:4259-4270. doi:10.1093/jxb/ern267

Feng W et al. (2018) The FERONIA receptor kinase maintains cell-wall integrity during salt stress through Ca^{2+} signaling. Curr Biol 28:666-675 e665. doi:10.1016/j.cub.2018.01.023

Feraru E et al. (2011) PIN polarity maintenance by the cell wall in *Arabidopsis*. Curr Biol 21:338-343. doi:10.1016/j.cub.2011.01.036

Fry BA, Loria R (2002) Thaxtomin A: evidence for a plant cell wall target. Physiol Mol Plant Pathol 60:1-8. doi:10.1006/pmpp.2001.0371

Fu J, Wang S (2011) Insights into auxin signaling in plant-pathogen interactions. Front Plant Sci 2:74. doi:10.3389/fpls.2011.00074

Garcia-Brugger A et al. (2006) Early signaling events induced by elicitors of plant defenses. Mol Plant Microbe Interact 19:711-724. doi:10.1094/MPMI-19-0711

Gopalan S (2008) Reversal of an immunity associated plant cell death program by the growth regulator auxin. BMC Res Notes 1:126. doi:10.1186/1756-0500-1-126

Goyer C, Vachon J, Beaulieu C (1998) Pathogenicity of *Streptomyces scabies* mutants altered in thaxtomin A production. Phytopathology 88:442-445. doi:10.1094/PHYTO.1998.88.5.442

Healy FG, Wach M, Krasnoff SB, Gibson DM, Loria R (2000) The txtAB genes of the plant pathogen *Streptomyces acidiscabies* encode a peptide synthetase required for phytotoxin thaxtomin A production and pathogenicity. Mol Microbiol 38:794-804. doi:10.1046/j.1365-2958.2000.02170.x

Hong JH et al. (2017) A sacrifice-for-survival mechanism protects root stem cell niche from chilling stress. Cell 170:102-113.e114. doi:10.1016/j.cell.2017.06.002

Hu XY, Neill SJ, Cai WM, Tang ZC (2004) Induction of defence gene expression by oligogalacturonic acid requires increases in both cytosolic calcium and hydrogen peroxide in *Arabidopsis thaliana*. Cell Res 14:234-240. doi:10.1038/sj.cr.7290224

Hutter JL, Bechhoefer J (1993) Calibration of atomic-force microscope tips. Rev Sci Instrum 64:1868-1873. doi:10.1063/1.1143970

Huysmans M, Lema AS, Coll NS, Nowack MK (2017) Dying two deaths - programmed cell death regulation in development and disease. Curr Opin Plant Biol 35:37-44. doi:10.1016/j.pbi.2016.11.005

Kazan K, Manners JM (2009) Linking development to defense: auxin in plant-pathogen interactions. Trends Plant Sci 14:373-382. doi:10.1016/j.tplants.2009.04.005

Keegstra K (2010) Plant cell walls. Plant Physiol 154:483-486. doi:10.1104/pp.110.161240

King RR, Lawrence CH, Calhoun LA (1992) Chemistry of phytotoxins associated with *Streptomyces scabies*, the causal organism of potato common scab. J Agric Food Chem 40:834-837. doi:10.1021/jf00017a025

King RR, Lawrence CH, Clark MC (1991) Correlation of phytotoxin production with pathogenicity of *Streptomyces scabies* isolates from scab infected potato tubers. Am Potato J 68:675-680. doi:10.1007/BF02853743

Kurusu T, Kuchitsu K, Nakano M, Nakayama Y, Iida H (2013) Plant mechanosensing and Ca^{2+} transport. Trends Plant Sci 18:227-233. doi:10.1016/j.tplants.2012.12.002

Larsson E, Sitbon F, Ljung K, von Arnold S (2008) Inhibited polar auxin transport results in aberrant embryo development in Norway spruce. New Phytol 177:356-366. doi:10.1111/j.1469-8137.2007.02289.x

Lawrence CH, Clark MC, King RR (1990) Induction of common scab symptoms in aseptically cultured potato tubers by the vivotoxin, thaxtomin. Phytopathology 80:606-608. doi:10.1094/Phyto-80-606

Lecourieux D, Ranjeva R, Pugin A (2006) Calcium in plant defence-signalling pathways. New Phytol 171:249-269. doi:10.1111/j.1469-8137.2006.01777.x

Lehman TA, Smertenko A, Sanguinet KA (2017) Auxin, microtubules, and vesicle trafficking: conspirators behind the cell wall. J Exp Bot 68:3321-3329. doi:10.1093/jxb/erx205

Levesque-Tremblay G, Pelloux J, Braybrook SA, Müller K (2015) Tuning of pectin methylesterification: consequences for cell wall biomechanics and development. Planta 242:791-811. doi:10.1007/s00425-015-2358-5

Link VL, Hofmann MG, Sinha AK, Ehness R, Strnad M, Roitsch T (2002) Biochemical evidence for the activation of distinct subsets of mitogen-activated protein kinases by voltage and defense-related stimuli. Plant Physiol 128:271-281. doi:10.1104/pp.010569

Lionetti V, Fabri E, De Caroli M, Hansen AR, Willats WG, Piro G, Bellincampi D (2017) Three Pectin Methylesterase Inhibitors protect cell wall integrity for *Arabidopsis* immunity to *Botrytis*. Plant Physiol 173:1844-1863. doi:10.1104/pp.16.01185

Löfke C, Dünser K, Scheuring D, Kleine-Vehn J (2015) Auxin regulates SNARE-dependent vacuolar morphology restricting cell size. Elife 4. doi:10.7554/eLife.05868

Loria R et al. (2008) Thaxtomin biosynthesis: the path to plant pathogenicity in the genus *Streptomyces*. Antonie van Leeuwenhoek 94:3-10. doi:10.1007/s10482-008-9240-4

Loria R, Kers J, Joshi M (2006) Evolution of plant pathogenicity in *Streptomyces*. Annu Rev Phytopathol 44:469-487. doi:10.1146/annurev.phyto.44.032905.091147

Maisch J, Nick P (2007) Actin is involved in auxin-dependent patterning. Plant Physiol 143:1695-1704. doi:10.1104/pp.106.094052

Majda M, Robert S (2018) The role of auxin in cell wall expansion. Int J Mol Sci 19, 951. doi:10.3390/ijms19040951

Manfield IW et al. (2004) Novel cell wall architecture of isoxaben-habituated *Arabidopsis* suspension-cultured cells: global transcript profiling and cellular analysis. Plant J 40:260-275. doi:10.1111/j.1365-313X.2004.02208.x

Marga F, Grandbois M, Cosgrove DJ, Baskin TI (2005) Cell wall extension results in the coordinate separation of parallel microfibrils: evidence from scanning electron microscopy and atomic force microscopy. Plant J 43:181-190. doi:10.1111/j.1365-313X.2005.02447.x

McFarlane HE, Döring A, Persson S (2014) The cell biology of cellulose synthesis. Annu Rev Plant Biol 65:69-94. doi:10.1146/annurev-arplant-050213-040240

Meimoun P et al. (2009) Two different signaling pathways for thaxtomin A-induced cell death in *Arabidopsis* and tobacco BY2. Plant Signal Behav 4:142-144. doi:10.4161/psb.4.2.7719

Mélida H, García-Angulo P, Alonso-Simón A, Encina A, Álvarez J, Acebes JL (2009) Novel type II cell wall architecture in dichlobenil-habituated maize calluses. Planta 229:617-631. doi:10.1007/s00425-008-0860-8

Nafisi M, Fimognari L, Sakuragi Y (2015) Interplays between the cell wall and phytohormones in interaction between plants and necrotrophic pathogens. Phytochemistry 112:63-71. doi:10.1016/j.phytochem.2014.11.008

Nick P (2010) Probing the actin-auxin oscillator. Plant Signal Behav 5:94-98. doi:10.4161/psb.5.2.10337

Paredez AR, Somerville CR, Ehrhardt DW (2006) Visualization of cellulose synthase demonstrates functional association with microtubules. Science 312:1491-1495. doi:10.1126/science.1126551

Perrot-Rechenmann C (2010) Cellular responses to auxin: division versus expansion. Cold Spring Harb Perspect Biol 2:a001446. doi:10.1101/cshperspect.a001446

Petrášek J, Černá A, Schwarzerová K, Elčkner M, Morris DA, Zažímalová E (2003) Do phytotropins inhibit auxin efflux by impairing vesicle traffic? Plant Physiol 131:254-263. doi:10.1104/pp.012740

Petti C, Reiber K, Ali SS, Berney M, Doohan FM (2012) Auxin as a player in the biocontrol of *Fusarium* head blight disease of barley and its potential as a disease control agent. BMC Plant Biol 12:224. doi:10.1186/1471-2229-12-224

Radotić K et al. (2012) Atomic force microscopy stiffness tomography on living *Arabidopsis thaliana* cells reveals the mechanical properties of surface and deep cell-wall layers during growth. Biophys J 103:386-394. doi:10.1016/j.bpj.2012.06.046

Reddy AS (2001) Calcium: silver bullet in signaling. Plant Sci 160:381-404. doi:10.1016/S0168-9452(00)00386-1

Rubery P, Sheldrake A (1974) Carrier-mediated auxin transport. Planta 118:101-121. doi:10.1007/BF00388387

Scheible WR, Eshed R, Richmond T, Delmer D, Somerville C (2001) Modifications of cellulose synthase confer resistance to isoxaben and thiazolidinone herbicides in *Arabidopsis Ixr1* mutants. Proc Natl Acad Sci USA 98:10079-10084. doi:10.1073/pnas.191361598

Scheible WR et al. (2003) An *Arabidopsis* mutant resistant to thaxtomin A, a cellulose synthesis inhibitor from *Streptomyces* species. Plant Cell 15:1781-1794. doi:10.1105/tpc.013342

Scheuring D et al. (2016) Actin-dependent vacuolar occupancy of the cell determines auxin-induced growth repression. Proc Natl Acad Sci U S A 113:452-457. doi:10.1073/pnas.1517445113

Schindelin J et al. (2012) Fiji: an open-source platform for biological-image analysis. Nat Methods 9:676. doi:10.1038/nmeth.2019

Seifertová D et al. (2014) Characterization of transmembrane auxin transport in *Arabidopsis* suspension-cultured cells. J Plant Physiol 171:429-437. doi:10.1016/j.jplph.2013.09.026

Smertenko A, Franklin-Tong VE (2011) Organisation and regulation of the cytoskeleton in plant programmed cell death. Cell Death Differ 18:1263-1270. doi:10.1038/cdd.2011.39

Steinwand BJ, Xu S, Polko JK, Doctor SM, Westafer M, Kieber JJ (2014) Alterations in auxin homeostasis suppress defects in cell wall function. PLoS ONE 9:e98193. doi:10.1371/journal.pone.0098193

Tateno M, Brabham C, DeBolt S (2016) Cellulose biosynthesis inhibitors - a multifunctional toolbox. J Exp Bot 67:533-542. doi:10.1093/jxb/erv489

Tegg RS, Gill WM, Thompson HK, Davies NW, Ross JJ, Wilson CR (2008) Auxin-induced resistance to common scab disease of potato linked to inhibition of thaxtomin A toxicity. Plant Dis 92:1321-1328. doi:10.1094/PDIS-92-9-1321

Tegg RS, Melian L, Wilson CR, Shabala S (2005) Plant cell growth and ion flux responses to the streptomycete phytotoxin thaxtomin A: calcium and hydrogen flux patterns revealed by the non-invasive MIFE technique. Plant Cell Physiol 46:638-648. doi:10.1093/pcp/pci069

Tegg RS, Shabala SN, Cuin TA, Davies NW, Wilson CR (2013) Enhanced resistance to the cellulose biosynthetic inhibitors, thaxtomin A and isoxaben in *Arabidopsis thaliana mutants*, also provides specific co-resistance to the auxin transport inhibitor, 1-NPA. BMC Plant Biol 13:76. doi:10.1186/1471-2229-13-76

Tolmie F, Poulet A, McKenna J, Sassmann S, Graumann K, Deeks M, Runions J (2017) The cell wall of *Arabidopsis thaliana* influences actin network dynamics. J Exp Bot 68:4517-4527. doi:10.1093/jxb/erx269

Tsang DL, Edmond C, Harrington JL, Nühse TS (2011) Cell wall integrity controls root elongation via a general 1-aminocyclopropane-1-carboxylic acid-dependent, ethylene-independent pathway. Plant Physiol 156:596-604. doi:10.1104/pp.111.175372

White PJ, Broadley MR (2003) Calcium in plants. Ann Bot 92:487-511. doi:10.1093/aob/mcg164

Yu T, Zhang H, Li X, Zheng X (2008) Biocontrol of *Botrytis cinerea* in apple fruit by *Cryptococcus laurentii* and indole-3-acetic acid. Biol Control 46:171-177. doi:10.1016/j.biocontrol.2008.04.008

Zhang J et al. (2018) Indole-3-acetic acid inhibits blue mold rot by inducing resistance in pear fruit wounds. Sci Hortic 231:227-232. doi:10.1016/j.scienta.2017.12.046

2.10 SUPPLEMENTARY MATERIAL

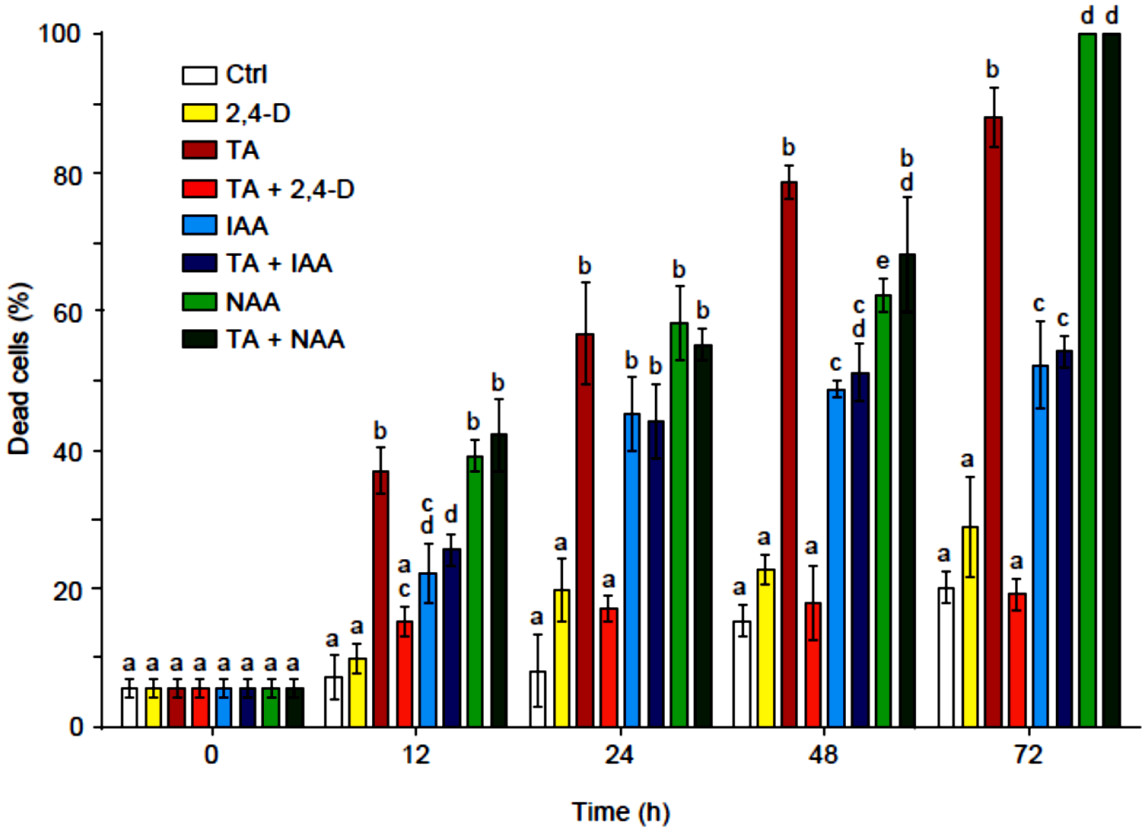

Suppl. Figure S1 Auxin increases cell survival in thaxtomin A-treated cells.
Percentage of cell death in *Arabidopsis* suspension-cultured cells at the indicate time after treatment with: 2,4-dichlorophenoxyacetic acid (2,4-D: 50 µM), thaxtomin A (TA: 1 µM), indole-acetic acid (IAA: 30 µM), 1-naphthaleneacetic acid (NAA; 30 µM) or combined treatments of TA with either 2,4-D, IAA or NAA.
Each time point represents the average value of three different experiments including 500 cells each. Error bars indicate SD. Statistically different values (t-test followed by Holm-Šídák method, $p < 0.05$) are indicated by a different letter within each time point.

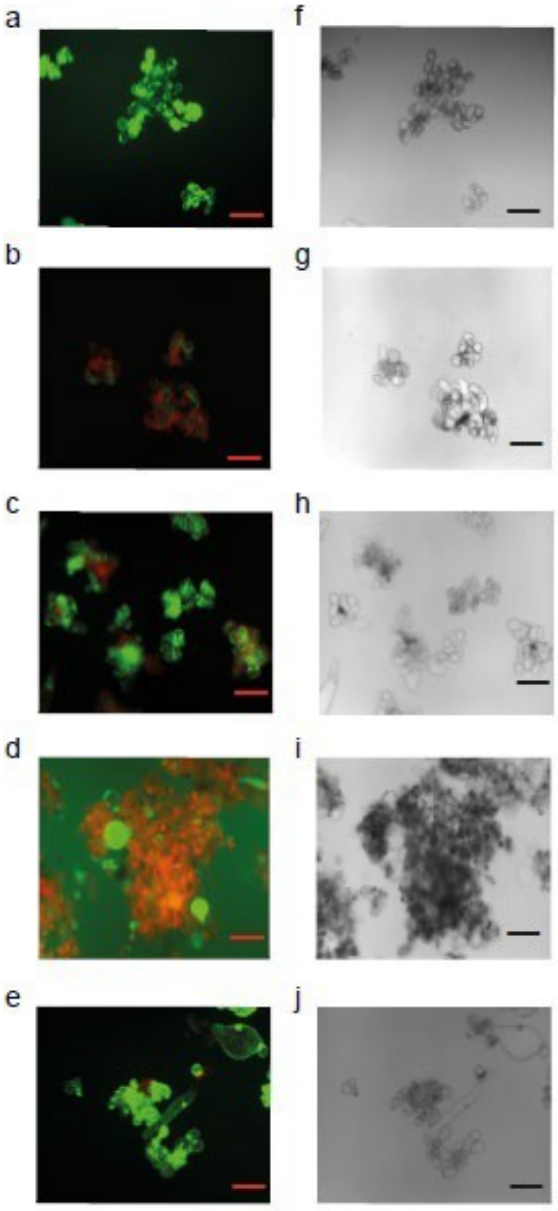

Suppl. Figure S2 Visualization of cell death in *Arabidopsis* suspension-cultured cells in presence of CBIs and auxin.

Cells were vizualized 48 h after the addition of auxin and/or cellulose biosynthesis inhibitor using epifluorescence microscopy (**a-e**) or light microscopy (**f-j**).Treatments: **a** and **f**: Control (methanol); **b** and **g**: Thaxtomin A (TA: 1 µM); **c** and **h**: TA (1 µM) + 2,4-dichlorophenoxyacetic acid (2,4-D: 50 µM); **d** and **i**: Isoxaben (IXB: 1 µM); **e** and **j**: IXB (1 µM) + IAA (1 µM). **a-e**: Cells were stained with propidium iodine (PI) and fluorescein diacetate (FDA) to detect dead (red) and living cells (green). **f-j**: Cells were stained with trypan blue to detect dead cells (black). Images were taken with upright microscope Zeiss Z1 imager. Scale = 200 µm.

CHAPITRE 3

Analyse de l'effet de la thaxtomine A sur la vitesse des cellulose synthases, la qualité de la cellulose produite et la dynamique des microtubules.

3.1 INTRODUCTION DE L'ARTICLE ET CONTRIBUTION DES AUTEURS

Bien que la TA soit étudiée depuis plus d'une vingtaine d'années maintenant, on ne sait toujours pas le mécanisme exact par lequel elle inhibe la synthèse de la cellulose. Dans cette partie de ma thèse, j'ai étudié la dynamique de la surface cellulaire en présence de la TA. Dans un premier temps, je montre, par microscopie à force atomique, que la TA affecte l'expansion des microfibrilles de cellulose dans les cellules en suspension d'*Arabidopsis thaliana*. De plus, je présente le comportement des microtubules en présence de la toxine, ainsi que les changements observés dans la vitesse des CeSA6 et ce dans des lignées transgéniques coexprimant la tubuline6 et CeSA6 avec des protéines fluorescentes. Enfin, je montre l'effet de la TA sur des mutants dont la cristallinité de la cellulose est altérée, ce qui suggère qu'une cristallinité élevée de la cellulose est capable d'alléger l'effet de la TA.

Ma contribution à ce projet comprend l'exécution de la totalité des expériences présentées et la préparation de l'article pour soumission. J'ai effectué une partie des travaux (imagerie en temps réel) sous la supervision du Dr. Geoff Wasteneys dans son laboratoire de l'université de Colombie Britannique (UBC) à Vancouver. J'ai réalisé la partie concernant l'analyse des extraits de la paroi en microscopie à force atomique dans le laboratoire du Dr. Michel Grandbois à l'Institut de pharmacologie de Sherbrooke à Fleurimont. La totalité des travaux a été dirigé par Dre Nathalie Beaudoin.

Le manuscrit présenté dans la section suivante est préparé pour être soumis à la revue internationale *The Cell Surface*.

OVERTHAXING CELL WALL DYNAMICS: THAXTOMIN A CHANGES CELLULOSE QUALITY AND MICROTUBULE ORIENTATION.

Fatima Awwad, Guillaume Bertrand, Miki Fujita, Marcus Woodley, Michel Grandbois, Geoffrey Wasteneys, Nathalie Beaudoin*.

*Corresponding author

3.2 ABSTRACT

The plant cell wall is an essential structure allowing plants to thrive and survive to biotic and abiotic stresses. The cell wall also plays a major role in growth and development mainly by its high dynamism. Several synthetic compounds act as cellulose biosynthesis inhibitors (CBI) to compromise cell wall stability in plant cells. In contrast, thaxtomin A is a natural CBI synthesized by the plant pathogen *Streptomyces scabies,* the main causal agent of common scab on potato tubers. The specific mode of action and target of thaxtomin A are still unknown. To better understand how thaxtomin A perturbs cellulose synthesis and cell wall organization, we analyzed cell wall and cellulose extracts from thaxtomin A-treated *Arabidopsis* cells using atomic force microscopy. We also studied the impact of thaxtomin A on cellulose synthase velocity and microtubule organization using *Arabidopsis* transgenic seedlings expressing tubulin and cellulose synthase linked to yellow and red fluorescent protein respectively. Our results show that cell wall dynamics is affected by thaxtomin A since it altered cellulose quality, changed microtubule orientation and reduced cellulose synthase velocity. Finally, we evaluated the effect of thaxtomin A on the growth of various microtubule-associated protein *Arabidopsis* mutants. We found that mutants with high cellulose crystallinity were more tolerant to thaxtomin A while mutants with reduced cellulose crystallinity were overly sensitive to thaxtomin A. These studies bring a deeper understanding of the specific mode of action of this toxin and demonstrate that thaxtomin A can be used as a novel tool to understand cell wall dynamics in living cells.

Keywords: Thaxtomin A, cellulose synthesis, cell wall, microtubules

Highlights

Cellulose synthase velocity in *Arabidopsis* seedlings decreases after short treatment with thaxtomin A.

Microtubules orientation is compromised by thaxtomin A.

Abbreviations

AFM Atomic Force Microscopy

CBI Cellulose Biosynthesis Inhibitor

CeSA Cellulose Synthase

CSC Cellulose Synthesis Complex

CDTA *t*-1,2-diaminecyclohexane-N,N,N′,N′-tetraacetic acid sodium salt

CTRL Control

MAP Microtubule Associated Protein

MTs Microtubules

PCD Programmed Cell Death

PCW Primary Cell Wall

TA Thaxtomin A

3.3 INTRODUCTION

The plant cell wall is important for cell structure, cell elongation, protection from the environment, plant growth and development. This dynamic structure of cellulose, hemicellulose and pectin can be modified by enzymatic and non-enzymatic proteins to modulate its elasticity and extensibility in response to growth signals or environmental changes (Chebli and Geitmann, 2017).

In primary cell walls (PCW), cellulose confers rigidity while pectin modulates elasticity depending on methylesterification and acetylation, ion linking and hormonal effect (Braybrook and Peaucelle, 2013; Chebli and Geitmann, 2017). All these factors are decisive for cell fate during morphogenesis and organogenesis and can control cell survival (Duval et al., 2005). Pectin and hemicellulose are most probably synthesized in the Golgi and can be branched, substituted and modified to permit cell growth (Voiniciuc et al., 2018). Cellulose, the main structural constituent of the plant cell wall, is made of chains of β-1-4 glucose subunits that are linked by hydrogen bonds to form microfibrils, which in turn assemble in bundles and macrofibrils of fibers. Cellulose synthesis is mediated by enzymatic complexes made of cellulose synthases (CeSA) associated with other proteins with enzymatic functions such as membrane-bound cellulase KORRIGAN1 (KOR1; Lei et al., 2014). Although it has been proven that each CeSA is capable of synthesizing single glucan chain independently (Morgan et al., 2012), CeSAs are mostly found in rosette complexes. CeSA complexes (CSC) are laid down to predefined positions in the plasma membrane so that cellulose microfibrils can grow in a specific direction and pattern (Lei et al., 2015; Lindeboom et al., 2008). In *Arabidopsis*, ten CeSAs have been identified and are responsible for synthesizing primary and secondary cell wall cellulose (Richmond and Somerville, 2000). CSCs have been observed in trans-Golgian vesicles, as well as in the plasma membrane where they synthesize cellulose. CSCs are linked to microtubules (MTs) with different proteins such as Cellulose Synthase Interactive 1 (CSI1; Li et al., 2012). The motility of CSCs within the plasma membrane (PM) is dictated by polymerizing cellulose fibrils. The trajectories of CSC are aligned with the cortical MTs

(Paredez et al., 2006). Live-cell imaging has led to the identification CeSA trafficking compartments that allow CeSA delivery to the membrane.

These compartments are known as small CeSA compartments (SmaCCs) or microtubule-associated cellulose synthase compartments (MASCs, Crowell et al., 2009; Gutierrez et al., 2009). Formation of SmaCCs/MASCs has been shown to be more important in response to abiotic stresses such as osmotic deregulation (Lei et al., 2015)

Since Ledbetter and Porter's discovery of plant microtubules and their possible roles in cell division and cell wall formation (Ledbetter and Porter, 1970), MTs have been deeply studied to further understand their role in cell wall organisation and synthesis. In particular, several studies have looked at the polymerization and orientation of MTs and have identified MT-associated proteins as well as other elements involved in the control of MTs' dynamic instability. In particular, it was found that during cell wall formation, MTs dictate CeSAs position thereby orienting cellulose microfibrils deposition in the PCW (Paredez et al., 2006).

Cell wall stability is often compromised by inhibition of cellulose synthesis as mediated by synthetic molecules known as Cellulose biosynthesis inhibitors (CBI) such as Dichlobenil and Isoxaben, which are also widely used as herbicides (Tateno et al., 2016). Thaxtomin A (TA) is a natural CBI (Scheible et al., 2003). Thaxtomin A (TA) is a phytotoxin produced by the soil bacterium *Streptomyces scabies,* the main causal agent of potato common scab (King et al., 1989). The presence of TA has been shown to be essential for *S. scabies* to induce scab lesions on the potato periderm (Healy et al., 2000). Recently, studies have shown that TA is able to reduce cell wall rigidity after 24 h of treatment (see chap 2). However, there is little information on how inhibition of cellulose synthesis by TA specifically modifies cell wall rigidity.

Our main objective is to better understand the mode of action of TA. In this work, we showed that cellulose quality was compromised in the presence of TA since less crystalline cellulose fibers and shorter cellulose microfibrils were detected using atomic force microscopy in cells treated with TA. We also showed that the presence of TA led to a decrease in CeSA velocity in transgenic seedlings expressing CeSA6 and Tubulin6 with associated fluorescent proteins. Microtubule orientation was also altered minutes after treatment with TA and this reorientation

could be associated with inhibition of cell elongation. Finally, we studied the effect of TA on few microtubule-associated proteins/cellulose synthase mutants and found an interesting link between cellulose crystallinity *in vivo* and TA's effect.

3.4 MATERIALS AND METHODS

3.4.1 Plant material and growth condition

Wild-type and mutant seeds were from *Arabidopsis thaliana* accession Columbia (Col0). Seeds from *microtubule organization 1-1* (*mor1-1*; Whittington et al., 2001) and *anisotropy-1* (*any1*; Fujita et al., 2013) mutants from Dr. Wasteneys lab. Wild-type and mutant seeds were surface sterilized in a solution of 3% (v/v) hydrogen peroxide and 50% (v/v) ethanol for 2 min. After rinsing in sterilized water 5 times, seeds were sown on Petri plates containing Hoagland's medium and stored at 4°C for 3-5 days before being transferred vertically into a growth cabinet under constant light (80 µmol m^{-2} $second^{-1}$) at 22°C for 11-12 days. For *mor1-1,* the temperature shift was performed in a cabinet with similar light intensity using a constant temperature of 29°C constant temperature. We used seeds of homozygous transgenic lines expressing the yellow fluorescent protein (YFP) linked to the CeSA6 protein under control of the native CeSA6 promoter in a *CeSA6*-null mutant background (*prc1-1* : *CeSA6*-null; Fagard et al., 2000) and the red fluorescent protein RFP linked to TUBULIN 6.These lines will be referred in the text as YFP-CeSA6/*prc1-1* expressing mRFP-TUB6 (Fujita et al., 2011).

3.43.2 Confocal microscopy

For CeSA and microtubule imaging, we used a spinning disk confocal microscope composed of a modified Yokogawa CSU-10 spinning-disk scan head (Yokogawa Electric Corporation, http://www.yokogawa.com) and a Leica DMI6000 inverted microscope (http://www.leica.com/) equipped with a 63 × NA 1.3 glycerol lens.

3.4.3 YFP–CeSA6 velocity measurement

CeSA velocity measurement was carried using Multiple Kymograph plugins in ImageJ/Fiji (Schindelin et al., 2012) as described previously (Fujita et al., 2011).

3.4.4 Thaxtomin A purification

Thaxtomin A (TA) was prepared as described before (Duval et al. 2005). TA (stock of 1 mM) were diluted in DMSO and added at a final concentration of 1 µM. The same volume of DMSO (less than 0.1% of final volume) was added to control cells.

3.4.5 Cellulose extraction

To extract cell wall, suspension cells were treated for 24 h with DMSO (control) or 1 µM of TA. Cell wall was extracted as described by Encina with slight modifications (Encina et al, 2002). Briefly, *Arabidopsis* suspension cells were washed sequentially with 100 mM and 500 mM cold potassium phosphate buffer (pH 7.0), homogenized and treated with type VI α-amylase (Sigma Aldrich) for 4 h at 37°C. Cell walls were then treated with *t*-1,2-diaminecyclohexane-N,N,N′,N′-tetraacetic acid sodium salt (CDTA) and Na_2CO_3 and $NaBH_4$ to remove pectins, followed by addition of potassium buffers and acetic acid to solubilize hemicellulose. The residue was then hydrolysed for 2.5 h at 100°C with 2 M trifluoroacetic acid.

For purification of cellulose microfibrils, we proceeded as described by Davies et al. (2003) with some modifications. Briefly, *Arabidopsis thaliana* cell suspensions treated with DMSO (control) or 10 µM of TA for 24 hours were harvested and homogenised in Hepes-KOH buffer (20 mM, pH 7.2) containing 10 mM 2-mercaptoethanol. Samples were centrifuged and filtrated, and 50 mg of cell wall extract was treated twice with CDTA (50 mM, pH 6.5) at 80°C for 1 h, followed by 50 mM of Na_2CO_3 containing 25 mM NaBH4 at 1°C for 16 h then twice

at 20°C for 3h. After concentrating and purifying the extracts, a final resuspension in ultrapure water was performed before storing the sample or examining it using AFM.

3.4.6 AFM analysis

Suspensions of cell walls and purified cellulose microfibrils (10 µL) in water were spread onto a clean Mica sheet glued to a glass slide and observed using a JPK instruments NanoWizard® 4 V.6 (Berlin, Germany) mounted on a Zeiss imager Z1 microscope (Carl Zeiss Canada Ltd, Ontario, Canada). Suspensions of cell walls or cellulose microfibrils (10 µL) in water were spread onto a mica sheet and dried for 5 minutes in ambient air. AFM observations were performed using a JPK Instruments NanoWizard® 4 V.6 (Berlin, Germany). The cantilever used was a Bruker RTESPA (Bruker AFM probes, California, USA) with a nominal spring constant of 20-80 N/m and a resonant frequency around 300 KHz. Images were taken in non-contact mode in air.

3.5 RESULTS

3.5.1 Thaxtomin A affects cellulose quality

In order to investigate TA's effect on cellulose within the plant cell wall, we performed two different extractions of PCW from *Arabidopsis* suspension cells treated for 24 hours with DMSO as a negative controlled and 1 µM of TA. First, we used a mild cell wall extraction that allows the purification of cellulose microfibrils in the cell wall context without pectin and hemicellulose residues from primary cell walls (Encina et al., 2002). AFM non-contact mode was used to visualize these microfibrils in the lamellar structure of the PCW. We observed that cellulose microfibrils from cells treated with TA (Fig. 3.1b) had a narrower diameter than that of control cells (Fig. 3.1a). The second method allowed the purification of individualized cellulose microfibrils (Davies et.al, 2003). We visualized these crystallites using AFM non-

contact mode and estimated their length using JPKSPM Data processing software (VERSION ++6.0.16) from three independent extractions. We observed in both conditions, some cellulose microfibrils with similar length. However, there was an important population of shorter crystallites in TA-treated cells (102.12 nm ± 49.20, Fig. 3.1d) compared to crystallites from mock-treated cells (275.66 nm ± 67.8, Fig. 3.1c).

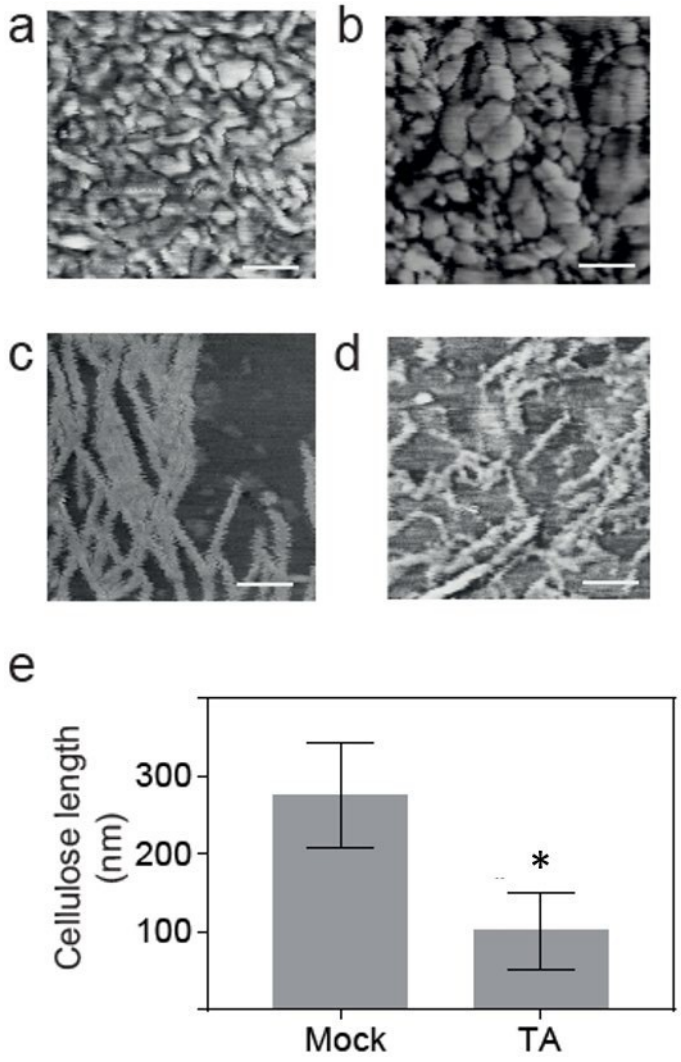

Figure 3.1 Effects of thaxtomin A on cellulose microfibrils in the cell wall surface of *Arabidopsis* cells.

Atomic force microscopy lock-in-phase topology maps of cellulose microfibrils in extracted cell wall (a-b) or purified cellulose microfibrils (c-d) from cells treated for 24 h with (a-c) DMSO as a control (b-d) 1 µM of thaxtomin A. Cellulose microfibrils length in nm was measured using ImageJ (e). Average length was calculated from 100 microfibrils from three

different cellulose extractions in each condition. Asterisks indicate significant differences using Student's *t* test with $P < 0.05$ ($P = 0.023$). Scale bars = 100 nm.

3.5.2 Cellulose synthase behavior in the presence of TA

To track cellulose synthase proteins behavior in the PCW in TA-treated cells, we used transgenic lines co-expressing CeSA6 tagged with yellow fluorescent protein reporter (CeSA6-YFP) and Tubulin 6 tagged with red fluorescent protein (mRFP-TUB6) in *CeSA6*-null mutant background *prc1-1* (Paredez et al., 2006). Observations were conducted on the upper hypocotyl cells since CeSA6 is expressed in fast elongating hypocotyls (Paredez et al., 2006). As shown in Fig. 3.2b, CeSA6 velocity was higher in mock cells (mean = 392.8 nm/min) than in cells treated with 5 µM of TA for 1 hour (mean = 311.7 nm/min). These results were confirmed in cells where TA was added at 10 µM for 1 h (mean= 303.8 nm/min) or in cells of seedlings that germinated on a medium containing 200 µM of TA (mean= 313.2 nm/min). The most affected velocity was in seedlings treated with 10 µM of TA for 30 s before mounting the sample for observation. In this case, CeSA6 velocity dropped more importantly than that of cells treated for 1 h (mean= 267.0 nm/min). This means that TA can compromise CeSA6 velocity from the first minutes of treatment.

On the other hand, there were some populations of non-motile CeSA6 observed in TA-treated seedlings (Video in S1-c). However, this was not detected in at least 5 of the15 cells that were used to calculate velocity in each condition, which prevents further generalization. We also observed higher compartmental fluorescence (brighter Golgi apparatus) as a result of CeSA6 internalization in the presence of TA (Fig.3.2a). Golgi apparatus compartments were identified due to the larger circular shape fluorescing in yellow. This observation suggests that TA promoted CeSA6 accumulation in Golgi.

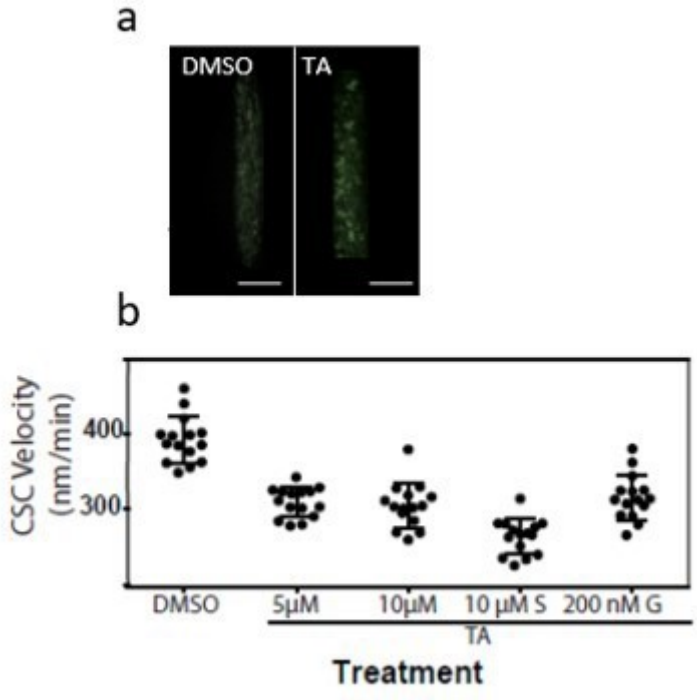

Figure 3.2 Thaxtomin A affects cellulose synthase 6 (CeSA6) velocity and distribution

Transgenic seedlings YFP-CeSA6/*prc1-1* expressing mRFP-TUB6 were treated with different concentrations of thaxtomin A (TA). Kymographs of YFP–CeSA6 particles, representing the position of particles in the selected trajectories over time at 29°C, were analysed in hypocotyl epidermal cells of dark-grown seedlings on Hoagland medium supplemented for 1 h with a) DMSO (less than 0.1%) on the left; 5 µM of thaxtomin A (right. Seedlings were visualized using a spinning disk confocal microscope with a 63 × NA 1.3 glycerol lens. Graph b) shows CeSA6 velocity variation (in nm/min) between four conditions (5 µM and 10 µM TA during one hour, 10 µM TA added spontaneously to the mounting medium (10 µM S) and finally velocity 3-days seedlings germinated in the presence of 200 nM TA in the growth medium (200 nM G). CeSA6 velocity was obtained by calculating 300 CeSA particles/condition in 5 different seedlings using ImageJ software to analyze individual CeSA particle slope from kymographs. Asterisks indicate significant differences by Student's *t* test at $P < 0.005$. Scale bars = 20 µm.

3.5.3 Thaxtomin A induces microtubule reorientation and arrests cell elongation

While observing CeSA6-YFP behavior in the presence of TA, we noticed a phenomenon in almost all cells treated spontaneously with TA. Before TA treatment, microtubules were found in a diagonal and perpendicular orientation to the cell elongation axis (Fig. 3.3 a). Upon TA addition, microtubules shifted toward a longitudinal and parallel orientation to the elongation axis 5 min (Fig. 3.3 b) and 30 min after TA addition (Fig. 3.3c). Within thirty minutes after adding TA, most microtubules (82%) were parallel to the elongation axis and cell elongation appeared to be arrested. This indicates that TA addition can disrupt microtubule organization and reorient the bundles toward the elongation axis in as fast as thirty minutes of time.

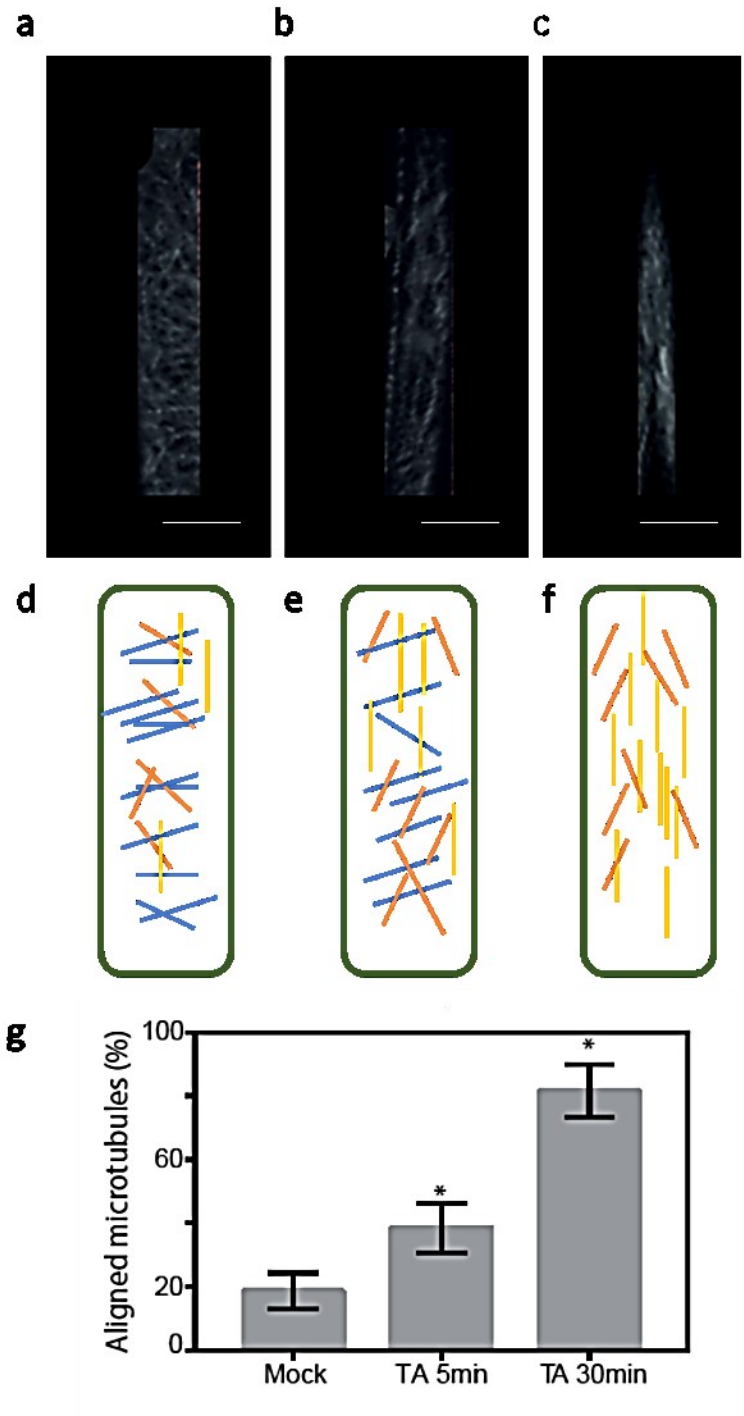

Figure 3.3 Thaxtomin A alters microtubule orientation.

Transgenic seedlings expressing YFP-CeSA6 and RFP-TUB6 in the CeSA6 mutant *prc1-1* were treated with different concentrations of thaxtomin A (TA). Kymographs of RFP–TUB6

particles, representing the trajectories of TUB6 over time at 29°C were taken from hypocotyl epidermal cells of dark-grown seedlings on Hoagland medium supplemented with a) DMSO as a negative control (less than 0.1%), b) 10 µM of thaxtomin A during 1 min, c) 10 µM of thaxtomin A during 30 min. The angle between microtubules and the cell elongation axis was measure using ImageJ. Schemes d, e and f represent symbolic distribution of the angle α formed between each microtubule and the elongation axis in each of the previous conditions (blue array for $60º<\alpha<90º$, orange for $30º<\alpha<60º$ and yellow for $0º<\alpha<30º$). Percentage of aligned microtubules ($0º<\alpha<30º$) are shown in graph e. Asterisks indicate significant differences by Student's *t* test at $P < 0.005$. Seedlings were visualized using a spinning disk confocal microscope with a 63 × NA 1.3 glycerol lens. Scale bars = 20 µm.

3.5.4 Mutants resistance and oversensitivity to TA

In order to further characterize TA's effect on cytoskeleton dynamics, we tested the response to TA of some of *Arabidopsis* mutants affected in either microtubule-associated protein genes (*spiral1-2, lefty-1, lefty-2*) or cellulose synthase genes (*radially swallen-1, procuste1-1, isoxaben resistant-1, isoxaben resistant-2*). The response of mutant seedlings to TA was compared to wild-type *Arabidopsis thaliana* seedlings of similar accession (Col0) and to the *Thaxtomin A resistant* (*txr1*) mutant. All control and mutant seedlings were grown in the same conditions in media containing DSMO as a control or 0.2 µM TA. Root elongation was measured at days 3, 5, 7 and 10 after transfer to light using ImageJ/Fiji. Wild type and *txr1* seed germination was similar in the absence and presence of TA. Similarly, TA did not affect seed germination in any of the mutants. However, we could measure changes in root elongation induced by TA in wild-type and mutant seedlings from three days after transfer to growth. In TA-containing medium, growth inhibition associated with cotyledon whitening was observed in 5-day-old WT seedlings. As expected, seedlings from the thaxtomin A resistant mutant *trx1* were not affected by TA. In the group of mutants tested, the seedlings of two mutants that are modified respectively for a microtubule associated protein and CeSA1, *'microtubule*

organization 1' (*mor1-1)* and *'anysotropy1'* (*any1),* were found to have a modified resistance to TA when compared to wild-type *Arabidopsis thaliana* seedlings and to the *Thaxtomin A resistant* (*txr1*) mutant. The *mor1-1* and *any1* mutants have altered cellulose crystallinity profiles (Fujita et al., 2013). In the mutant *any1,* seedling dwarfism is apparent on control medium as reported in the literature (Fujita et al., 2013). However, when germinated on TA medium, we observed cotyledons discoloration and inhibition of root elongation as soon as 3 days after germination (Fig.3. 4b) compared to WT seedlings where root elongation only stopped 5 days after germination. This observation led us to further investigate *any1* sensitivity to TA. We measured *any1* root growth on a range of TA concentrations (0, 10, 20, 50, 200 nM TA) and compared these results to WT seedlings grown at the same time on the same Petri dishes containing TA-supplemented medium. While WT Col-0 seed germination and seedling growth were not affected by low concentration (10 nM) of TA, *any1* seedlings were overly sensitive and died (within 3 days, indicating that *any1* is highly sensitive to TA (SI, 2).

In contrast, root elongation in *mor1-1* was only decreased by 200 nM TA while this concentration arrested root elongation in WT seedlings (Fig. 3.4a). This indicates that *mor1-1* is moderately resistant to TA when compared to WT. The *mor1-1* mutant has no obvious phenotype when grown in a non-restrictive temperature, and its growth on control medium is almost similar to the wild type growth. The relative root growth of each mutant on TA was compared to control (Fig. 3.4c). Compared to WT, whose relative root growth inhibition on TA compared to control medium was close to 70%, we observed that *mor1-1* relative root growth was inhibited by only 20%, indicating that *mor1-1* is more resistant to TA than WT. To further investigate this effect, we triggered *mor1-1* thermosensitive phenotype by growing vertically 3 days-old seedlings at 23 °C then transferring plates at restrictive temperature of 29 °C for 48 h. At this temperature, *mor1-1* roots skewing is observed (Fig. 4d) and crooked root hair are abundant (Whittington et al., 2001). In presence of TA, this phenotype was visibly more intense (Fig. 4e) compared to root grown in mock medium at restrictive temperature (Fig. 3.4d).

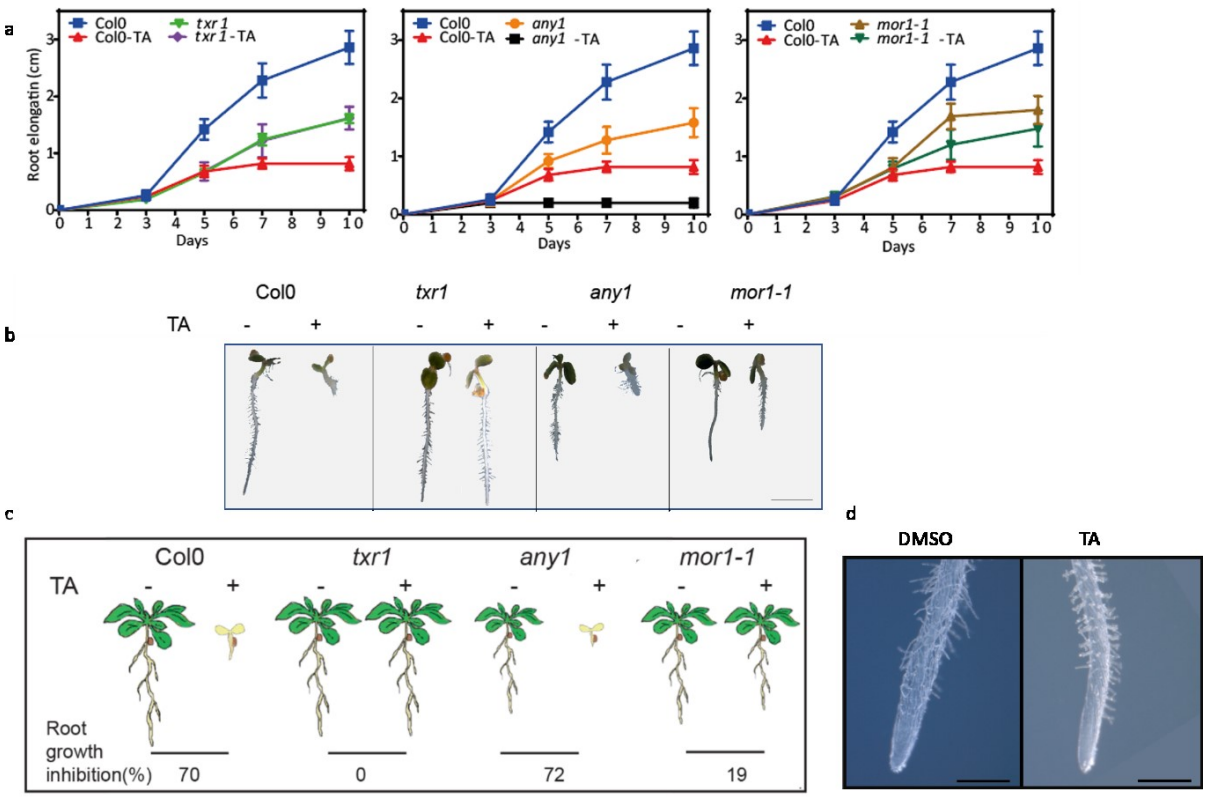

Figure 3.4 Acute sensitivity to thaxtomin A in *any-1* mutant, resistance to thaxtomin A in *mor1-1*. a) Effects of thaxtomin A (0.2 µM) on root elongation of *Arabidopsis* seedlings in wild type Col0, TA-resistant mutant *txr1*, microtubule organization mutant *mor1-1* and CeSA1 mutant *any1*. The primary root lengths were measured using ImageJ after seedlings were grown for 10 days on media containing DMSO as negative control or 0.2 µM of thaxtomin A. (b) Growth of 5-day-old seedlings in the presence or absence of 0.2 µM TA (c) Schematic representation of relative root elongation on TA compared to control medium of wild type Col 0, *txr1, any-1* and *mor1-1* in, (d) detail of *mor1-1* root twisting phenotype after 48 h in restrictive temperature of 29 °C. All values are means ± SD (n = 50). Scale in b = 0.5 mm, in d = 100 µm.

3.6 DISCUSSION

We previously reported that CBIs like TA and isoxaben induced decreased cell wall stiffness (Chap. 2) as detected in AFM analyses. During those experiments, it was repeatedly occurring that the cantilever would show zero retraction in a few spots of the cell wall as if holes in the

PCW were caused by TA/isoxaben treatment. We attributed this result to uncomplete synthesis of cellulose. Since TA was already shown to decrease ^{14}C-glucose incorporation into the cell wall of *Arabidopsis* seedlings (Scheible et al., 2003), we were interested in characterizing further more the effect of TA on cellulose quality. We first used a mild extraction that removes pectin and hemicellulose from the PCW. This revealed that TA causes the enlargement of the diameter of partially rehydrated cellulose microfibrils (Fig. 3.1b). This could be due to a less crystalline and more amorphous fraction of cellulose. It t is known that amorphous cellulose is less organized and prone to absorb more water and swell since it contains less intra and inter molecular bonding between different microfibrils of the same crystallite (Ciolacu et al., 2011). Using another method to purify cellulose microfibrils, we found that TA promoted the formation of shorter microfibrils fragments when compared to untreated samples. This could be attributed to a modification in CeSA activity in the presence of the toxin.

To test this hypothesis, we analyzed CeSA6 velocity using transgenic lines coexpressing YFP-CeSA6 and RFP-TUB6 in the CeSA6 mutant *prc1-1*. In previous work, Bischoff et al. (2009) had showed that a 2.5 h treatment with TA leads to non-motile CeSA3 in *Arabidopsis* seedlings. In this work, we used CeSA6 transgenic lines instead of CeSA3, which were not available. We think that the effect of TA on CeSA motility may occur much more rapidly after the addition of the toxin. Accordingly, we found that CeSA6 velocity was rapidly reduced (5-10 min after TA addition) compared to its velocity in mock treated seedlings. However, almost 1h after TA treatment, CeSA6 velocity was even further reduced close to immobility, suggesting a possible non-motility for CeSA6. This observation was combined to a reorientation of cortical microtubules within the same cells to a longitudinal orientation parallel to the longitudinal elongation axis, suggesting that the elongation is inhibited by TA addition (Chan, 2012). In addition, even though an important population of CeSA6s was non-motile after 1 h, this was only detected in a fraction of cells tested. Hence, we can not conclude that there is an absolute relationship between TA addition and CeSA6 non-motility. For these reasons combined, we think that the decrease in CeSA6 velocity and microtubule reorientation are correlated with elongation arrest in dark grown hypocotyl.

Microtubule orientation plays an essential role during cell elongation., It has been proven that cells actively elongating show highly organized microtubules (Chan, 2012). More precisely, plant cells use dynamic microtubule reorientation to dictate the developmental phase in most tissues. When cell elongation is completed, cortical microtubules will reorient from transversal to longitudinal organization (Yuan et al., 1994). Anisotropic plant cell growth is characterized by growth rate and growth direction, where both parameters mimics patterns of stress and strain of the plant cell wall, patterns that are often implicating microtubule reorientation as a response (Hamant and Traas, 2010). Interestingly, auxin has been shown to have a rapid action on microtubule reorientation (Chen et al, 2004). We also previously reported that addition of auxin to thaxtomin A-treated cells limits cell death caused by TA-induced cell wall perturbations (Chap. 2). These results suggest that TA is inhibiting cell elongation via microtubule reorientation (Fig. 3.3), Microtubules align transversally to allow cell elongation, and reorient to longitudinal direction after the end of this phase to procure higher resistance to mechanical stress (Schopfer and Palme, 2016).

Interestingly, TA did not only affect cellulose microfibrils length, CeSA6 velocity and induced microtubule reorientation, we also found that the effect of TA is modified in mutants exhibiting altered cellulose crystallinity. On one hand, we found that *mor1-1*, which has a high level of cellulose crystallinity is much less affected than WT by TA during root elongation. However, it is still possible that loss of function of MOR1 itself could explain *mor1-1* resistance, since this line showed a failure in decreasing crystallinity correlated with high CSCs velocity and a reduced MT polymer mass (Fujita et al., 2011). This could mean that TA treatment was not able to decrease crystallinity in *mor1-1* and the cell wall was less perturbated in presence of TA, in comparison with the wild type. Also, it is important to note that the temperature restrictive phenotype of *mor1-1* seedlings was accentuated by the presence of TA since both twisting and root hair deformation appeared faster in presence of TA than in control. This phenotype is a result of cortical MT disruption (Whittington et al., 2001). This may suggest that TA interacts with MOR1 leading to microtubule organization in wild type. This will need

to be further investigated by using transgenic lines expressing fluorescent protein and tubulin in *mor1-1*.

. On the other hand, the mutant *any1*, which shows an important reduction of cellulose crystallinity is more sensitive to TA than WT during seedling development and root elongation. The mutation D604N in *any1*, affects the catalytic domain of AtCeSA1 causing a null-mutant. This mutation is correlated with a reduced cell wall crystallinity and a decreased velocity of CSCs (Fujita et al., 2013). Together, these elements show that TA effect on the cell wall is reduced when crystallinity is high.

Because of the importance of plant cell walls in protecting cells against the outside environment as well as providing mechanical strength (resisting to~10 MPa or more, Cosgrove, 2016), plant physiologists discuss currently the cause to effect relationship between cell wall loosening and microtubule reorientation (Hamant 2004, Chen et al., 2014, Schopfer and Palme, 2016). In this article, thaxtomin A's effect on microtubule reorientation has been seen as soon as 5 minutes post-treatment. We suggest that thaxtomin A is firstly acting on microtubule orientation resulting in a subsequentdecrease in cellulose synthase velocity (Fig.3. 2) and leading to less yield; consequently, cellulose microfibrils are shorter under CBI treatment (Fig.3.1) which would cause cell wall loosening.

3.7 ACKNOWLEDGMENT

This work was supported by a discovery grant from National Sciences and Engineering Council of Canada (NSERC) to N. Beaudoin and Centre SÈVE collaboration grant to F. Awwad. All authors declare no financial conflict of interest.

3.8 REFERENCES

Braybrook, S.A., and Peaucelle, A. (2013). Mechano-Chemical Aspects of Organ Formation in Arabidopsis thaliana: The Relationship between Auxin and Pectin. PLoS ONE *8*, e57813.

Chan, J. (2012). Microtubule and cellulose microfibril orientation during plant cell and organ growth. Journal of Microscopy *247*, 23–32.

Chebli, Y., and Geitmann, A. (2017). Cellular growth in plants requires regulation of cell wall biochemistry. Current Opinion in Cell Biology *44*, 28.

Ciolacu, D., Ciolacu, F., and Popa, V.I. (2011). Amorphous cellulose—structure and characterization. Cellulose Chemistry and Technology *45*, 13.

Crowell, E.F., Bischoff, V., Desprez, T., Rolland, A., Stierhof, Y.-D., Schumacher, K., Gonneau, M., Höfte, H., and Vernhettes, S. (2009). Pausing of Golgi bodies on microtubules regulates secretion of cellulose synthase complexes in Arabidopsis. The Plant Cell *21*, 1141–1154.

Duval, I., Brochu, V., Simard, M., Beaulieu, C., and Beaudoin, N. (2005). Thaxtomin A induces programmed cell death in Arabidopsis thaliana suspension-cultured cells. Planta *222*, 820–831.

Encina, A., Sevillano, J.M., Acebes, J.L., and Alvarez, J. (2002). Cell wall modifications of bean (Phaseolus vulgaris) cell suspensions during habituation and dehabituation to dichlobenil. Physiologia Plantarum *114*, 182–191.

Fagard, M., Desnos, T., Desprez, T., Goubet, F., Refregier, G., Mouille, G., McCann, M., Rayon, C., Vernhettes, S., and Höfte, H. (2000). PROCUSTE1 encodes a cellulose synthase required for normal cell elongation specifically in roots and dark-grown hypocotyls of Arabidopsis. The Plant Cell *12*, 2409–2423.

Fujita, M., Himmelspach, R., Ward, J., Whittington, A., Hasenbein, N., Liu, C., Truong, T.T., Galway, M.E., Mansfield, S.D., Hocart, C.H., et al. (2013). The anisotropy1 D604N Mutation in the Arabidopsis Cellulose Synthase1 Catalytic Domain Reduces Cell Wall Crystallinity and the Velocity of Cellulose Synthase Complexes. PLANT PHYSIOLOGY *162*, 74–85.

Gutierrez, R., Lindeboom, J.J., Paredez, A.R., Emons, A.M.C., and Ehrhardt, D.W. (2009). Arabidopsis cortical microtubules position cellulose synthase delivery to the plasma membrane and interact with cellulose synthase trafficking compartments. Nature Cell Biology *11*, 797–806.

Healy, F.G., Wach, M., Krasnoff, S.B., Gibson, D.M., and Loria, R. (2000). The txtAB genes of the plant pathogen Streptomyces acidiscabies encode a peptide synthetase required for phytotoxin thaxtomin A production and pathogenicity. Molecular Microbiology *38*, 794–804.

King, R.R., Lawrence, C.H., Clark, M.C., and Calhoun, L.A. (1989). Isolation and characterization of phytotoxins associated with Streptomyces scabies. J. Chem. Soc., Chem. Commun. *0*, 849–850.

Ledbetter, M.C., and Porter, K.R. (1970). Introduction to the Fine Structure of Plant Cells (Berlin Heidelberg: Springer-Verlag).

Lei, L., Singh, A., Bashline, L., Li, S., Yingling, Y.G., and Gu, Y. (2015). CELLULOSE SYNTHASE INTERACTIVE1 Is Required for Fast Recycling of Cellulose Synthase Complexes to the Plasma Membrane in Arabidopsis. The Plant Cell *27*, 2926–2940.

Li, S., Lei, L., Somerville, C.R., and Gu, Y. (2012). Cellulose synthase interactive protein 1 (CSI1) links microtubules and cellulose synthase complexes. Proc Natl Acad Sci USA *109*, 185.

Lindeboom, J., Mulder, B.M., Vos, J.W., Ketelaar, T., and Emons, A.M.C. (2008). Cellulose microfibril deposition: coordinated activity at the plant plasma membrane. Journal of Microscopy *231*, 192–200.

Morgan, J.L.W., Strumillo, J., and Zimmer, J. (2012). Crystallographic snapshot of cellulose synthesis and membrane translocation. Nature *493*, 181.

Paredez, A.R., Somerville, C.R., and Ehrhardt, D.W. (2006). Visualization of Cellulose Synthase Demonstrates Functional Association with Microtubules. Science *312*, 1491–1495.

Richmond, T.A., and Somerville, C.R. (2000). The Cellulose Synthase Superfamily. Plant Physiology *124*, 495–498.

Scheible, W.-R., Fry, B., Kochevenko, A., Schindelasch, D., Zimmerli, L., Somerville, S., Loria, R., and Somerville, C.R. (2003). An Arabidopsis mutant resistant to thaxtomin A, a cellulose synthesis inhibitor from Streptomyces species. The Plant Cell *15*, 1781–1794.

Tateno, M., Brabham, C., and DeBolt, S. (2016). Cellulose biosynthesis inhibitors -- a multifunctional toolbox. Journal of Experimental Botany *67*, 533–542.

Whittington, A.T., Vugrek, O., Wei, K.J., Hasenbein, N.G., Sugimoto, K., Rashbrooke, M.C., and Wasteneys, G.O. (2001). MOR1 is essential for organizing cortical microtubules in plants. Nature *411*, 610–613.

3.9 SUPPLEMENTARY MATERIAL

3.9.1 Supplementary information 1

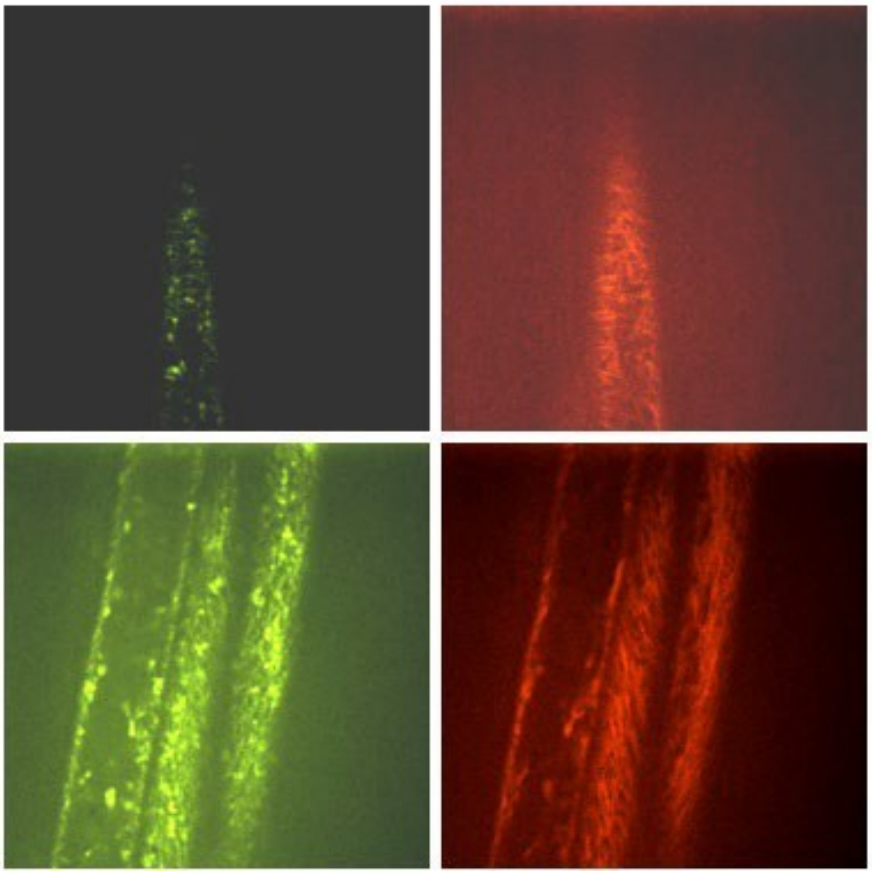

Video SI.1 : Visualization of YFP:CeSA6 YFP-CeSA6 was visualized in absence (upper left) or in presence of 5µM thaxtomin A and RFP:TUB6 in absence (upper right) or in presence of 5µM thaxtomin A (lower right) in Arabidopsis seedlings expressing YFP-CeSA 6/RFP-TUB 6 in *prc1-1* grown in dark for 3 days and transferred on a mounting medium containing DMSO as a control or 5µM thaxtomin A for 1 hour. 61 frames were taken each 5 seconds

using modified Yokogawa spinning-disk scan head and a Leica DMI6000 inverted microscope equipped with a 63 × NA 1.3 glycerol lens.

3.9.2 Supplementary information 2

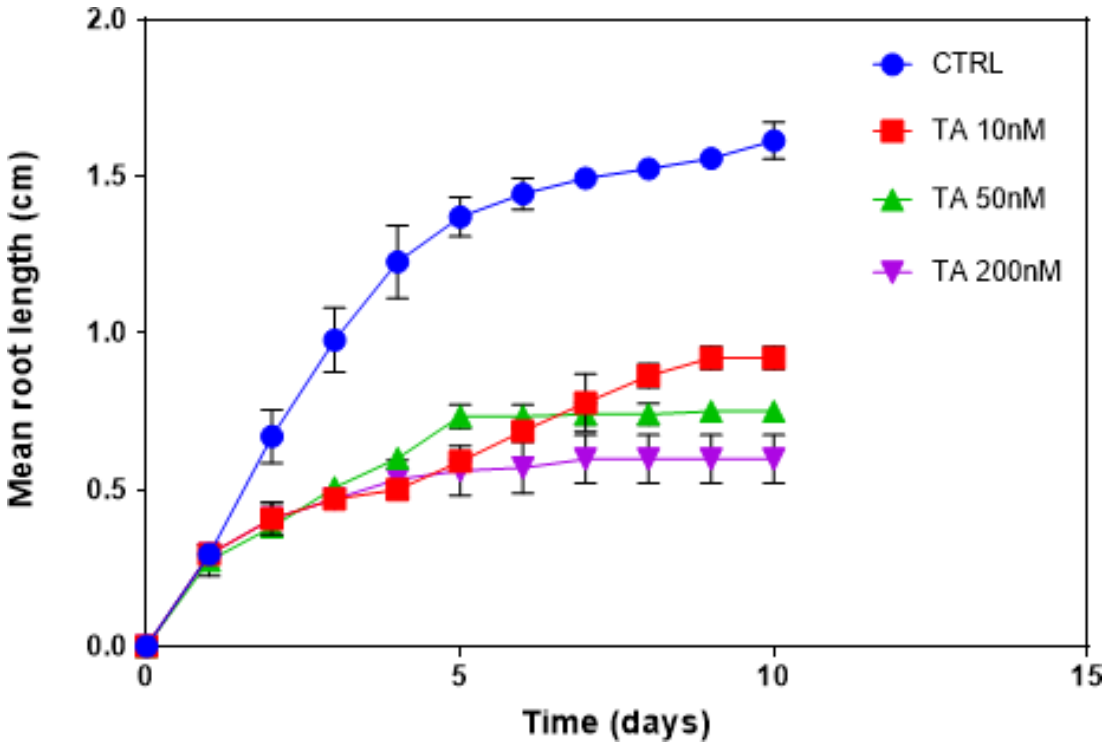

Figure SI.1: Thaxtomin A-sensitive mutant *anysotropy1* growth.
Mean root growth of *anysotropy1* (*any1*) seedlings on medium containing DMSO (CTRL), 10 nM, 50 nM or 200 nM Thaxtomin A during 10 days. Each point represents the mean value of three repetitions with 50 seedlings each. Error bars represent SD.

CHAPITRE 4

Analyse de l'importance des espèces réactives à l'oxygène dans la protection contre la mort cellulaire induite par la thaxtomine A chez *Arabidopsis thaliana*.

4.1 INTRODUCTION DE L'ARTICLE ET CONTRIBUTIONS DES AUTEURS

Ce dernier manuscrit est présenté sous forme de courte communication dans laquelle on montre que l'absence de production des ROS lors d'un traitement à la TA contribue à l'induction de la MCP. On montre aussi que l'ajout d'une quantité sublétale de peroxyde d'hydrogène est capable de réduire cette MCP. D'autre part, on montre qu'en présence de peroxyde d'hydrogène, une rigidification de la paroi est observée, d'où l'importance du peroxyde dans des petites concentrations pour l'homéostasie pariétale.

Ma contribution est l'exécution de la totalité des expériences présentées et la préparation du manuscrit pour le soumettre. J'ai réalisé une partie des travaux dans le laboratoire du Dr. Michel Grandbois à l'Institut de pharmacologie de Sherbrooke à Fleurimont. La totalité des travaux a été dirigé par Dre Nathalie Beaudoin.

Le manuscrit présenté dans la section suivante a été préparé pour être soumis à la revue internationale *Plant Signaling and Behavior*.

Reactive oxygen species alleviate cell death induced by thaxtomin A treatment in *Arabidopsis* cell cultures

Fatima Awwad, Guillaume Bertrand, Michel Grandbois, Nathalie Beaudoin*

*Corresponding author

4.2 ABSTRACT

Thaxtomin A is a cellulose biosynthesis inhibitor produced by the soil bacterium *Streptomyces scabies*. It is essential for the induction of common scab lesions on potato tuber periderm. It was shown that thaxtomin A induces an atypical programmed cell death that is not associated with reactive oxygen species (ROS) production. We show that the absence of ROS is not due to the activation by TA of antioxidant enzymes. In contrast, we present evidence that the absence of ROS production is at least partially involved in the induction of cell death by TA. Using *Arabidopsis thaliana* cell suspensions, we show that the addition of H_2O_2 before adding TA can reduce cell death. This was associated with increased cell wall rigidity, as revealed by investigation of the cell surface mechanics in atomic force microscopy mode. Hence, the production of ROS may stimulate cell survival in response to cell wall damage by increasing cell wall rigidity.

4.3 INTRODUCTION

At high concentrations, hydrogen peroxide (H_2O_2) is a form of reactive oxygen species (ROS) known for its toxicity for all living cells. Interestingly, plant cells and tissues are able to tolerate important amounts (up to 200 mM) compared to animal cells (100 µM; Ślesak et al., 2007). Several biotic and abiotic stress result in H_2O_2 production in plant cells such as heat stress (Volkov et al., 2006) and response to bacterial pathogen *Pseudomonas syringae* (Torres et al., 2002). We know today that H_2O_2 plays an important signaling role at different physiological and cellular levels, like in programmed cell death signaling (Petrov et al., 2015), root system development (Hernández-Barrera et al., 2015), seed germination (Barba-Espin, 2011), and many other examples. Generation of H_2O_2 can be mediated by several enzymes like cell wall peroxidases (Francoz et al., 2015), amine oxidase (Cona et al., 2006) and oxalate. ROS production could also occur non-enzymatically, during photosynthesis and respiration, through

electron transport chain reactions occurring in chloroplasts or in mitochondria (Niu and Liao, 2016).

Thaxtomin A (TA) is a toxin produced by the common scab phytopathogen *Streptomyces scabies*. TA is classified as a cellulose biosynthesis inhibitor (CBI) that reduces cellulose synthesis, inhibits root growth and causes root swelling in *Arabidopsis* (Scheible et al., 2003). Further studies aimed at characterizing the specific effects and target of TA have shown that it activates a programmed cell in death in *Arabidopsis* seedling and suspension cells (Duval et al., 2005), it also induced changes in cell wall related gene expression (Duval et al., 2005; Tegg et al, 2013). Also, TA-induced programmed cell death was found to be highly atypical, since no ROS production was detected and no MAPK activation was detected (Duval et al., 2005; Errakhi et al., 2008). In this study, we are interested in studying why ROS are not produced during TA-induced cell death, and why this may be important to compromise cell survival.

4.4 MATERIALS AND METHODS

4.4.1 Plant material and treatments

Cell suspension cultures of *Arabidopsis thaliana* accession Landsberg *erecta* were graciously provided by Dr. Jean Rivoal (IRBV, Montréal, PQ, Canada). Unless otherwise indicated, all chemicals were purchased from Sigma Aldrich. Cell suspensions were grown in 45 mL Murashige and Skoog (MS) medium (pH 5.7) supplemented with B5 vitamins and 1 mg L^{-1} 2,4-dichlorophenoxyacetic acid (2,4-D) in 125 mL Erlenmeyer flasks kept on a rotary shaker (120 rpm) at 22°C in the dark. *Arabidopsis* cell cultures were subcultured weekly by diluting 15 mL cells into fresh medium. Treatments were performed using 10 mL log-phase cells 3 to 4 d after subculture. Thaxtomin A (TA) was prepared as described before (Duval et al. 2005). TA (stock of 1 mM) were prepared in methanol and added at a final concentration of 1 µM. The same volume of methanol (less than 0.1% of final volume) was added to control cells. Hydrogen peroxide (H_2O_2) was diluted in water at a final concentration of 1 M. Hydrogen

peroxide treatments were performed by adding 10 mM directly to cell suspensions. To investigate the effect of H_2O_2 on the induction of cell death by TA, H_2O_2 was added 3 hours prior to TA treatment. Different time/dose responses were performed before choosing H_2O_2 concentration and treatment duration.

4.4.2 Cell death assay

Cell death was assessed using trypan blue staining as described before (Duval et al., 2005). For each condition, at least 500 cells in groups of 100 were counted. Each experiment was repeated at least three times.

4.4.3 ROS visualization

For microscopic evaluation of ROS production, cells or seedlings were incubated for 30 min in a phosphate buffer solution (PBS) containing 10 µM H_2DCFDA (2',7'-dichlorofluorescein diacetate probe) then washed twice with PBS before mounting in a medium containing 2.78 µM propidium iodide (PI; Leshem et al., 2006). Images were taken with a Zeiss Imager Z1 microscope (Carl Zeiss Canada Ltd, Ontario, Canada) equipped with a monochromatic camera using AxioVision 4.8.2 version. 40 µL of cell culture were examined using an excitation wavelength of 488 nm (H_2DCFDA) and 535 nm (PI). H_2DCFDA fluorescence was detected in the presence of ROS in cells with a FITC filter (520 nm) and PI marked dead cells and cell frontiers with a rhodamine filter (617 nm).

4.4.4 Antioxidant enzymes activity assays

Catalase (CAT), ascorbate peroxidase (APX) and superoxide dismutase (SOD) activities were measured using three samples per condition and repeated in three independent experiments

using protocols described previously (Bergmeyer, 1970; Nakano and Asada, 1981; Beyer and Fridovich, 1987).

4.4.5 Cell surface mechanics

The cells elastic modulus (Young's modulus) of individual cells was quantified from force/tip-sample separation curves recorded using atomic force microscopy (AFM). The cells were pre-treated for 24 h with different combinations of methanol (control), TA or H_2O_2, using the concentrations indicated in each experiment. A 40 µl-aliquot of each culture was laid on a poly-L-lysine (0.1 mg mL^{-1}) coated slide cover slip for 5 min to allow adhesion. The cover slip was washed three times with culture medium before fixing it with a minute drop of vacuum grease in a small petri dish filled with 2 mL of culture medium prior to analysis. AFM analysis was conducted in contact mode as described before (Radotić et al. 2012). Force-curves were recorded at five different arbitrary locations in a 5 µm radius over the cell surface leading to five batches of 30 to 50 points per cell, repeated in 3-5 cell per condition. Also, the reference protocol was based on different measurements and variations regarding the depth of the cantilever before contact with the cell surface (Radotić et al., 2012). Based on the different settings and conditions, AFM-measurements allowed measuring the cell wall rigidity in cell culture media allowing minimal changes in osmosis and vacuole size among the different treatments.

4.4.6 Statistics

Statistical analysis was performed with GraphPad Prism 7. For cell death assay and measurements, cells were counted in groups of 100 and the mean was calculated from 3 to 15 replicates. Each experiment was repeated at least three times. Data was analyzed using t-test

followed by Holm-Šídák method with alpha = 0.05. Results were considered statistically different when p-value was < 0.05.

4.5 RESULTS

4.5.1 Hydrogen peroxide protects *Arabidopsis* cells from CBI-induced cell death

We know that no ROS production was detected in TA induced PCD (Duval et al., 2005; Errakhi et al., 2008). We aimed to confirm that the absence of ROS production is also observed in our suspension cells before going for further testing. ROS were detected using H_2DCFDA which emits fluorescence in the presence of ROS. In control cells, we observed some fluorescence, indicating a basal ROS production (Fig 1a-left) but very little H_2DCFDA fluorescence was detected in in TA-treated cells, confirming the absence of ROS production after TA addition (Fig1a -right). H_2O_2 production was also quantified using ferrous oxidation of xylenol orange (FOX) modified assay and lead to the same result (Supplementary data, Fig SI; Wei et al., 2002).

We also compared cell death induction in the presence of TA and H_2O_2. For this test, we treated *Arabidopsis* cells with methanol as a control, with 10 mM H_2O_2 or 1 µM TA, or with a combination of both where H_2O_2 was added prior to TA treatment (Fig. 4.1 b). For H_2O_2 and TA co-treatment, we tried different doses and times. As shown in Fig, 1b, addition of TA alone led to a drastic increase in cell death with up to 70% of dead cells 48 h after addition of TA compared to control cells which had less than 10% dead cells or compared to cells treated only with H_2O_2, where 38% of cells were dead. Interestingly, when cells were pretreated with H_2O_2 3 h prior to TA addition, we found that the percentage of dead cells (40% dead cells, Fig. 4.1b). was similar to that of H_2O_2 treated cells (38% dead cells, Fig. 4.1b). This shows that pre-treatment with H_2O_2 prevents cell death caused by TA in *Arabidopsis* cell suspensions.

It is possible that the reduced ROS production in the presence of TA could be the result of increased anti-oxydant enzyme activity. To test this possibility, assays were performed in order to measure various antioxidant enzymes activities. Catalase, Ascorbate peroxidase and Superoxide dismutase activities assays were performed in cell suspensions. As shown in Fig. 4.1 c, d and e, there was non-significant differences in these enzyme activities between control and TA-treated cells.

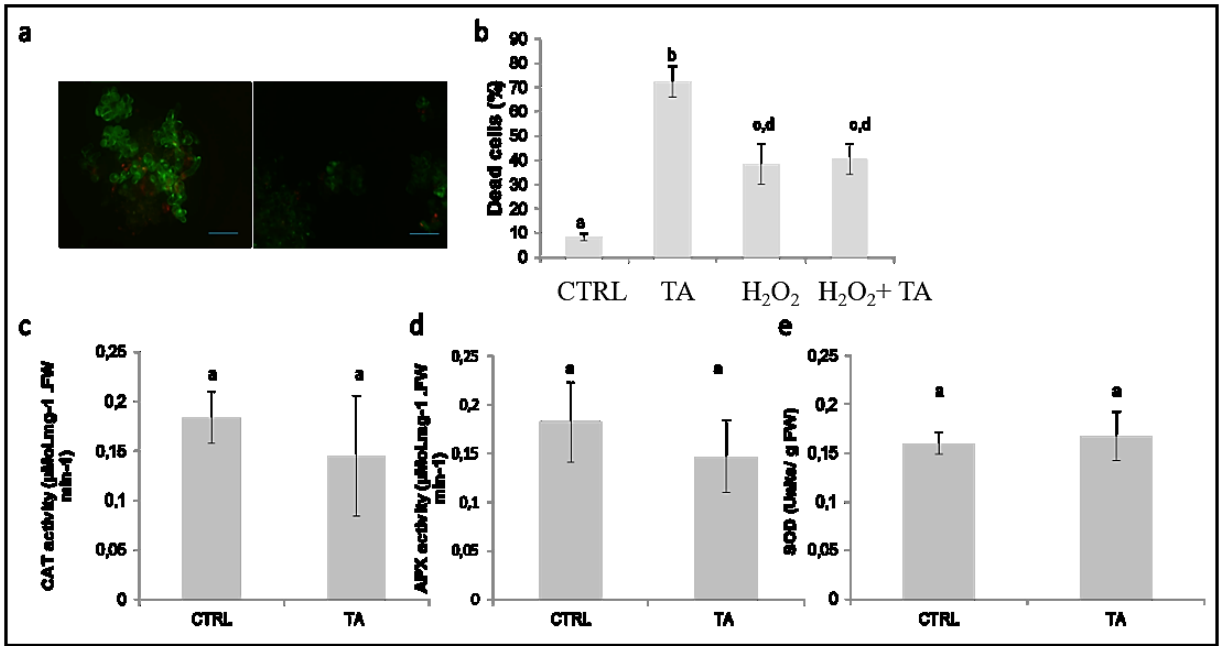

Figure 4.1: Reduced ROS production in *Arabidopsis* cell suspension in response to thaxtomin A.

Reactive oxygen species were detected (a) using H_2DCFDA (green) in suspension cells treated for 24 h with methanol (left) or 1 µM thaxtomin A (right). Scale = 100 µm. Graph (b) shows percentage of dead cells in suspension cells treated for 48 h with methanol (CTRL), 1 µM TA, 10 mM H_2O_2 or a 3 h pretreatment of 1 mM H_2O_2 followed by 1 µM TA. Catalase (CAT) activity, Ascorbate peroxidase (APX) activity and Superoxide dismutase (SOD) activity in cells treated with methanol (CTRL) or 1 µM TA for 24 h are shown respectively in (c), (d) and (e). In (a), cells were counted in groups of 100 and the mean was calculated from 3 to 15 replicates. Each experiment was repeated at least three times. In (c), (d) and (e), each value is the mean of three samples per conditions, and each experiment was repeated three times with similar results. Error bars indicate standard deviation and different letter indicate statistical difference with $p<0.05$. Data was analyzed using t-test followed by Holm-Šídák method with alpha = 0.05.

4.5.2 Hydrogen peroxide increased cell wall rigidity

Since there was no change in antioxidant enzyme activities within TA-treated cells, we speculated that H_2O_2 may protect cells from TA by altering the cell wall. It was shown by different studies that H_2O_2 can increase cell wall rigidity (Lin and Kao, 2001; Passardi et al., 2004). Using atomic-force microscopy in contact mode, we investigated the mechanical propreties of the cell surface of cell suspension-cultured cells. Although each value shown in Fig. 4.2 corresponds to the rigidity in each point of measurement, we can compare the overall cell wall stiffness between different cells that were treated in the same conditions with different treatments (Radotić et al., 2012). As shown in Fig. 4.2, we noticed that the distribution of Young's modulus values in control cells is spread almost evenly in the range of 100-600 MPa, while in TA-treated cells, values were mainly concentrated below 200 MPa, showing a reduced stiffness of the cell surface, as described before (Chap 2). In contrast, cells treated with H_2O_2 showed an increase in stiffness with Young's modulus values distributed mainly above 500 MPa. Finally, cells treated with both H_2O_2 and TA also showed a higher stiffness with more than 50% of Young's modulus values higher than 500 MPa. These results show that cell wall rigidity is increased in presence of hydrogen peroxide oppositely to TA's weakening action on cell wall.

4.6 DISCUSSION

Reactive oxygen species are key players in signaling and defense responses in plants (Choudhury et al., 2017; Herrera-Vásquez et al., 2015; Huang et al., 2016).

Despite TA's capacity to induced PCD, no ROS production was detected in the presence of TA (Fig. 4.1a; Duval et al., 2005, Errakhi et al., 2008). Also, H_2O_2 quantification via ferrous oxidization of xylenol orange (FOX) modified assay showed significantly lower production in

TA treated cells compared to control cells and compared to H_2O_2 production induced by high temperature as a positive control (Fig SI). These results, combined with the absence of enhanced antioxidant enzymes activity, show that TA presence does not lead to ROS production. Moreover, H_2O_2 levels in TA treated cells is lower than the basal level in *Arabidopsis* suspension cells.

To study whether the absence of H_2O_2 production could play a role in TA-induced PCD, we provided exogenous peroxide to cells, 0.5, 1, 3 and 6 hours before adding TA. Our results showed that H_2O_2 presence was able to reduce TA-induced PCD in suspension cells. This means that the absence of H_2O_2 production in the presence of TA is negatively affecting cell survival. Also, AFM investigation showed that the addition of sublethal concentration of H_2O_2 increased cell wall stiffness (Fig. 4.2 b). This increased stiffness was not affected by the addition of TA later (Fig.4. 2d) and was associated with a reduction of cell death induced by TA, suggesting that the high cell wall rigidity may contribute to inhibiting TA's effect in cell suspension. This protection by H_2O_2 could be both direct and indirect, since in one hand H_2O_2 presence caused higher stiffness, and on another hand, H_2O_2 effect could be caused by its function as a signaling messenger. Interestingly, recent studies show that the mutation in *Thaxtomin-resistant mutant txr1* 's mutation is located in a gene that encodes for ATPAM16. ATPAM16 plays a major role in transporting plant immunity regulator into mitochondria and protects plants from accumulating ROS in certain conditions (Huang et al., 2013).

The increased rigidity in presence of H_2O_2 could be a result of its interaction with cell wall proteins such as cell wall peroxidase that are responsible of scavenging H_2O_2 as a substrate and modifying links between cell wall components allowing higher stiffness and increased cell wall strength (Wakabayashi et al., 2012). At low concentrations of H_2O_2, cell wall peroxidases are not able to increase stiffness, and in high concentrations of H_2O_2, the reduction will result in high hydroxyl radical production which will lead to sugar cleavage and then cell wall loosening (Renew et al., 2005).

In TA-induced cell death, the lack of H_2O_2 production suggests that cell wall peroxidases would not be able to modify cross-linkage between cell wall components and thus rigidity is compromised. In conclusion, a slightly high level of H_2O_2 is essential for plant cells to achieve normal signal transduction and cell wall remodeling.

We choose to publish these results in a short communication form to communicate our few findings with the scientific committee and researchers that might be interested in leading further investigation on H_2O_2 function in cell wall remodeling.

4.7 CONCLUSION

Thaxtomin A-induced cell death is not associated with production of reactive oxygen species. The low amount of ROS found in TA-treated cells is due to lower production of ROS and is not due to antioxidant enzyme activity since CAT, APX and SOD activity were unchanged upon TA treatment. Alleviation of ROS production in the presence of TA could lead to death by decreasing cell wall rigidity in the absence of hydrogen peroxide. Hydrogen peroxide protection in this case could be partially due to the increased rigidity of the cell wall, but also to the signanling roles of hydrogen peroxide in plant cells. TA might be perturbing ROS production and hence ROS-mediated signal transduction.

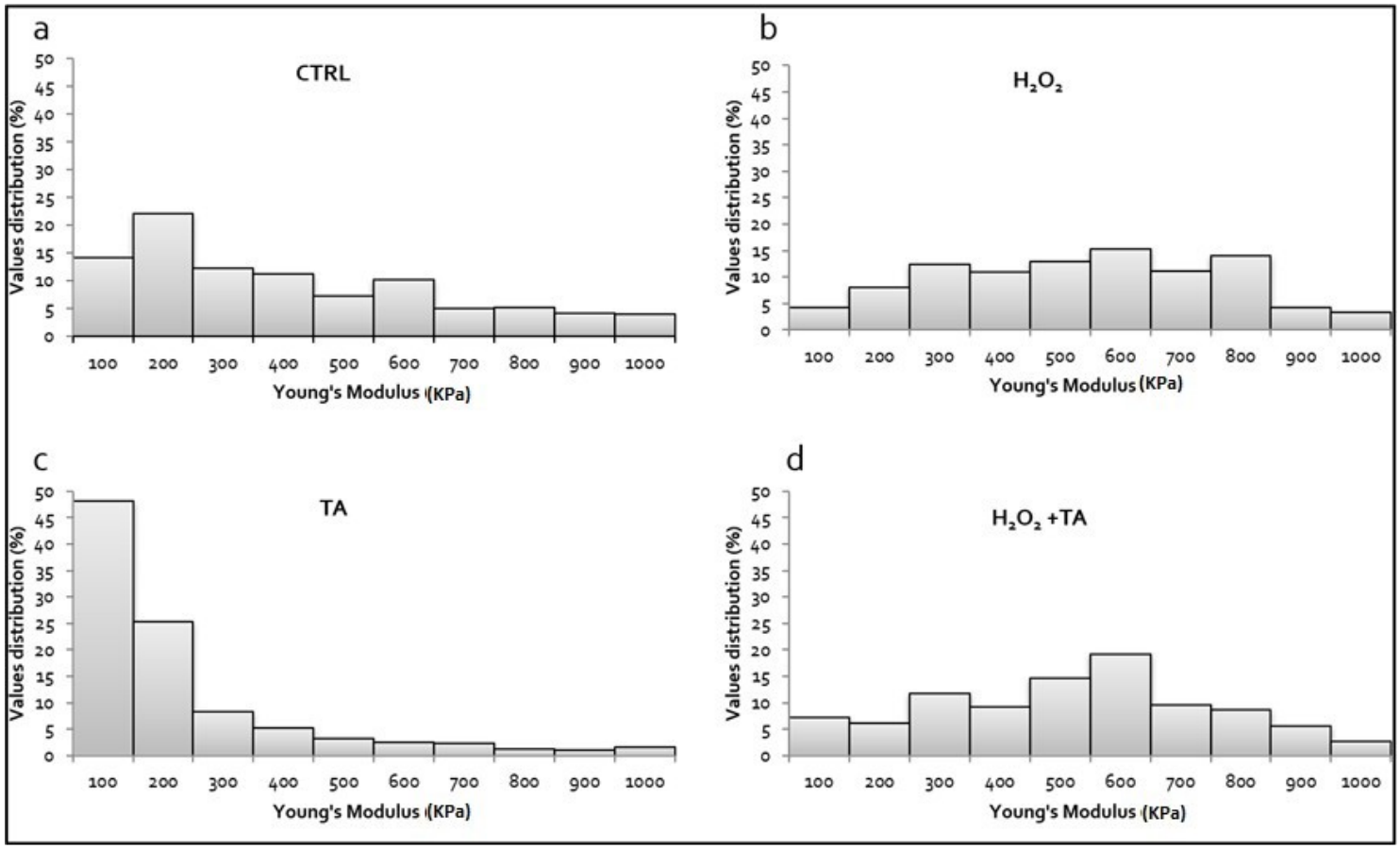
a
CTRL
b
H_2O_2
c
TA
d
H_2O_2 +TA
Values distribution (%)
Young's Modulus (KPa)
0
5
10
15
20
25
30
35
40
45
50
100
200
300
400
500
600
700
800
900
1000

4.8 REFERENCES

BARBA-ESPÍN, G., DIAZ-VIVANCOS, P.,Job, D., Belghazi, M., Job, C and HERNÁNDEZ, J. A. (2011). Understanding the role of H2O2 during pea seed germination: a combined proteomic and hormone profiling approach. Plant, cell & environment, *34*(11), 1907-1919.

Bergmeyer, H. U. (1970). Standardization of methods for estimation of enzyme activity in biological fluids. Z. Klin. Chem. Biochem., *8*, 658-660.

Beyer Jr, W. F., & Fridovich, I. (1987). Assaying for superoxide dismutase activity: some large consequences of minor changes in conditions. Analytical biochemistry, *161*(2), 559-566.

Choudhury, F.K., Rivero, R.M., Blumwald, E., and Mittler, R. (2017). Reactive oxygen species, abiotic stress and stress combination. The Plant Journal *90*, 856–867.

Cona, A., Rea, G., Angelini, R., Federico, R., & Tavladoraki, P. (2006). Functions of amine oxidases in plant development and defence. Trends in plant science, *11*(2), 80-88.

Duval, I., Brochu, V., Simard, M., Beaulieu, C., and Beaudoin, N. (2005). Thaxtomin A induces programmed cell death in Arabidopsis thaliana suspension-cultured cells. Planta *222*, 820–831.

Errakhi, R., Dauphin, A., Meimoun, P., Lehner, A., Reboutier, D., Vatsa, P., Briand, J., Madiona, K., Rona, J.P., Barakate, M., et al. (2008). An early Ca2+ influx is a prerequisite to thaxtomin A-induced cell death in Arabidopsis thaliana cells. Journal of Experimental Botany *59*, 4259–4270.

Francoz, E., Ranocha, P., Nguyen-Kim, H., Jamet, E., Burlat, V., & Dunand, C. (2015). Roles of cell wall peroxidases in plant development. *Phytochemistry*, *112*, 15-21.

Hernández-Barrera, A., Velarde-Buendía, A., Zepeda, I., Sanchez, F., Quinto, C., Sánchez-Lopez, R. & Cardenas, L. (2015). Hyper, a hydrogen peroxide sensor, indicates the sensitivity of the Arabidopsis root elongation zone to aluminum treatment. Sensors, *15(1)*, 855-867.

Herrera-Vásquez, A., Salinas, P., and Holuigue, L. (2015). Salicylic acid and reactive oxygen species interplay in the transcriptional control of defense genes expression. Front. Plant Sci. *6*.

Huang, Y., Chen, X., Liu, Y., Roth, C., Copeland, C., McFarlane, H. E., ... & Li, X. (2013). Mitochondrial AtPAM16 is required for plant survival and the negative regulation of plant immunity. Nature communications, *4*, 2558.

Huang, S., Aken, O.V., Schwarzländer, M., Belt, K., and Millar, A.H. (2016). The Roles of Mitochondrial Reactive Oxygen Species in Cellular Signaling and Stress Response in Plants. Plant Physiology *171*, 1551–1559.

Leshem, Y., Melamed-Book, N., Cagnac, O., Ronen, G., Nishri, Y., Solomon, M., ... & Levine, A. (2006). Suppression of Arabidopsis vesicle-SNARE expression inhibited fusion of H2O2-containing vesicles with tonoplast and increased salt tolerance. Proceedings of the National Academy of Sciences, *103*(47), 18008-18013.

Lin, C.C., and Kao, C.H. (2001). Cell wall peroxidase activity, hydrogen peroxide level and NaCl-inhibited root growth of rice seedlings. Plant and Soil *230*, 135–143.

Nakano, Y., & Asada, K. (1981). Hydrogen peroxide is scavenged by ascorbate-specific peroxidase in spinach chloroplasts. Plant and cell physiology, *22*(5), 867-880.

Niu, L., & Liao, W. (2016). Hydrogen peroxide signaling in plant development and abiotic responses: crosstalk with nitric oxide and calcium. Frontiers in plant science, *7,* 230.

Passardi, F., Penel, C., and Dunand, C. (2004). Performing the paradoxical: how plant peroxidases modify the cell wall. Trends in Plant Science *9*, 534–540.

Petrov, V., Hille, J., Mueller-Roeber, B., & Gechev, T. S. (2015). ROS-mediated abiotic stress-induced programmed cell death in plants. Frontiers in plant science, 6, 69.

Radotić K et al. (2012) Atomic force microscopy stiffness tomography on living Arabidopsis thaliana cells reveals the mechanical properties of surface and deep cell-wall layers during growth. Biophys J *103*:386-394.

Renew, S., Heyno, E., Schopfer, P., and Liszkay, A. (2005). Sensitive detection and localization of hydroxyl radical production in cucumber roots and Arabidopsis seedlings by spin trapping electron paramagnetic resonance spectroscopy. The Plant Journal *44*, 342–347.

Scheible, W.-R., Fry, B., Kochevenko, A., Schindelasch, D., Zimmerli, L., Somerville, S., Loria, R., and Somerville, C.R. (2003). An Arabidopsis mutant resistant to thaxtomin A, a cellulose synthesis inhibitor from Streptomyces species. The Plant Cell *15*, 1781–1794.

Slesak, I., Libik, M., Karpinska, B., Karpinski, S., & Miszalski, Z. (2007). The role of hydrogen peroxide in regulation of plant metabolism and cellular signalling in response to environmental stresses. ACTA BIOCHIMICA POLONICA-ENGLISH EDITION-, *54(1)*, 39.

Tenhaken, R. (2015). Cell wall remodeling under abiotic stress. Front. Plant Sci. *5*. 771.

Torres, M. A., Dangl, J. L., & Jones, J. D. (2002). Arabidopsis gp91phox homologues AtrbohD and AtrbohF are required for accumulation of reactive oxygen intermediates in the plant defense response. Proceedings of the National Academy of Sciences, *99*(1), 517-522.

Volkov, R. A., Panchuk, I. I., Mullineaux, P. M., & Schöffl, F. (2006). Heat stress-induced H 2 O 2 is required for effective expression of heat shock genes in Arabidopsis. Plant molecular biology, *61*(4-5), 733-746.

Wakabayashi, K., Soga, K., and Hoson, T. (2012). Phenylalanine ammonia-lyase and cell wall peroxidase are cooperatively involved in the extensive formation of ferulate network in cell walls of developing rice shoots. Journal of Plant Physiology *169*, 262–267.

Wei H, Zhang X, Wang Y, Lebwohl M. 2002. Inhibition of ultraviolet light-induced oxidative events in the skin and internal organs of hairless mice by isoflavone genistein. Cancer Letters *185*, 21–29.

Supplementary information

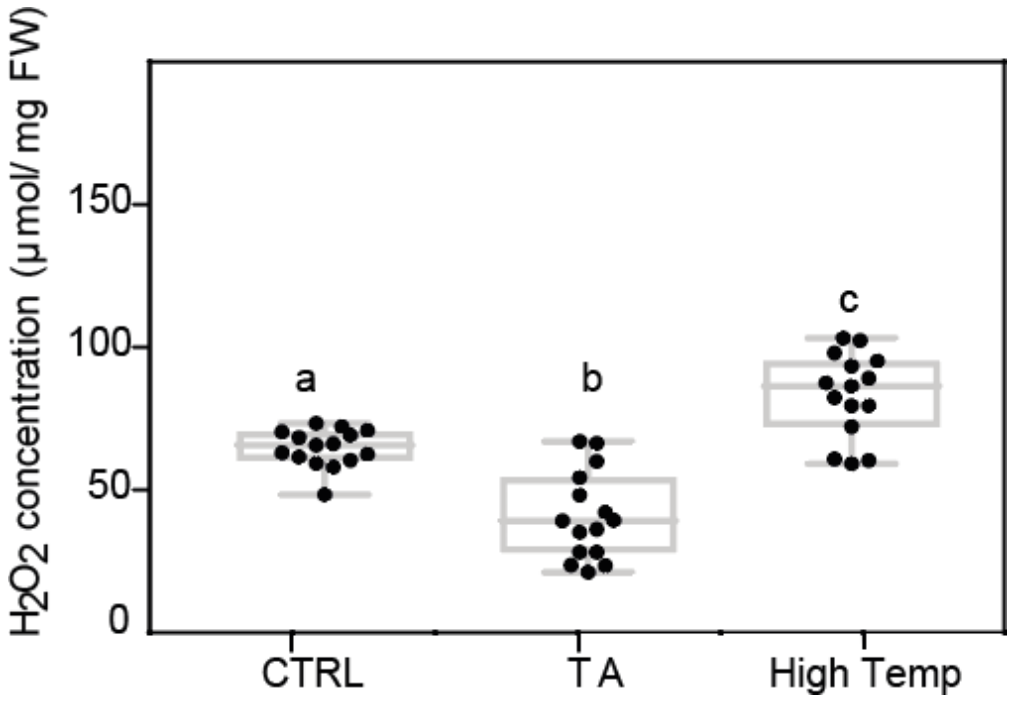

Figure SI : Hydrogen peroxide quantification using ferrous ammonium sulphate/xylenol orange (FOX).

Hydrogen peroxide (H_2O_2) concentration in µmol/mg of fresh weight was measured in methanol (CTRL), 10 µmol thaxtomin A dissolved in methanol (TA) treated cells and as a positive control, cells were placed in 45ºC heated medium (High Temp). All treatments were of 30 min of duration. Measurements were made according to modified FOX assay (Wei et al., 2002) on 5 samples/condition repeated in three independent experiments. All 15 measurements (black points) of each condition were pooled in this graph. The three groups were compared by Dunnett's multiple comparison test. Different letters indicate statistically significant difference.

CHAPITRE 5

DISCUSSION ET CONCLUSION GÉNÉRALE

La paroi pectocellulosique est une structure de grande importance pour les cellules végétales. Elle permet la survie de ces cellules face aux contraintes environnementales et aux agents phytopathogènes. Dans notre étude, nous avons montré que l'inhibiteur de synthèse de cellulose, la thaxtomine A, agit sur plusieurs niveaux avant de finir par activer une mort cellulaire programmée.

5.1 La protection par l'auxine contre la MCP induite par les CBI

Dans le deuxième chapitre, nous avons confirmé que l'ajout d'auxine protège les cellules en suspension de façon importante contre l'effet de la TA. De même, nous avons montré que l'efflux d'auxine est indispensable pour la mise en place du programme de mort suite à un traitement de TA. Ainsi, nos résultats confirment que le flux calcique est une étape importante dans la MCP induite par la TA. Ces résultats confirment les travaux ultérieurs (Duval et al., 2005; Scheible et al, 2009) montrant l'importance de l'auxine et du flux calcique dans la réponse cellulaire à la présence de la TA. De même, les travaux présentés dans ce chapitre comparent la MCP induite par la TA à celle induite par l'isoxabène et confirment pour la première fois que l'efflux d'auxine est indispensable dans les deux cas. Des expériences supplémentaires (Annexe 1) montrent que le transporteur polaire d'auxine, PIN2, subit une internalisation rapide dans les minutes qui suivent l'application de la TA. Ces résultats font appel aux travaux de transcriptomique menés sur des cellules traitées à la TA ou à l'IXB qui

montrent une augmentation de l'expression de quelques gènes reliés au transport de l'auxine ou à la réponse à l'auxine (PINOID et ARF; Duval et Beaudoin, 2010).

En outre, les résultats obtenus par la microscopie à force atomique en surface des cellules traitées au CBI ont montré que la paroi cellulaire est moins rigide en présence de TA ou d'IXB. Il est intéressant de noter que l'ajout d'auxine (IAA ou 2,4-D) au milieu a mené tout de même à la diminution de la rigidité de la paroi. Cette diminution de rigidité de la paroi peut être la cause derrière la protection conférée par l'auxine aux cellules contre la MCP induite par les CBI. En effet, il est possible que le pré-ramollissement de la paroi perturbe l'action des CBI sur cette dernière. Ce phénomène de diminution de la rigidité de la paroi en présence d'auxine a été reporté par plusieurs études (Bhalerao et al., 2002; Braybrook et Peaucelle, 2013) pour son importance durant l'élongation cellulaire et l'organogenèse.

Nous pensons que, suite à l'application de la TA ou de l'IXB, un efflux d'auxine a lieu, dirigeant l'auxine des cellules centrales aux cellules distales d'une file cellulaire. Les cellules distales, ayant une grande concentration d'auxine, subissent un gonflement et une diminution de la rigidité de leurs parois, ce qui permet de diminuer le stress mécanique perçue au niveau de la paroi suite à la perturbation mené par la TA. Ce mécanisme permet aux cellules distales (gonflées) de survivre à la TA. Le gonflement a lieu aussi durant un traitement à l'IXB, ce qui peut s'expliquer par le même mécanisme.

L'action de l'auxine peut avoir lieu sur plusieurs niveaux, premièrement au niveau du ramollissement de la paroi (Braybrook et Peaucelle, 2013) ou encore au niveau de l'activation de la synthèse de cellulose (Tegg et al., 2005). De même, l'efflux d'auxine via les transporteurs PIN activent la mise en place d'un gradient d'auxine qui mènera à des patrons d'expansion cellulaire ou de différenciation (Blilou et al., 2005).

Les travaux présentés dans la Chap. 2 montrent l'importance de l'efflux de l'auxine dans l'induction de la MCP suite à l'ajout de l'isoxabène ou de la TA. Mais ces tests ne dépassent pas le fait qu'ils sont basés sur des inhibiteurs pharmacologiques et que ces inhibiteurs visent tous les transporteurs d'efflux sans donner d'indice plus spécidique. Pour compléter les travaux présentés dans cette thèse, il serait intéressant d'étudier chez les cellules traitées avec l'auxine

et la TA l'expression des gènes de réponse à l'auxine qui ont été surexprimés suite à traitement par la TA seule comme At1g72430 (Duval et Beaudoin, 2009) De même, il serait intéressant de voir comment les deux calmodulines TOUCH3 et Pinoid-Binding Protein-1 dont les gènes sont aussi surexprimés en réponse à la TA se comportent dans les co-traitements auxine-TA. Il est connu que ces deux protéines se lie à la protéine PINOID qui est un régulateur positif de l'efflux de l'auxine (Duval et Beaudoin, 2009). En regardant ces gènes cibles, nous pouvons avoir une idée précise de la cinétique qui a lieu quand la TA est ajoutée au milieu cellulaire, et ce en suivant l'expression de gènes en fonction du temps avant et durant un traitement à la TA.

5.2 L'effet de la TA sur la dynamique de la paroi

Les résultats que nous avons obtenus démontrant la diminution de la rigidité de la paroi observé en présence de la TA nous ont amené à étudier davantage comment les composants de la paroi sont altérés par la TA pour permettre cette diminution. Nous nous sommes intéressés particulièrement à l'effet de la TA sur la synthèse de la cellulose, le composant qui confère la rigidité à la paroi (Chebli et Geitmann, 2017), et plus spécifiquement sur son effet sur les celluloses synthases mêmes.

Dans cette partie des travaux, nous avons montré qu'en présence de la TA la longueur des microfibrilles de cellulose est compromise par rapport aux conditions normales. De même, nous avons montré un effet rapide de la TA sur la diminution de la vélocité des CeSA6. Ce mécanisme a été accompagné d'une réorientation des microtubules d'une direction transversale en une longitudinale. Ces observations corrèlent avec un arrêt apparent de l'élongation cellulaire et une internalisation des CeSA6. Ces résultats suggèrent que la TA affecte la synthèse de la cellulose en réorientant les microtubules qui affecteront à leurs tours la position des CeSA6 ralenties. Ceci perturbe la synthèse de la cellulose et génère des chaînes moins longues.

La présence des chaînes compromises en longueur peut justifier la diminution de la rigidité de la paroi observé dans le chapitre 2.

D'autre part, nos travaux ont montré le comportement opposé de deux mutants très différent, *any1* qui est un mutant nul de *CeSA1* (Fujita et al., 2013) qui se trouve extrêmement sensible à la TA, et *mor1-1* qui présente une protéine associée au microtubules MOR1 altérée mais partiellement fonctionnelle (Kawamura et Wasteneys, 2008) et qui est relativement résistant à la TA. Une caractéristique commune entre les deux mutants est le fait que les deux ont un niveau de cristallinité de cellulose anormale. *any1* présente une réduction dans la cristallinité de la cellulose alors que *mor1-1* possède une cellulose plus cristalline comparé à l'écotype sauvage. À la lumière de ces résultats, il apparait donc possible que le mécanisme de tolérance/sensibilité à la TA est lier au niveau de cristallinité de la paroi. Toutefois, on ne peut pas exclure la possibilité que la protéine MOR1 soit une cible ou interagisse avec une cible de la TA, vue que le phénotype à température restrictive de *mor1-1* s'accentue en présence de la TA.

Finalement, bien que cette partie ajoute plusieurs nouveaux éléments pouvant contribuer à la compréhension du mode d'action de la TA sur la paroi, il est important de souligner d'autres possibilités. Par exemple, nous avons peu d'information sur l'effet de la TA sur les autres composants de la paroi. Si les moyens et le temps le permettaient, j'aurais pu tester l'effet de la TA sur les pectines de la paroi en regardant l'état de méthyl estérification. Également, il serait intéressant d'étudier si la composition en pectines et en hémicellulose (en différent types) changeait sous l'action de la TA. De même, il serait intéressant de connaître l'action de la TA sur un autre composant du cytosquelette, l'actine, vu le fait que la polymérisation de l'actine est altérée selon le gradient et l'efflux de l'auxine (Nick, 2010), et que la TA nécessite cet efflux pour induire la mort.

5.3 Le peroxyde d'hydrogène et son absence durant la MCP induite par la TA

Après avoir démontrer l'effet de l'auxine sur la MCP induite par la TA, ainsi que l'effet de la TA sur la synthèse de la cellulose, nous nous sommes intéressés à caractériser d'autres éléments propres à cette MCP atypique. La dernière partie des travaux se consacrait à un aspect

présent dans la littérature, l'absence de production des ROS suite à l'action de la TA (Duval et al., 2005; Errakhi et al., 2008). Après avoir confirmé que la production des ROS n'a pas lieu après l'ajout de la TA, nous avons montré que justement si elle avait eu lieu, ceci aurait probablement favoriser la survie de la cellule. Cette hypothèse a été démontré par l'ajout exogène de peroxyde d'hydrogène avant un traitement à la TA et qui a mené à une diminution du pourcentage de cellules mortes. De même, nos résultats montrent que la présence du peroxyde exogène était responsable d'une rigidification de la paroi comme mesuré par microscopie à force atomique. L'ajout de la TA aux cellules traitées par le peroxyde n'affecte pas cette rigidification.

On peut conclure que l'absence de production de ROS et particulièrement du H_2O_2 durant une MCP induite par la TA est un élément essentiel qui fait la différence entre cette MCP et les autres types de mort programmée. En perspective, il serait intéressant de regarder le comportement des peroxydase de la paroi et voir si leurs expressions ou leurs activités sont effectivement changées en présence de TA vu que ces enzymes produisent des ROS, oxydent les composés phénolique et contribuent au remodelage de la paroi (Francoz et al., 2015). Ces résultats démontreraient l'importance des ROS pour protéger la cellule lors de dommages au niveau de la paroi.

5.4 Conclusion

Lors de cette étude, nous avons montré que l'inhibiteur de synthèse de cellulose, la TA, affecte la vitesse de synthèse de la cellulose, la qualité de la cellulose produite et ainsi la rigidité de la paroi en la diminuant.

De même, nous avons démontré que la TA induit une réorientation des microtubules affectant l'élongation cellulaire et probablement la taille des cellules.

D'autre part, cette étude ajoute deux éléments concernant la MCP induite par la TA, le premier étant le mode d'action de l'auxine dans la protection contre cette mort, et le deuxième celui du peroxyde d'hydrogène.

Ces éléments contribuent à la compréhension du mode d'action de la TA, ce qui peut s'inscrire plus tard dans des cibles de traitement contre la maladie de la gale commune de la pomme de terre dont la TA est un important facteur.

Il sera important pour la continuité du projet de tester la présence des interactions moléculaires entre la protéine TCH3 et la TA et ceux en présence et en absence d'auxine. Il se peut que cette protéine soit sensible à une interaction de TA avec un récepteur pariétale, TCH3 pourrait dans ce contexte se lier aux PIDs pour activer un efflux d'auxine. L'auxine qui baisse dans certaines cellules et qui augmente dans d'autre mène à la survie des cellules riches en auxine qui expérimenteront une croissance acide au niveau de la paroi ce qui justifie le gonflement de ces cellules.

De point de vue fondamentale, les approches et les résultats obtenus durant cette étude pourront être poussés afin d'utiliser la thaxtomine A comme outil de compréhension de la paroi cellulaire dans ses différents composants.

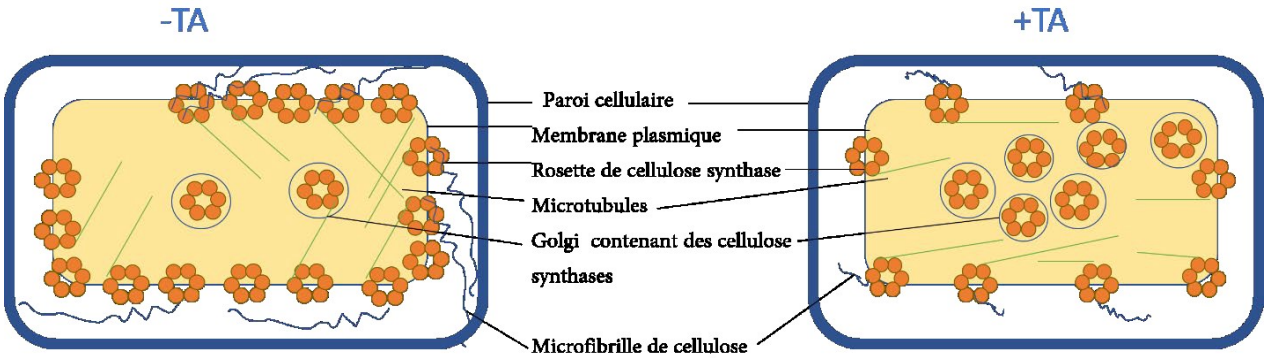

Figure 5.1 : Schéma symbolisant l'effet de la thaxtomine A (TA) sur la paroi.
En présence de TA, une réorientation des microtubules a lieu en limitant l'élongation cellulaire, ainsi qu'une diminution de la vélocité des celluloses synthases (environ 370 nm/min en absence de TA vs 260 nm/min en présence de TA). Les particules celluloses synthases sont plus abondantes dans les Golgi en présence de TA. De même, les micro fibrilles de cellulose nouvellement synthétisées sont plus courtes en présence de TA.

ANNEXE

Table A1 : Estimation de la fluorescence relative des particules PIN2-GFP sous différents traitments avec ImageJ.

Conditions	Répartition membranaire	Répartition cytoplasmique	Ration membranaire/ cytoplasmique
GM+DMSO	14692 ± 12,6 %	758 ±4,8%	19,3
GM+TA 100nM	16025 ±8,2%	626 ±8,9%	25,6
10µM TA à 5min	826 ±14%	12536 ±6.5%	0,06

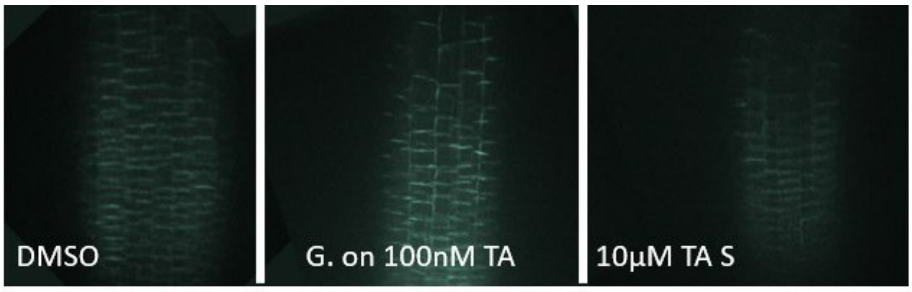

Figure annexe : Visualisation du transporteur PIN2 en présence de la TA. Les photos représentent des racines de plantules pPIN2::PIN2–GFP âgées de 4 jours germées sur milieu contenant du DMSO comme témoin. Germée sur milieu contenant 100 nM de TA, ou germées sut milieu contenant du DMSO puis transférées pendant 30 minutes dans une solution de 10µM de TA.

BIBLIOGRAPHIE

Almagro, G., Baroja-Fernández, E., Muñoz, F.J., Bahaji, A., Etxeberria, E., Li, J., Montero, M., Hidalgo, M., Sesma, M.T., and Pozueta-Romero, J. (2012). No evidence for the occurrence of substrate inhibition of Arabidopsis thaliana sucrose synthase-1 (AtSUS1) by fructose and UDP-glucose. Plant Signal. Behav. 7, 799–802.

Alushin, G.M., Lander, G.C., Kellogg, E.H., Zhang, R., Baker, D., and Nogales, E. (2014). High-Resolution Microtubule Structures Reveal the Structural Transitions in αβ-Tubulin upon GTP Hydrolysis. Cell 157, 1117–1129.

Amor, Y., Haigler, C.H., Johnson, S., Wainscott, M., and Delmer, D.P. (1995). A membrane-associated form of sucrose synthase and its potential role in synthesis of cellulose and callose in plants. Proc. Natl. Acad. Sci. 92, 9353–9357.

Arioli, T., Peng, L., Betzner, A.S., Burn, J., Wittke, W., Herth, W., Camilleri, C., Höfte, H., Plazinski, J., Birch, R., et al. (1998). Molecular Analysis of Cellulose Biosynthesis in Arabidopsis. Science 279, 717–720.

Atmodjo, M.A., Hao, Z., and Mohnen, D. (2013). Evolving Views of Pectin Biosynthesis. Annu. Rev. Plant Biol. 64, 747–779.

Beckman, C.H. (2000). Phenolic-storing cells: keys to programmed cell death and periderm formation in wilt disease resistance and in general defence responses in plants? Physiol. Mol. Plant Pathol. 57, 101–110.

Bignell, D.R., Francis, I.M., Fyans, J.K., and Loria, R. (2014). Thaxtomin A Production and Virulence Are Controlled by Several bld Gene Global Regulators in Streptomyces scabies. Mol. Plant. Microbe Interact. 27, 875–885.

Bischoff, V., Cookson, S.J., Wu, S., and Scheible, W.-R. (2009). Thaxtomin A affects CeSA-complex density, expression of cell wall genes, cell wall composition, and causes ectopic lignification in Arabidopsis thaliana seedlings. J. Exp. Bot. 60, 955–965.

Bradley, D.J., Kjellbom, P., and Lamb, C.J. (1992). Elicitor-and wound-induced oxidative cross-linking of a proline-rich plant cell wall protein: a novel, rapid defense response. Cell 70, 21–30.

Brochu, V. (2005). Caracterisation des effets de la thaxtomine a chez les plantes. Mémoire de maîtrise, Université de Sherbrooke, Québec.

Buschmann, H., and Lloyd, C.W. (2008). Arabidopsis Mutants and the Network of Microtubule-Associated Functions. Mol. Plant 1, 888–898.

Chebli, Y., and Geitmann, A. (2017). Cellular growth in plants requires regulation of cell wall biochemistry. Curr. Opin. Cell Biol. 44, 28.

Cosgrove, D.J. (2005). Growth of the plant cell wall. Nat. Rev. Mol. Cell Biol. 6, 850–861.

Cosgrove, D.J. (2016). Plant cell wall extensibility: connecting plant cell growth with cell wall structure, mechanics, and the action of wall-modifying enzymes. J. Exp. Bot. 67, 463–476.

Daher, F.B., and Braybrook, S.A. (2015). How to let go: pectin and plant cell adhesion. Front. Plant Sci. 6.

Daneva, A., Gao, Z., Van Durme, M., and Nowack, M.K. (2016). Functions and Regulation of Programmed Cell Death in Plant Development. Annu. Rev. Cell Dev. Biol. 32, 441–468.

Desprez, T., Juraniec, M., Crowell, E.F., Jouy, H., Pochylova, Z., Parcy, F., Höfte, H., Gonneau, M., and Vernhettes, S. (2007). Organization of cellulose synthase complexes involved in primary cell wall synthesis in Arabidopsis thaliana. Proc. Natl. Acad. Sci. 104, 15572–15577.

Dixit, R., and Cyr, R. (2004). Encounters between Dynamic Cortical Microtubules Promote Ordering of the Cortical Array through Angle-Dependent Modifications of Microtubule Behavior. Plant Cell 16, 3274–3284.

Doblin, M.S., Kurek, I., Jacob-Wilk, D., and Delmer, D.P. (2002). Cellulose Biosynthesis in Plants: from Genes to Rosettes. Plant Cell Physiol. 43, 1407–1420.

Doblin, M.S., Johnson, K.L., Humphries, J., Newbigin, E.J., and Bacic, A. (Tony) (2014). Are designer plant cell walls a realistic aspiration or will the plasticity of the plant's metabolism win out? Food Biotechnol. Plant Biotechnol. 26, 108–114.

Drechsel, D.N., Hyman, A.A., Cobb, M.H., and Kirschner, M.W. (1992). Modulation of the dynamic instability of tubulin assembly by the microtubule-associated protein tau. Mol. Biol. Cell 3, 1141–1154.

Duval, I., and Beaudoin, N. (2009). Transcriptional profiling in response to inhibition of cellulose synthesis by thaxtomin A and isoxaben in Arabidopsis thaliana suspension cells. Plant Cell Rep. 28, 811–830.

Duval, I., Brochu, V., Simard, M., Beaulieu, C., and Beaudoin, N. (2005). Thaxtomin A induces programmed cell death in Arabidopsis thaliana suspension-cultured cells. Planta 222, 820–831.

Ehrhardt, D.W., and Shaw, S.L. (2006). Microtubule Dynamics and Organization in the Plant Cortical Array. Annu. Rev. Plant Biol. 57, 859–875.

Endler, A., Kesten, C., Schneider, R., Zhang, Y., Ivakov, A., Froehlich, A., Funke, N., and Persson, S. (2015). A Mechanism for Sustained Cellulose Synthesis during Salt Stress. Cell 162, 1353–1364.

Errakhi, R., Dauphin, A., Meimoun, P., Lehner, A., Reboutier, D., Vatsa, P., Briand, J., Madiona, K., Rona, J.P., Barakate, M., et al. (2008). An early Ca2+ influx is a prerequisite to thaxtomin A-induced cell death in Arabidopsis thaliana cells. J. Exp. Bot. 59, 4259–4270.

Francoz, E., Ranocha, P., Nguyen-Kim, H., Jamet, E., Burlat, V., and Dunand, C. (2015). Roles of cell wall peroxidases in plant development. Phytochemistry 112, 15–21.

Fry, S.C. (2001). Plant Cell Walls. In ELS, (American Cancer Society), p.

Fry, B.A., and Loria, R. (2002). Thaxtomin A: evidence for a plant cell wall target. Physiol. Mol. Plant Pathol. 60, 1–8.

Fujita, M., Himmelspach, R., Hocart, C.H., Williamson, R.E., Mansfield, S.D., and Wasteneys, G.O. (2011). Cortical microtubules optimize cell-wall crystallinity to drive unidirectional growth in Arabidopsis. Plant J. 66, 915–928.

Fujita, S., Pytela, J., Hotta, T., Kato, T., Hamada, T., Akamatsu, R., Ishida, Y., Kutsuna, N., Hasezawa, S., Nomura, Y., et al. (2013). An Atypical Tubulin Kinase Mediates Stress-Induced Microtubule Depolymerization in Arabidopsis. Curr. Biol. 23, 1969–1978.

Fukuda, H. (2004). Signals that control plant vascular cell differentiation. Nat. Rev. Mol. Cell Biol. 5, 379–391.

Gallavotti, A. (2013). The role of auxin in shaping shoot architecture. J. Exp. Bot. 64, 2593–2608.

Gilroy, S. (2017). Pollen tube vs CHUKNORRIS: the action is pulsatile. J. Exp. Bot. 68, 3041–3043.

Gutierrez, R., Lindeboom, J.J., Paredez, A.R., Emons, A.M.C., and Ehrhardt, D.W. (2009). Arabidopsis cortical microtubules position cellulose synthase delivery to the plasma membrane and interact with cellulose synthase trafficking compartments. Nat. Cell Biol. 11, 797–806.

Hashimoto, T. (2015). Microtubules in Plants. Arab. Book Am. Soc. Plant Biol. 13.

Hématy, K., Cherk, C., and Somerville, S. (2009). Host–pathogen warfare at the plant cell wall. Curr. Opin. Plant Biol. 12, 406–413.

Hill, J.L., Hammudi, M.B., and Tien, M. (2014). The Arabidopsis Cellulose Synthase Complex: A Proposed Hexamer of CeSA Trimers in an Equimolar Stoichiometry. Plant Cell tpc.114.

Hon, D.N.-S. (1994). Cellulose: a random walk along its historical path. Cellulose 1, 1–25.

Horio, T., and Murata, T. (2014). The role of dynamic instability in microtubule organization. Front. Plant Sci. 5, 511.

Huang, Y., Chen, X., Liu, Y., Roth, C., Copeland, C., McFarlane, H.E., Huang, S., Lipka, V., Wiermer, M., and Li, X. (2013). Mitochondrial AtPAM16 is required for plant survival and the negative regulation of plant immunity. Nat. Commun. 4, 2558.

Hückelhoven, R. (2007). Cell Wall–Associated Mechanisms of Disease Resistance and Susceptibility. Annu. Rev. Phytopathol. 45, 101–127.

Kärkönen, A., and Kuchitsu, K. (2015). Reactive oxygen species in cell wall metabolism and development in plants. Phytochemistry 112, 22–32.

Kaur, S., Dhugga, K.S., Gill, K., and Singh, J. (2016). Novel Structural and Functional Motifs in cellulose synthase (CeSA) Genes of Bread Wheat (Triticum aestivum, L.). PLOS ONE 11, e0147046.

Kers, J.A., Wach, M.J., Krasnoff, S.B., Widom, J., Cameron, K.D., Bukhalid, R.A., Gibson, D.M., Crane, B.R., and Loria, R. (2004). Nitration of a peptide phytotoxin by bacterial nitric oxide synthase. Nature 429, 79–82.

Kim, H.J., and Triplett, B.A. (2001). Cotton Fiber Growth in Planta and in Vitro. Models for Plant Cell Elongation and Cell Wall Biogenesis. Plant Physiol. 127, 1361–1366.

Kim, S.H., Lee, C.M., and Kafle, K. (2013). Characterization of crystalline cellulose in biomass: Basic principles, applications, and limitations of XRD, NMR, IR, Raman, and SFG. Korean J. Chem. Eng. 30, 2127–2141.

King, R.R., Lawrence, C.H., Clark, M.C., and Calhoun, L.A. (1989). Isolation and characterization of phytotoxins associated with Streptomyces scabies. J. Chem. Soc. Chem. Commun. 0, 849–850.

Kumar, M., and Turner, S. (2015). Plant cellulose synthesis: CeSA proteins crossing kingdoms. Phytochemistry 112, 91–99.

Lei, L., Li, S., Du, J., Bashline, L., and Gu, Y. (2013). CELLULOSE SYNTHASE INTERACTIVE3 Regulates Cellulose Biosynthesis in Both a Microtubule-Dependent and Microtubule-Independent Manner in Arabidopsis. Plant Cell tpc.113.116715.

Leucci, M.R., Lenucci, M.S., Piro, G., and Dalessandro, G. (2008). Water stress and cell wall polysaccharides in the apical root zone of wheat cultivars varying in drought tolerance. J. Plant Physiol. 165, 1168–1180.

Levesque-Tremblay, G., Pelloux, J., Braybrook, S.A., and Müller, K. (2015). Tuning of pectin methylesterification: consequences for cell wall biomechanics and development. Planta 242, 791–811.

Li, S., Lei, L., Somerville, C.R., and Gu, Y. (2012). Cellulose synthase interactive protein 1 (CSI1) links microtubules and cellulose synthase complexes. Proc. Natl. Acad. Sci. 109, 185.

Lopez-Galvez, G. (1996). Wound-induced phenylalanine ammonia lyase activity: factors affecting its induction and correlation with the quality of minimally processed lettuces. Postharvest Biol Technol 9, 223–233.

Loqué (2015). Engineering of plant cell walls for enhanced biofuel production. Curr. Opin. Plant Biol. 25, 151–161.

McFarlane, H.E., Döring, A., and Persson, S. (2014). The Cell Biology of Cellulose Synthesis. Annu. Rev. Plant Biol. 65, 69–94.

Meents, M.J., Watanabe, Y., and Samuels, A.L. (2018). The cell biology of secondary cell wall biosynthesis. Ann. Bot. 121, 1107–1125.

Menéndez, M., Rivas, G., Díaz, J.F., and Andreu, J.M. (1998). Control of the Structural Stability of the Tubulin Dimer by One High Affinity Bound Magnesium Ion at Nucleotide N-site. J. Biol. Chem. 273, 167–176.

Moneva, E. (2011). Étude de la mort cellulaire programmée induite par la thaxtomine A ou l'isoxabène chez Arabidopsis thaliana. Mémoire de maîtrise. Université de Sherbrooke, Québec.

Morgan, J.L.W., Strumillo, J., and Zimmer, J. (2012). Crystallographic snapshot of cellulose synthesis and membrane translocation. Nature 493, 181.

Morgan, J.L.W., McNamara, J.T., Fischer, M., Rich, J., Chen, H.-M., Withers, S.G., and Zimmer, J. (2016). Observing cellulose biosynthesis and membrane translocation in crystallo. Nature 531, 329.

Mueller, S.C., and Brown, R.M. (1980). Evidence for an intramembrane component associated with a cellulose microfibril-synthesizing complex in higher plants. J. Cell Biol. 84, 315–326.

Nick, P. (2010). Probing the actin-auxin oscillator. Plant signaling & behavior, *5*(2), 94-98.

Nixon, B.T., Mansouri, K., Singh, A., Du, J., Davis, J.K., Lee, J.-G., Slabaugh, E., Vandavasi, V.G., O'Neill, H., Roberts, E.M., et al. (2016). Comparative Structural and Computational Analysis Supports Eighteen Cellulose Synthases in the Plant Cellulose Synthesis Complex. Sci. Rep. 6, 28696.

Oda, Y., Mimura, T., and Hasezawa, S. (2005). Regulation of secondary cell wall development by cortical microtubules during tracheary element differentiation in Arabidopsis cell suspensions. Plant Physiol. 137, 1027–1036.

Oehme, D.P., Downton, M.T., Doblin, M.S., Wagner, J., Gidley, M.J., and Bacic, A. (2015). Unique aspects of the structure and dynamics of elementary Iβ cellulose microfibrils revealed by computational simulations. Plant Physiol. 168, 3–17.

Pacifici, E., Mambro, R.D., Ioio, R.D., Costantino, P., and Sabatini, S. (2018). Acidic cell elongation drives cell differentiation in the Arabidopsis root. EMBO J. 37, e99134.

Padilla-reynaud, R., Simao-beaunoir, A., Lerat, S., and Bernards, M.A. (2015). Suberin Regulates the Production of Cellulolytic Enzymes in Streptomyces scabiei, the Causal Agent of Potato Common Scab.

Paredez, A.R., Somerville, C.R., and Ehrhardt, D.W. (2006). Visualization of Cellulose Synthase Demonstrates Functional Association with Microtubules. Science 312, 1491–1495.

Park, Y.B., and Cosgrove, D.J. (2012). Changes in Cell Wall Biomechanical Properties in the Xyloglucan-Deficient xxt1/xxt2 Mutant of Arabidopsis. Plant Physiol. 158, 465–475.

Pear, J.R., Kawagoe, Y., Schreckengost, W.E., Delmer, D.P., and Stalker, D.M. (1996). Higher plants contain homologs of the bacterial celA genes encoding the catalytic subunit of cellulose synthase. Proc. Natl. Acad. Sci. 93, 12637–12642.

Pubchem Thaxtomin A. Kim S, Thiessen PA, Bolton EE, Chen J, Fu G, Gindulyte A, Han L, He J, He S, Shoemaker BA, Wang J, Yu B, Zhang J, Bryant SH. PubChem Substance and Compound databases. Nucleic Acids Res. 2016 Jan 4; 44(D1):D1202-13. Epub 2015 Sep 22 [PubMed PMID: 26400175] doi: 10.1093/nar/gkv951.

Purushotham, P., Cho, S.H., Díaz-Moreno, S.M., Kumar, M., Nixon, B.T., Bulone, V., and Zimmer, J. (2016). A single heterologously expressed plant cellulose synthase isoform is sufficient for cellulose microfibril formation in vitro. Proc. Natl. Acad. Sci. U. S. A. 113, 11360–11365.

Richmond, T.A., and Somerville, C.R. (2000). The Cellulose Synthase Superfamily. Plant Physiol. 124, 495–498.

Romero-Arias, J.R., Hernández-Hernández, V., Benítez, M., Alvarez-Buylla, E.R., and Barrio, R.A. (2017). Model of polar auxin transport coupled to mechanical forces retrieves robust morphogenesis along the $\mathit{Arabidopsis}$ root. Phys. Rev. E 95, 032410.

Scheible, W.-R., Fry, B., Kochevenko, A., Schindelasch, D., Zimmerli, L., Somerville, S., Loria, R., and Somerville, C.R. (2003). An Arabidopsis mutant resistant to thaxtomin A, a cellulose synthesis inhibitor from Streptomyces species. Plant Cell 15, 1781–1794.

Sedbrook, J.C., and Kaloriti, D. (2008). Microtubules, MAPs and plant directional cell expansion. Trends Plant Sci. 13, 303–310.

Tateno, M., Brabham, C., and DeBolt, S. (2016). Cellulose biosynthesis inhibitors -- a multifunctional toolbox. J. Exp. Bot. 67, 533–542.

Taylor, N. G., Howells, R. M., Huttly, A. K., Vickers, K., & Turner, S. R. (2003). Interactions among three distinct CesA proteins essential for cellulose synthesis. Proceedings of the National Academy of Sciences, 100(3), 1450-1455.

Tegg, R.S., Melian, L., Wilson, C.R., and Shabala, S. (2005). Plant cell growth and ion flux responses to the streptomycete phytotoxin thaxtomin A: calcium and hydrogen flux patterns revealed by the non-invasive MIFE technique. Plant Cell Physiol. 46, 638–648.

Tegg, R.S., Gill, W.M., Thompson, H.K., Davies, N.W., Ross, J.J., and Wilson, C.R. (2008). Auxin-induced resistance to common scab disease of potato linked to inhibition of thaxtomin A toxicity. Plant Dis. 92, 1321–1328.

Tenhaken, R. (2015). Cell wall remodeling under abiotic stress. Front. Plant Sci. 5.

Van Hautegem, T., Waters, A.J., Goodrich, J., and Nowack, M.K. (2015). Only in dying, life: programmed cell death during plant development. Trends Plant Sci. 20, 102–113.

Vergara, C. E., & Carpita, N. C. (2001). β-D-Glycan synthases and the CesA gene family: lessons to be learned from the mixed-linkage (1→ 3),(1→ 4) β-D-glucan synthase. In Plant Cell Walls (pp. 145-160). Springer, Dordrecht.

Voiniciuc, C., Pauly, M., and Usadel, B. (2018). Monitoring Polysaccharide Dynamics in the Plant Cell Wall. Plant Physiol. 176, 2590–2600.

Wang, J., Howles, P.A., Cork, A.H., Birch, R.J., and Williamson, R.E. (2006). Chimeric Proteins Suggest That the Catalytic and/or C-Terminal Domains Give CeSA1 and CeSA3 Access to Their Specific Sites in the Cellulose Synthase of Primary Walls. Plant Physiol. 142, 685–695.

Wang, T., Park, Y.B., Daniel, J.C., and Hong, M. (2015). Cellulose-pectin spatial contacts are inherent to never-dried Arabidopsis thaliana primary cell walls: evidence from solid-state NMR. Plant Physiol. pp–00665.

Wasteneys, G.O., and Ambrose, J.C. (2009). Spatial organization of plant cortical microtubules: close encounters of the 2D kind. Trends Cell Biol. 19, 62–71.

Williamson, R.E., Burn, J.E., Birch, R., Baskin, T.I., Arioli, T., Betzner, A.S., and Cork, A. (2001). Morphology of rsw1, a cellulose-deficient mutant of Arabidopsis thaliana. Protoplasma 215, 116–127.

Xuan, W., Band, L.R., Kumpf, R.P., Damme, D.V., Parizot, B., Rop, G.D., Opdenacker, D., Möller, B.K., Skorzinski, N., Njo, M.F., et al. (2016). Cyclic programmed cell death stimulates hormone signaling and root development in Arabidopsis. Science 351, 384–387.

Yokoyama, R., and Nishitani, K. (2004). Genomic Basis for Cell-Wall Diversity in Plants. A Comparative Approach to Gene Families in Rice and Arabidopsis. Plant Cell Physiol. 45, 1111–1121.